2020

RENCA Macrobeads Inhibit Tumor Cell Growth via EGFR Activation and Regulation of MEF2 Isoform Expression

Prithy Caroline Martis
Wright State University

RENCA MACROBEADS INHIBIT TUMOR CELL GROWTH VIA EGFR ACTIVATION AND REGULATION OF MEF2 ISOFORM EXPRESSION

A dissertation submitted in partial fulfillment of the
requirements for the degree of
Doctor of Philosophy

By

PRITHY CAROLINE MARTIS
B.S., University of Cincinnati, 2003

2020
Wright State University

WRIGHT STATE UNIVERSITY
GRADUATE SCHOOL

July 27, 2020

I HEREBY RECOMMEND THAT THE DISSERTATION PREPARED UNDER MY SUPERVISION BY Prithy Caroline Martis ENTITLED RENCA macrobeads inhibit tumor cell growth via EGFR activation and regulation of MEF2 isoform expression BE ACCEPTED IN PARTIAL FULFILLMENT OF THE REQUIREMENTS FOR THE DEGREE OF Doctor of Philosophy.

_____
Lawrence S. Gazda, Ph.D.
Dissertation Director

_____
Madhavi Kadakia, Ph.D.
Dissertation Co-Director

_____
Mill W. Miller, Ph.D.
Director, Biomedical Sciences Ph.D. Program

_____
Barry Milligan, Ph.D.
Interim Dean of the Graduate School

Committee on Final Examination:

_____
Lawrence S. Gazda, Ph.D.

_____
Madhavi Kadakia, Ph.D.

_____
Weiwen Long, Ph.D.

_____
Michael Markey, Ph.D.

_____
David Cool, Ph.D.

ABSTRACT

Martis, Prithy Caroline, Ph.D., Biomedical Sciences Ph.D. Program, Wright State University, 2020. RENCA macrobeads inhibit tumor cell growth via EGFR activation and regulation of MEF2 isoform expression

Tumors are heterogeneous systems, whose growth is influenced by intrinsic properties of malignant cells, external systemic factors (i.e. immune, neural, endocrine, etc.), and the dynamic interactions between tumor cells and their microenvironment. Given the inherent complexity of cancers, combined with the continual evolution of tumors and the development of treatment resistance, a precision medicine approach may not provide an optimal clinical response. Exploring a new paradigm that focuses on regulating cancer as a system may not only control tumor progression but also address the extraordinary challenges of tumor heterogeneity and disease recurrence in order to improve clinical outcomes. As a group of discrete, growth-restricted tumor colonies that regulate their own growth and secrete a large number of tumor-inhibitory signals, RENCA macrobeads function as a biological-system, providing the opportunity for a systems-therapeutic approach to cancer management.

Previous work has demonstrated that RENCA macrobeads restrict the growth of various cancer cells both in vitro as well as in preclinical and clinical studies; however, the molecular mechanism(s) of this inhibition is unknown. In this study, we demonstrated that factors secreted by RENCA macrobeads significantly altered the transcript levels of multiple MEF2 isoforms in targeted tumor cells. Suppression of various MEF2 isoforms

markedly reduced the growth inhibitory effect of RENCA macrobeads and abrogated macrobead induced S-phase arrest. Importantly, we identified an essential role for the MEF2D isoform in mediating RENCA macrobead-induced inhibition. In addition, the cell-surface receptor, EGFR, was shown to be involved in the anti-proliferative response to RENCA macrobeads. Growth inhibition was more robust in cells overexpressing EGFR and was associated with cell accumulation in S-phase. In cell lines with reduced EGFR kinase activity or low-levels of cell-surface receptor, we demonstrated that RENCA macrobeads inhibited growth, although to a lesser degree and exhibited G2/M arrest, supporting the notion that factors secreted by RENCA macrobeads regulate multiple cell cycle checkpoints. Lastly, we identified three proteins in conditioned media of RENCA macrobeads (RTN4, TSP1, TIMP2) that partially contribute to growth regulation of external tumor cells with functional EGFR activity. Moreover, we identified a novel role for these proteins in modulating MEF2 activity and regulating MEF2 expression, particularly the MEF2D isoform.

Overall, these studies support a mechanism by which RENCA macrobeads, at least partially, regulate tumor growth external to the macrobead. These findings could identify patients most likely to benefit from RENCA macrobead therapy.

TABLE OF CONTENTS

LIST OF FIGURES

LIST OF TABLES

ACKNOWLEDGEMENTS

This has been a journey more spirited and unexpected than I could have ever imagined. Like all graduate students who have survived the Ph.D. process, there were many good times and some rather frustrating moments; but more importantly, there were a number of remarkable people who helped me along the way.

Without question, I owe my deepest gratitude to my advisor, Dr. Lawrence S. Gazda. Thank you for your constant support, encouragement and guidance throughout the years. You have been an incredible mentor and have taught me a great deal about looking at science through a broad lens. I feel honored to be your first Ph.D. student and am grateful to you for preparing me for the next step in my career. I know that if I become only half the thinker, half the visionary, half the person that you are, it will surely be one of my greatest accomplishments.

I would also like to express my sincere appreciation to my co-advisor, Dr. Madhavi Kadakia. Thank you for giving me the opportunity to study under your guidance and all the time and support you have given me with my research. In addition to being a model example of what it takes to be a successful scientist, you have taught me the skills required to be an independent, critical thinker. Thank you for challenging me to be a better researcher.

I am especially grateful to my dissertation committee: Dr. David Cool, Dr. Weiwen Long, Dr. Michael Markey and for a short while, Dr. Katherine Excoffon. Each of you have generously given your time and expertise to offer me valuable comments toward improving my work. Your insights fill these pages.

Of course, this was only possible with the support of Dr. Mill Miller and Karen Luchin. I thank you for accepting the challenges of having a non-traditional Ph.D. student in your program and going the extra mile to make the process less stressful throughout my time at Wright State.

A special thanks to all members of The Rogosin Institute, especially Atira Dudley, Melissa Bemrose, Madeline Wiles and the entirety of the Cancer team. Working with a one-of-a-kind 3D-biological system presents unique challenges – to this end, each of you have provided tremendous support and valuable advice for which I am incredibly thankful. I also want to use this opportunity to thank Brian Doll. Over the years, you have given me many useful suggestions, saved me from being defeated by technology, and provided me with the “occasional” (but much needed) distraction.

It is truly a pleasure to acknowledge all my friends. True friends are hard to find and impossible to replace – all of you mean so much to me. Thank you for the love, encouragement, and lots of laughs over the years. I officially promise to once again listen to stories about your lives without interrupting with science.

Not least of all, I owe a debt of gratitude to my family. This journey would have been far more difficult without all of you in my life.
To my amazing mother: For as long as I can remember, you have been a continuous source of love, support and patience. I wish there was a better way to tell you how much I admire you, how much I appreciate you and how much I thank you, for everything you've done. I love you with all my heart.
To my brothers: In your own ways, each of you have been my role models and have encouraged me to follow my dreams. You have taught me to aim high, work hard and value those that we meet along the way.
To Joseph: You have blessed and enriched my life in more ways than I can count (…and that does not include your six-pack). You bring infinite joy and laughter to my life, and I love you beyond words.
As for my husband, James (who told me repeatedly that he does not need to be acknowledged, but also knows by now that I never listen to him): I find it hardest to express my appreciation for you because it is so boundless. You are my best friend, my most enthusiastic cheerleader and the most amazing husband. From near or far, you have been there for me from the beginning, supplied me with gummies, followed my "crazy" (but very normal) cleaning regimens, supported and encouraged me in the most positive way throughout this process, especially when tasks seemed arduous and insurmountable. Without your willingness to help with all of life's aspects; without your love and unwavering support; without you, this would not be possible. I love you so very much.

DEDICATION

"When you change the way you look at things, the things you look at will change"
-Max Planck

This thesis is dedicated to my late father, Henry A. Martis who is missed more than words can express. Thank you for always believing in me, and showing by example that with determination, dedication and compassion, anything is possible. You inspire me every day to be – and give – my very best. Although this comes too late to help you, I hope that it will someday make a difference.

CHAPTER 1: INTRODUCTION

1.1. Burden and Impact of Cancer

Cancer has long been one of the most devastating and confounding health concerns worldwide. Accounting for one in every six deaths, cancer is the second leading cause of global mortality, surpassed only by cardiovascular disease [2, 3]. Based on World Health Organization (WHO) estimates, in 2018 alone, there were 18.1 million new cases of cancer diagnosed and more than 9.6 million deaths [3, 4]. To add to the existing burden, worldwide incidence of cancer and death rates are forecasted to rise rapidly as populations grow, age, and adopt lifestyles that increase cancer risk [4].

1.2. Tumor biology

Cancer is not a singular, specific disease but a group of more than 150 disease processes that can involve any tissue in the body. Rather than responding appropriately to signals that control normal cell behavior, defects in the regulatory circuits of cancerous cells allows for continual proliferation, dissemination, invasion into adjacent tissues and colonization of abnormal cells at distant sites, termed metastases [5].

Based on the somatic mutation theory (SMT), initiation and progression of cancers hinge on the acquisition of driver mutations of key genes, related RNA and protein products that activate oncogenic pathways [6, 7]. These molecules typically coordinate signaling to

regulate the balance of proliferation, survival and apoptosis in normal quiescent cells [8, 9]. However, the mutant phenotype confers selective growth and survival advantages that allow transformed cells to expand and achieve clonal dominance [10], eventually forming a tumor mass.

An alternative theory of tumorigenesis, the tissue organization field theory (TOFT), posits that cancer is a tissue-based disease wherein proliferation is the default state of all cells [11]. In this model, carcinogens act to disrupt the reciprocal interactions between parenchymal and stromal components of tissues [12-14]. Disruption of normal tissue architecture alters the cells' ability to appropriately recognize and respond to positional and contextual cues, resulting in excessive proliferation (hyperplasia), disorganization of epithelia with abnormal histology (dysplasia) and cell transformation (metaplasia). Ultimately, epithelial cells unable to restrain their intrinsic proliferative properties form a tumor mass [12].

Tumors are classified according to anatomical site, histopathological and morphological profiles, as well as stage [15]. Tumor stage, a critical determinant of prognosis, is based on the TNM system developed by Pierre Denoix and the Union for International Cancer Control (UICC) [16]. In the TNM classification, the T category describes the extent of the primary tumors, by size, depth of invasion or invasion of adjacent structures; the N categorizes the absence or extent of regional lymph node involvement; and the M category indicates the absence or presence of distant metastasis [16, 17]. For instance, pathological evaluation of a tumor identified in the sigmoid colon that has invaded the submucosa with

no lymph node involvement or distant metastasis is classified as T1N0M0 (Stage I colorectal cancer). This combination of TNM categories, since its implementation in the 1940's, has described cancer diagnoses and guided the approach to treatment [16]. In the genomic era, the influx of complex multi-omics data has captured a new spectrum of biological diversity, providing novel diagnostic and personalized treatment targets [18, 19].

1.3. Cancer treatments

The ultimate goal of treatment programs has been to *cure* cancer using a multidisciplinary approach – combining surgery, radiotherapy and chemotherapy – directed at the primary tumor and potential metastases [20]. In recent years, molecular-targeted therapy and immunotherapy have expanded the cancer treatment arsenal in an effort to improve tumor control [21-23].

Surgery: As the earliest form of cancer therapy, surgery remains the mainstay for the treatment of most solid tumors. Surgery is most effective for localized tumors with well-defined borders. This is accomplished by resection of lesions encompassed by a continuous margin of healthy tissue and removal of associated lymph nodes [24, 25]. As such, surgery alone has a limited role in disease management in patients with advanced disease or in the presence of distant metastases.

Radiotherapy: Radiation therapy uses high-energy particles (e.g., x-rays, gamma rays or proton beams) guided by computed tomography to damage and destroy cancer cells [26-28]. When used to treat localized cancers, radiation therapy can provide a complete

response but only offers supportive care in advanced or disseminated disease [26, 28]. Neoadjuvant radiotherapy is frequently used to reduce tumor burden prior to surgery or in cases of incomplete surgical resection, postoperatively, to tackle residual disease and minimize tumor recurrence [29]. However, one of the fundamental problems of radiation oncology is tumor resistance to radiation doses which cause an acceptable degree of normal tissue toxicity, leading to locoregional control failure and disease progression [30, 31].

Chemotherapy: An aggressive form of chemical drug therapy, chemotherapy targets rapidly proliferating cells in the body [32, 33]. Chemotherapeutic drugs, classified according to their chemical composition and function, halt cell division. These include (1) alkylating agents, such as cyclophosamide and platinum based drugs, that intercalate with DNA resulting in DNA cross-links and single-strand DNA breaks [34, 35]; (2) antimetabolites, such as 5-fluorouracil, gemcitabine and methotrexate, which are structural analogs of folic acid, purines or pyrimidines that interfere with nucleic acid synthesis [36, 37]; (3) anthracyclines, such as doxorubicin, that inhibit the activity of DNA replication enzymes [38-40]; (4) plant alkaloids, such as taxanes and vinorelbine, that interfere with microtubule dynamics [41, 42] and (5) corticosteroids, such as prednisone and dexamethasone, that induce DNA fragmentation at high doses [43, 44]. These drugs disrupt core cellular processes to achieve systemic growth control of malignant cells. As such, chemotherapy remains the standard treatment modality for many advanced cancers, although it is not always curative as a stand-alone protocol. Often used in conjunction with surgery, chemotherapy acts to eradicate tumor cells that have already metastasized or in addition to radiotherapy, to sensitize malignant cells and enhance the cytotoxic effect of

radiation [32, 33]. However, chemotherapeutic drugs indiscriminately destroy replicating cells, normal (e.g., hair follicles, bone marrow, gastrointestinal epithelium, and immune) and cancerous alike, causing systemic toxicity and long-term health issues that adversely affect a patients' quality of life. Despite data supporting the survival benefit of chemotherapy, chemoresistance remains a major obstacle to successful treatment, leading to disease recurrence and metastases [45].

Targeted Therapy: Targeted therapies block the proliferation of cancer cells by interfering with specific molecules required for tumor development and growth. Although these molecules may be present in normal tissues, they are often mutated or overexpressed in tumors, representing promising therapeutic targets in the management of cancer [46, 47]. Pathways associated with these molecules can be inhibited at multiple levels: (1) neutralizing ligands; (2) occluding receptor-binding sites; (3) blocking intracellular receptor signaling; or (4) interfering with intracellular downstream molecules. Monoclonal antibodies and small molecule inhibitors are the two main approaches of specific molecular targeting available for use in clinical practice [48]. Monoclonal antibodies, which are usually large (~150 kDa) and water soluble, target extracellular components of these pathways while small molecule cancer drugs, because of their size (≤500 Da), can translocate through the plasma membrane and affect intracellular processes that play a key role in transducing downstream cell growth signaling [49-52]. Despite an explosion of information about the biological basis of cancer, identifying actionable alterations that drive cancer progression and thus define molecular targets remains a challenge for researchers [53]. Moreover, targeted therapies are only producing appreciable therapeutic

responses in a fraction of patients of a particular type, and even within a specific subtype. Some tumors, while envisioned to respond, instead continue to grow and progress to states of heightened malignancy [54-56].

Immunotherapy: Immunotherapies aim to exploit the therapeutic potential of tumor-specific antibodies and cellular immune effector mechanisms to restore the anti-tumor response of a patient's suppressed immune system [57, 58]. Immunotherapeutic agents currently in development, such as monoclonal antibodies, cancer vaccines, chimeric antigen receptor (CAR)-T-cell therapies and immune checkpoint inhibitors, are designed to (1) block negative regulatory signals that promote immune evasion of tumors; and (2) stimulate immunogenic pathways. Despite the successful application of cancer immunotherapies across a broad range of cancers, durable responses are only observed in a minority of patients with advanced disease [59, 60]. Besides, intravenous administration of immunotherapies believed to be essential for systematically regulating the immune response against disseminated tumors often result in debilitating toxicities [61-63]. These limitations, along with an incomplete understanding of the intricacies of immune regulation in cancer, the lack of predictive biomarkers, and the development of resistance to immunotherapies present formidable obstacles to treatment [64].

1.4. Tumor heterogeneity: A hurdle for cancer treatment

Tumor heterogeneity represents one of the greatest challenges to effective cancer treatment. The nonuniformity of cancer has long been appreciated, reflected most visibly in the widely divergent responses of histologically similar tumors to a given treatment

(interpatient heterogeneity) [65]. The extent of tumor heterogeneity is only beginning to be realized with the advent of novel sequencing technologies. The coexistence of different cancer cell subpopulations within a single tumor, described as intratumor heterogeneity [66-68], generates substantial complexity in cancer. Intratumor heterogeneity appears through different stages of tumor progression (temporal), varied locations within the tumor (spatial) as well as in response to cancer therapies [69-72]. This non-homogeneous mass of cells displays genetic, epigenetic and phenotypic diversity [73-76]. Illustrating this astounding heterogeneity, in one analysis of a single hepatocellular tumor, approximately the size of a golf ball, a sampling of 286 regions from a single slice of the tumor revealed more than 100 million coding region mutations [77]. Adding to that complexity are the increasing differences between primary tumors and metastatic foci (intrapatient heterogeneity). Metastatic lesions at secondary sites can arise from different cell populations within a single primary tumor, contributing to heterogeneity among metastases, and since metastatic lesions can acquire new mutations and evolve independently, variability within metastases can also exist [78]. Furthermore, the cellular environment surrounding a tumor, the tumor microenvironment (TME), composed of stromal (e.g., fibroblasts, adipocytes, endothelial cells etc.) and immune cells can be another source of heterogeneity. Mediated by chemokines, angiogenic factors, and cytokines, crosstalk between the tumor and non-malignant cells can alter both tumor and normal cell behavior, thereby influencing clinical outcomes [79, 80]. Overall, this measured heterogeneity reflects only a static snapshot of the cells within a continually evolving tumor and its environment. Ultimately, what emerges is a view of cancer as an extraordinarily diverse group of neoplastic cells in the context of a complex tumor

microenvironment that functions at various spatial and temporal scales, cooperating as a highly dynamic organ system. It is therefore not surprising that universally applied treatments, even in combination, lead to inconsistent therapeutic responses, residual or refractory disease, tumor recurrence and eventually treatment failure [81].

1.5. RENCA macrobead therapy

The chaotic, adaptive nature of cancer constitutes a compelling reason to explore a new paradigm that focuses on regulating cancer as a system. This approach requires shifting from a reductionistic framework that seeks to block specific pathways and destroy aberrant cells to a systems biological approach aimed at simultaneously controlling multiple levels of dysfunction. In other 'system' diseases, such as diabetes or cardiovascular disease, where multiple systems (e.g., endocrine, immune, neural and circulatory systems) interact to influence pathogenesis and prognosis, clinicians have demonstrated tremendous success in disease management by regulating various components of such systems to function in a normal physiological manner. Effectively treated as a lifelong condition, medications serve to control disease progression and improve quality of life. Similar to diabetes and cardiovascular disease, cancer may be able to be treated as a chronic, systems disease, wherein the growth and lifespan of cancer cells can be continually regulated, allowing patients to live with the disease. *Chronic*, according to the CDC, means controlled but not cured [82]. Although this terminology is as relevant for cancer as it is for heart disease or diabetes, current cancer treatment protocols are not sustainable – high toxicity and drug-related complications associated with existing therapies preclude long-term use. As a solution to the avoidance of such toxicities, a *biological-based system,* in which normal

physiology is continuously regulated, may provide a therapy that is capable of inhibiting cancer cell proliferation and thereby long-term growth control leading to tumor regression. As a biocompatible, cell-system anti-cancer therapy, RENCA macrobeads meet these requirements [1, 83-87].

What are RENCA macrobeads? RENCA macrobeads are mouse renal adenocarcinoma cells encapsulated in a double layer of agarose (6-8 mm in diameter) [1] (Figure 1A). Upon encapsulation, cells are uniformly distributed throughout the inner coat as single cells or small cell clusters. Over multiple weeks, cells proliferate, forming ellipsoid-shaped tumor colonies (Figure 1B). These colonies recapitulate many of the basic three-dimensional structures of tumors, including a multicellular framework, centralized necrosis, and proliferation gradients. In addition, RENCA macrobeads exhibit comparable growth kinetics as in vivo tumors [88-90]. Characterized by an exponential growth phase when macrobeads are young and colonies are small, growth decelerates as colonies within the macrobead enlarge [1], similar to proliferation plateaus experienced by large tumors in vivo [88, 90]. Colonies that have reached a maximal size in mature RENCA macrobeads remain stable indefinitely but exhibit continuous cell turnover, with cells positive for molecular markers of proliferation (e.g., PCNA, BrdU) or apoptosis (e.g., p27, caspase-3) [1]. The double-layer architecture of the agarose hydrogel provides key elements to RENCA macrobead structure, function and stability. The higher agarose concentration of the outer coat contributes to structural integrity as well as prevents tumor cell outgrowth from the macrobead. This structural feature also provides a physical barrier to protect encapsulated cells from direct interaction with host immune cells while the porous

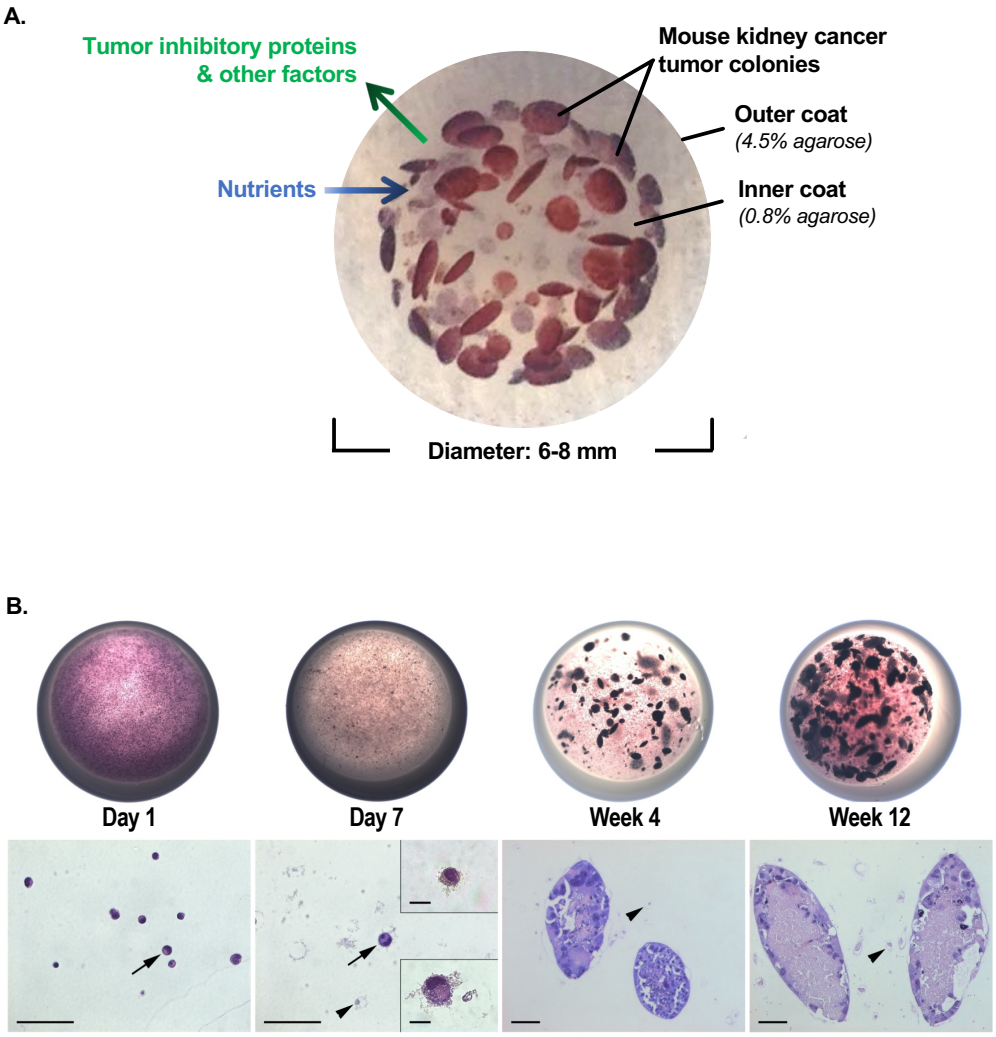

Figure 1: The RENCA macrobead. (A) Photograph of a RENCA macrobead stained with 0.33% (w/v) neutral red. RENCA macrobeads are an agarose matrix containing mouse renal adenocarcinoma cells. Macrobeads consist of two spherical layers of agarose with mouse RENCA cells contained within the inner coat. Each macrobead has a diameter of 6-8 mm. (B) Natural history of the RENCA macrobead. Macroscopic and microscopic appearances of day 1 through Wk. 12 RENCA macrobeads. Top, macroscopic photographs of RENCA macrobeads taken during an MTT assay demonstrate metabolically active cells and colonies (purple color) on day 1, Wk. 4, and Wk. 12 with a significant loss of metabolically active cells on day 7. Bottom, micrographs of H&E-stained sections of RENCA macrobeads demonstrating significant loss of day 1 encapsulated viable cells by day 7 in which two distinct types of cells survive (insets day 7) that produce ellipsoid tumor colonies that enlarge over time reaching a final size around 12 weeks of age. Arrows indicate viable cells and arrowheads denote cell debris. Scale bars for large micrographs are 50 μm and for insets at day 7 are 10 μm [1].

hydrogel allows sustained release of signals (e.g., peptides, proteins, exosomes, various forms of RNA) from growth-restricted tumor colonies [1, 85].

Safety and efficacy of RENCA macrobead therapy: In vitro studies have indicated that RENCA macrobeads (or macrobead conditioned media) inhibit the growth of various cancer cell lines, including mouse renal carcinoma (RENCA), osteosarcoma (K7M2), human prostate (DU145), bladder (J82) and colorectal cancer (HCT116) [85]. The anti-proliferative effect is dependent on the age of RENCA macrobeads. At early stages of development, young RENCA macrobeads (2-3 weeks post encapsulation) that have not formed tumor colonies do not inhibit the growth of external tumor cells. As macrobeads mature, their inhibitory capacity increases to approximately 50% at 24 weeks post-encapsulation and remains consistent for at least two years. Moreover, the observed inhibition is neither species nor tumor-type specific, although distinct cell lines are differentially inhibited by RENCA macrobead treatment [85].

Preclinical studies indicate that RENCA macrobeads are effective in reducing tumor burden in orthotopic murine models [85]. Mice with RENCA cells placed under the renal capsule had significantly smaller tumors (30-60%) following implantation of RENCA macrobeads into the peritoneal cavity as compared to control mice treated with empty macrobeads (double layer of agarose without cells). In companion cats and dogs with end-stage, spontaneous cancers, RENCA macrobead treatment also showed evidence of tumor growth control [85]. In cases of gastrointestinal lymphoma and mammary carcinoma, RENCA macrobead treatment prolonged survival following multiple implants. Maximum

growth control was observed in canines with prostatic adenocarcinoma. These dogs survived a median of 177 days from diagnosis as compared with no treatment (21-30 days), partial prostatectomy (<14 days for 7 out of 10 dogs), or total prostatectomy (<50 days, *n* = 10) [85]. Moreover, a majority of the animals demonstrated positive quality of life indicators, including an increased appetite, weight gain, higher activity and improved well-being [85].

Clinical data also supports the safety and efficacy of RENCA macrobead therapy in multiple tumor types. These patients are classified with Stage IV disease (metastatic cancer) and had failed all available, approved therapies prior to enrollment in RENCA macrobead trials [83, 84, 86, 87]. Only mild and transient treatment-related adverse events were observed in Phase I clinical trials which included patients with advanced, refractory peritoneal and thoracic cancers [87]. A decrease in the level of circulating tumor markers, carcinoembryonic antigen (CEA) and carbohydrate antigen (CA19-9), was noted in approximately 70% of treated patients regardless of cancer type. In addition, PET-CT measurements of tumor burden indicated suppression of metabolic activity and induction of peripheral necrosis [87]. Results from open-label Phase II clinical trials investigating RENCA macrobeads in patients with metastatic, treatment-resistant colorectal cancer (mCRC) also demonstrated decreased CEA and CA19-9 levels, stable to decreased tumor volumes, reduced uptake of ^{18}F-FDG, and stable levels of lactate dehydrogenase (LDH) in responders (R) as compared to non-responders (NR) [83, 84, 86]. Response to RENCA macrobead therapy correlated with increased overall survival (OS) (R mean OS = 10.76 months; NR mean OS = 4.9 months) and good quality of life scores [86]. While being safe

and effective in a wide variety of cancers, this data indicates that RENCA macrobead therapy offers a broad-spectrum treatment approach that provides a genuine benefit in clinical outcomes for cancer patients.

Exploring RENCA macrobead mechanism of action: RENCA macrobeads inhibit cell proliferation by inducing apoptosis following cell accumulation in S-phase [85]. Following culture in replete media (concentrated RENCA macrobead conditioned media brought up in fresh media), time-lapse microscopy studies indicated that fewer target tumor cells enter mitosis. Of the cells that entered mitosis, a significantly lower fraction (56%) successfully completed cell division while nearly all RENCA cells (>99%) in fresh media transitioned through mitosis. Mitotic failure resulted in cell death [85]. Culture in replete media also caused a delay in cell cycle time as compared to fresh media (30h vs. 24h) and induced S-phase arrest [85]. Gene expression profiles of target tumor cells exposed to replete media identified a prevalence of S-phase checkpoint genes with significant upregulation of transcripts associated with the DNA damage response (e.g., Gadd45, CHOP, Gas5, homologs of Chk2, etc.) [85]. Although this data suggests that RENCA macrobeads inhibit the growth of RENCA cells by inducing cell cycle checkpoint delays with upregulation of DNA damage surveillance and repair programs followed by abortion of the cell cycle and death via apoptosis, the molecular mechanism(s) of this inhibition remains unknown.

Communication between RENCA macrobeads and physically distant tumor cells is likely mediated through diverse mechanisms. As mediators of essential cellular processes, proteins facilitate intercellular communication, offering one avenue of research. Mass

spectrometry studies performed in our laboratory demonstrated that RENCA macrobeads release more than 700 proteins into their environment, many of which limit cancer cells' proliferative and survival advantages [85]. Given the large number of proteins secreted by RENCA macrobeads, predicting relevant signaling pathways involved in macrobead-mediated inhibition is challenging. Since extracellular stimuli regulate gene expression by controlling the activity of transcription factors, we utilized a 45-pathway reporter array to identify signaling pathway-associated transcriptional regulators responsive to factors secreted by RENCA macrobeads [91]. This study found increased activity of the transcription factor myocyte-enhancer factor 2 (MEF2) in target tumor cells in parallel to the antiproliferative effect of RENCA macrobeads.

Myocyte-enhancer factor 2

MEF2 proteins belong to the MADS (minichromosome maintenance genes (MCM1) – agamous (AG) – deficiens (DEFA) – serum response factor (SRF)) family of transcription factors [92, 93]. In vertebrates, MEF2 proteins are encoded by four genes – namely, MEF2A, MEF2B, MEF2C, and MEF2D which are expressed in distinct but overlapping patterns in tissues [94]. All MEF2 proteins share a highly conserved MADS-box and MEF2 domain in the N-terminus that mediate dimerization, DNA binding and co-factor interactions [95-97]. In contrast, the carboxy-terminus is structurally diverse amongst isoforms and features the transactivation domain which is subject to alternative splicing and covalent modifications, such as phosphorylation, acetylation, and sumoylation [95, 98, 99]. MEF2 responds to signals originating from multiple cell surface receptors, including G-protein coupled receptors [100], epidermal growth factor receptor (EGFR) [101-103],

the lipopolysaccharide receptor [104], as well as others. MEF2 proteins bind to the consensus DNA sequence (C/T)TA(A/T)$_4$TA(G/A) as homo- or heterodimers, thereby integrating extracellular signals into cellular processes by regulating a specific set of genes [95, 105-107].

Initially identified as key components of muscle cell differentiation, the activities of MEF2 are just beginning to be recognized in cancers [108-110]. However, their involvement is controversial – as MEF2 transcription factors interact with distinct co-factors and can be influenced by post-translational modifications, they have been described to function both as transcriptional activators or repressors in selective contexts and tissues.

Altered MEF2A expression associated with a proliferative phenotype in some cancers suggest a tumorigenic role for this isoform. In pancreatic cancer, a frequent *MEF2A* single nucleotide polymorphism (SNP) (Y105C) was considered a negative prognostic marker [111]. MEF2A protein levels are also frequently upregulated together with MEF2C in hepatocellular carcinoma as compared to levels in normal or cirrhotic livers [112]. Similar data is available for gastric cancer wherein 10% of patients are characterized by a significant increase in MEF2A mRNA. In gastric cancer cells, p38/MAPK signaling can activate MEF2A to promote glycolysis and proliferation [113]. In the same cells, MEF2A is described to have a tumor suppressive role. Activated MEF2A induced G0/G1 arrest and inhibited proliferation of NCI-N87 cells by inducing expression of p21 and decreasing cyclin D1 [114].

From a phylogenetic perspective, MEF2B is the most divergent of the MEF2 proteins [115]. *MEF2B* is amplified in a fraction of ovarian carcinomas, uterine cancers, adrenocortical carcinomas and esophageal cancers indicating that this isoform may act as an oncogene in these tumors [116-118]. Supporting a malignant phenotype, ectopically expressed MEF2B in HEK293A cells promoted cell migration and increased expression of the anti-apoptotic protein, Bcl2 [119]. Among MEF2B target genes is *BCL6*, an oncogene identified in B-cell lymphomas that influences expression of genes involved in the DNA damage response, cell cycle control and differentiation [120, 121]. As such, knockdown of MEF2B is associated with decreased cell cycle progression linked to G1 arrest [122] and has also been shown to diminish expression of DNA damage induced apoptosis suppressor (DDIAS), an anti-apoptotic protein that promotes cancer cell survival [123]. Moreover, *MEF2B* heterozygous somatic mutations were described in a small percentage of lymphomas, including diffuse large B-cell lymphomas (DLBCL), follicular lymphomas and mantle cell lymphomas [124-127]. In cells modeling common hotspot mutations identified in DLBCL, MEF2B transcriptional activity was increased and promoted cell migration and survival [119].

A role of *MEF2C* as an oncogene was initially suggested in leukemic cells. Increased *MEF2C* expression is characteristic of immature T-cell acute lymphoblastic leukemia [128]. Furthermore, MEF2C was described to act as a cooperating oncogene in combination with *Irf8* deficiency [129] or *Sox4* activation [130] to accelerate myeloid leukemia development. Myeloid leukemias demonstrated increased *MEF2C* expression and required elevated MEF2C levels to induce colony formation [131]. MEF2C also

promoted migration and invasion of leukemic cells [129]. Additional data supports a pro-oncogenic function of MEF2C in some solid tumors. In colorectal cancer, MEF2C levels were increased during disease progression [132]. MEF2C expression was also associated with tumor invasion of breast cancer [133]. Although MEF2C is overexpressed in hepatocellular carcinoma (HCC) [112, 134, 135], this isoform displays both oncogenic and tumor suppressive properties. MEF2C mediated VEGF-induced angiogenesis and promoted HCC invasion through p38/MAPK and PKC signaling while inhibiting cancer cell proliferation by blocking β-catenin nuclear translocation [135]. Supporting a tumor suppressive role, overexpression of MEF2C in rhabdomyosarcoma cells abrogated proliferation and anchorage-independent growth [136].

Early evidence for the involvement of MEF2D in tumorigenesis came from studies of childhood acute lymphoblastic leukemia (ALL). In ALL, chromosomal translocations involving MEF2D, although rare, were associated with increased proliferation and a worse prognosis [137, 138]. Several other reports have also supported an oncogenic role for MEF2D in different solid tumor models. High levels of MEF2D in HCC are associated with poor prognosis [139]. In these cells, MEF2D silencing limited proliferation and abolished tumorigenicity in mouse xenograft models [139]. In addition, elevated expression of MEF2D has been observed in lung cancer [140], gastric cancer [141], and pancreatic cancer models [142]. However, MEF2D has been described to have anti-proliferative functions in rhabdomyosarcomas, low grade uterine leiomyosarcomas and breast cancers [143-145]. Expression of exogenous MEF2D in rhabdomyosarcoma cell lines promoted differentiation, inhibited cell proliferation and limited cell migration [145].

In a model of rhabdomyosarcoma, MEF2D repression was linked to genes regulating cell cycle progression, namely *GADD45* and *CDKN1A* [146].

Studies in non-cancerous cells have also highlighted a role of MEF2 in cell cycle regulation. In multiple cell types, including myoblasts, fibroblasts and mammary epithelial cells, levels of specific MEF2 isoforms have been described to fluctuate during the cell cycle. In G1, S, and early G2 phases, MEF2C levels are high but sharply decline as cells progress from G2 to M phase [147]. Likewise, MEF2D levels remain relatively low following S phase through the G2/M transition and increase as cells exit the cell cycle [144, 148]. Stabilization of MEF2C inhibits nuclear accumulation of Cyclin B1 and impairs progression through mitosis [147]. Unscheduled MEF2 transcription during the cell cycle induces p21, a MEF2C and -D target gene that prompts growth arrest and reduces cell proliferation [148]. While no direct evidence for MEF2A expression during cell cycle progression has been reported, vascular myocytes display increased levels of MEF2A when induced to proliferate in serum [149]. Inhibition of MEF2A induces a G1 block followed by forced cell cycle reentry [150, 151] while increased levels of constitutively active MEF2A positively correlates with CHOP expression [152]. This protein participates in ER stress-induced and mitochondria-mediated apoptosis [153]. Accordingly, transcriptional regulation of homologous members of the MEF2 family could be a mechanism by which RENCA macrobeads coordinate cell cycle programs to mediate growth inhibition.

Transcriptional control can be modulated by signal transmission from the cell surface to the nucleus. Receptors span the interface of cells, facilitating communication between the

extracellular and intracellular environments. To gain insight into which cell surface receptors transduce RENCA macrobead protein signals into intracellular responses, we assessed the effect of RENCA macrobead conditioned media on the activity of a panel of transmembrane receptors, comparing young vs. mature RENCA macrobeads (none vs. partial inhibition). In our preliminary studies, total and phosphorylated levels of EGFR positively correlated with increased growth inhibition of RENCA cells.

Epidermal growth factor receptor

EGFR, also known as ErbB1/HER1, is a N-linked glycosylated membrane bound receptor tyrosine kinase (RTK) that belongs to the ErbB receptor family [154]. EGFR was originally characterized as an oncogene, due to its homology to v-ErbB, a retroviral protein that enables avian erythroblastosis virus to transform chicken erythroblasts [155]. Subsequent research reporting *EGFR* gene amplification and hyperactivity in multiple malignancies cemented EGFR signaling as a driver of oncogenesis [156, 157]. As such, pharmacological inhibition of EGFR has been a topic of intense research for several decades. Yet, other studies have featured a paradoxical growth inhibitory property of EGFR activation [158-163]. For example, multiple cell lines, such as epidermoid carcinoma (A431), non-small cell lung carcinoma (A549), and basal-like breast cancer cells (MDA-MB-468), undergo apoptosis following exposure to high doses of EGF [164-172]. Data has shown that the observed apoptosis requires an active tyrosine kinase [167, 168]. Decreasing EGFR phosphorylation with a tyrosine kinase inhibitor increased cell viability compared to EGF treated cells [167].

However, there is no consensus as to the mechanism by which EGFR activation limits cell growth and promotes apoptosis. Astuti et al. demonstrated that EGF stimulates the MAPK pathway and blocks exit from G2 checkpoint arrest by destabilizing cdc25, the phosphatase responsible for activating CDKs [173]. EGF has also been shown to promote de novo synthesis of the cyclin-dependent kinase inhibitor, p21 via activation of Stat1/Stat3. Depending on the study, Stat-mediated p21 expression delays progression through G2/M phase [174-176] or induces apoptosis [177, 178]. Subsequent research has provided evidence that Etk/Bmx, a member of the Tec family of tyrosine kinases, potentiated EGF-induced Stat1 activation [179]. Other groups have linked EGFR-mediated cellular toxicity to intracellular Ca^{2+} overload. In breast cancer cells, elevated cytoplasmic Ca^{2+} levels triggered by EGFR activation contributes to oxidative stress and mitochondria-mediated apoptosis via p38/JNK activation [180]. This is associated with increased expression of the pro-apoptotic proteins CHOP and Bim [180]. A similar effect was observed in xenografted NSCLC tumors treated with EGF. EGF-injected A549 tumors were significantly smaller than controls and exhibited reduced proliferation rates as evidenced by decreased $Ki67^{+}$ cells [172]. Moreover, markers of mitochondrial dysfunction (e.g., Rac1, $p22^{phox}$, Ref-1) were higher in tumor tissues from EGF-treated mice as compared to PBS-treated controls [172].

Synthesized as a 1210 residue precursor that is cleaved at the N-terminus to form a 1186 residue mature transmembrane protein [154], EGFR consists of an extracellular ligand-binding region, a single membrane-spanning a-helix and a cytoplasmic tyrosine kinase C-terminal domain [181]. EGFR functions to sense and respond to extracellular signals.

Binding of soluble ligands to the EGFR ectodomain promotes homo- or heterodimer formation, with a stoichiometry of 2:2 ligand:receptor [182, 183], activation of the kinase domain and autophosphorylation of multiple tyrosine residues in the cytoplasmic tail [184-186]. In addition, ligand-receptor interactions induce EGFR internalization and intracellular sorting to vesicular transport systems that recycle receptors to the cell surface or direct internalized EGFR to lysosomes for degradation [187-190]. EGFR binds at least seven different activating ligands: EGF, transforming growth factor-α (TGFα), amphiregulin (ARG), betacellulin (BTC), heparin-binding EGF-like growth factor (HB-EGF), epiregulin (EPR), and epigen (EGN) [191]. EGFR activation initiates multiple intracellular signaling pathways, including the MAPK, PI3K, SRC, PLC-γ, JNK, and JAK-STAT pathways [192-194]. These pathways, which are estimated to encompass 122 proteins, are interlinked at the molecular level [195]. As such, the activation of EGFR stimulates a complex, integrated signaling network, producing a diverse repertoire of biological responses [196]. Adding to this signaling diversity, EGF-like sequences present in other proteins can also activate EGFR [197-199]. These EGF motif-containing ligands can directly bind the receptor or transactivate EGFR through crosstalk with heterologous receptors [200-202]. For example, reticulon-4 (RTN4), thrombospondin-1 (TSP1), and tissue inhibitor of metalloproteinase-2 (TIMP2) have been shown to regulate EGFR activity. These proteins, identified in conditioned media of RENCA macrobeads at different stages of development, have been described to suppress tumor growth in diverse contexts and may participate in RENCA macrobead-mediated growth inhibition of target tumor cells.

Reticulon-4 (RTN4)

RTN4 is a highly conserved member of the reticulon family of proteins predominantly associated with the smooth endoplasmic reticulum (ER) [203-205]. RTN4 functions to establish ER membrane curvature [206-208] and vesicle formation [203]. In addition to defining the architecture of lipid membranes, the best studied function of RTN4 is inhibiting neurite outgrowth and axonal regeneration following spinal cord injury [209-216]. Evidence also points to the involvement of RTN4 in the progression of glioma [217] and prostate cancer cell lines [218]. In these studies, RTN4 overexpression slowed proliferation and induced cell cycle arrest. In addition, recent studies have reported a role for RTN4 in inducing apoptosis in neural systems [219-221], atherosclerotic models [222] and multiple cancer cell lines [223]. In Hela cells, RTN4 has been shown to contribute to endoplasmic stress-mediated apoptosis triggered by depletion of ER Ca^{2+} stores and upregulation of pro-apoptotic transcription factors [224]. Stable overexpression of RTN4 in a neuroblastoma model upregulated activated caspase-3 and Bax, a pro-apoptotic member of the Bcl-2 family that promotes loss of mitochondrial membrane potential [225]. RTN4 has also been shown to associate with the anti-apoptotic proteins Bcl-2 and Bcl-X_L and alter their sub-cellular localization, thereby reducing their anti-apoptotic activity [226].

RTN4 preferentially interacts with the RTN4 receptor (RTN4R) [227]. However, RTN4 receptors lack a transmembrane and signaling domain, thereby requiring a co-receptor or signal transducer to transmit intracellular messages. The transmembrane protein LINGO-1, the neurotrophin receptor p75, and the orphan tumor necrosis factor family member TAJ/TROY have all been shown to bind RTN4R and facilitate inhibition of neurite

outgrowth [228-233]. Epidermal growth factor receptor acts a signal transducer for RTN4R. While EGFR does not directly bind RTN4R, the kinase activity of EGFR has been shown to be required for the inhibitory action of RTN4 in neuronal cultures [234].

Thrombospondin-1 (TSP1)

TSP1 is an extracellular matrix molecule that belongs to a family of homologous glycoproteins with diverse effects on cell behavior [235, 236]. Disruption of the *thbs1* gene in mice results in craniofacial dysmorphism, spinal deformity, exaggerated inflammatory responses, and altered rates of wound healing and tissue remodeling in various injury models [237-240]. The role of TSP1 in cancer growth control is controversial, as it exerts complex and sometimes opposing effects. For example, TSP1 is overexpressed by invasive and metastatic melanoma cells, in which it actively contributes to epithelial-to-mesenchymal transition [241, 242]. On the contrary, suppression of *THBS1* expression in metastatic clones of several tumor cell lines suggested that loss of TSP1 expression may contribute to tumor progression [243]. Evidence indicates that overexpression of TSP1 in breast cancer cells, intestinal carcinoma, renal cell carcinoma, a transformed endothelial cell line, and glioblastoma cells decreases tumor growth in animal models [244-249]. In these contexts, it has been suggested that anti-angiogenic activity is the major mechanism for tumor growth suppression in vivo wherein TSP1 antagonizes growth factor-stimulated proliferation of endothelial cells and regulates vascular endothelial growth factor bioavailability and activity [243, 250, 251]. However, high doses of exogenous TSP1 and TSP1 peptide mimetics have demonstrated direct inhibition of breast cancer cell proliferation in vitro [252].

The diverse effects of TSP1 have been linked to specific epitopes in the multi-domain molecule. As a homo-trimeric thrombospondin, TSP1 is formed by globular domains at the N- and C-terminals. The TSP1 core contains three properdin-like type I repeats, three epidermal growth factor (EGF)-like type II repeats and a series of calcium-binding-wire-type III repeats [253, 254]. Although not all TSP1 domains have ascribed cognate cell surface receptors, the array of identified TSP1 receptors are extremely diverse. TSP1 has been described to recognize integrins, proteoglycans and glycolipids among others [255-258]. TSP1 directly engages CD36 and CD47 on endothelial cells to promote apoptosis and functions related to angiogenesis [259]. TSP1 also indirectly influences the activity and bioavailability of various mediators of angiogenesis. For example, TSP1 has the ability to activate TGFβ, a signal critical for the stability of microvasculature [260]. Recent studies have added EGFR to the numerous signaling partners of TSP1. Although TSP1 does not directly bind to EGFR, the EGF-like type II repeats of TSP1 promote EGFR tyrosine phosphorylation and downstream signaling by an indirect mechanism involving matrix metalloproteinases [261].

Tissue inhibitor of metalloproteinase-2 (TIMP2)

TIMP2, a member of the tissue inhibitor of metalloproteinase family, regulates the proteolytic activity of matrix metalloproteinases (MMPs) [262]. Consequently, TIMP2 affects extracellular matrix (ECM) turnover, tissue remodeling and cellular behavior [262]. Independent of MMP inhibition, TIMP2 also influences cell growth, angiogenesis and apoptosis in a context-dependent manner [262, 263]. TIMP2 induces G1 growth arrest in

endothelial cells through de novo synthesis of the cyclin dependent kinase inhibitor p27, resulting in inhibition of cyclin dependent kinase 2 (CDK2) and CDK4 [264, 265]. TIMP2 also promotes cell cycle arrest of post-mitotic neurons through increased production of cyclin dependent kinase inhibitor, p21 and decreased expression of cyclins B and D [266]. Evidence has shown that exogenous TIMP2 enhances stabilization and activation of death receptors such as TNF and Fas in metastatic colorectal cancer [267-270]. TIMP2 overexpression also exerts direct cytotoxic effects in hepatocellular carcinoma and osteosarcoma models [271-273] wherein the pro-apoptotic effect was associated with decreased expression of Bcl-2 and elevated levels of Bax, cleaved caspase-3 and cleaved caspase-9 [271].

Cell surface binding of TIMP2 to distinct sites on MMPs generally regulates ECM degradation [274-276]. The interaction of TIMP2 to MMPs is enhanced by integrins, specifically $\alpha_v\beta_3$ and $\alpha_3\beta_1$ [277], which also modulate phosphatase activity and related interactions with tyrosine kinase receptors such as FGFR1, IGF-R1, VEGFR2 and EGFR [278-281]. In these contexts, TIMP2 indirectly suppresses growth-factor mediated mitogenic signaling by short-circuiting tyrosine kinase receptor activation [278-281].

1.6. Specific Aims

This study aims to elucidate molecular mechanism(s) underlying RENCA macrobead-mediated growth regulation of target tumor cells. Specifically, this work evaluates distinct RENCA macrobead-secreted proteins, the contribution of EGFR signaling as well as the requirement of MEF2 in mediating the inhibitory response of RENCA macrobeads.

Mechanistic insight may help stratify future clinical trials to focus on patients more likely to respond to RENCA macrobead therapy. Identification of relevant tumor-inhibitory proteins may also allow for the development of additional assays to quantitatively evaluate the functionality and efficacy of RENCA macrobeads prior to therapy. In the long-term, information about the mode of action may reveal methods to potentiate the action of RENCA macrobeads as well as expose novel vulnerabilities in tumor cells.

Our *central hypothesis* is that RENCA macrobeads release proteins that interact with the cell-surface receptor EGFR and ultimately change MEF2 expression in order to restrict the growth of external tumor cells (Figure 2).

In Aim 1, we test the hypothesis that RENCA macrobeads promote growth arrest through regulation of MEF2 expression. 1.1) Assess whether RENCA macrobead exposure alters MEF2 transcript levels in target tumor cells. 1.2) Determine if MEF2 expression in target cells is required for RENCA macrobead-mediated growth inhibition, and 1.3) whether the depletion of MEF2 isoforms in target tumor cells alters cell-cycle distribution in the presence of RENCA macrobeads.

In Aim 2, we test the hypothesis that signaling through EGFR correlates with RENCA macrobead-induced growth arrest and inhibition. 2.1) Assess the effect of RENCA macrobead conditioned media on EGFR abundance and activity in target tumor cells. 2.2) Determine whether RENCA macrobead-induced MEF2 activity is associated with EGFR

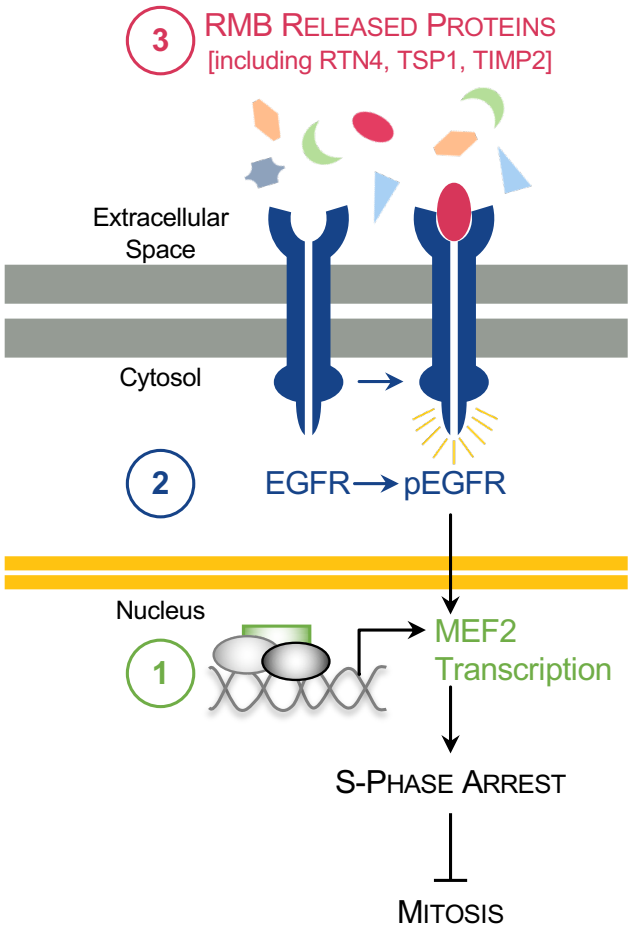

Figure 2: Proposed model of RENCA macrobead-mediated inhibition. This thesis tests the central hypothesis that RENCA macrobeads release proteins that interact with the cell-surface receptor EGFR and ultimately change MEF2 expression in order to restrict the growth of external tumor cells. The numbering refers to the three specific aims that were pursued in this work.

expression. 2.3) Evaluate the relationship between RENCA macrobead-mediated EGFR phosphorylation and growth of target tumor cells, and 2.4) assess whether RENCA macrobead-induced S-phase accumulation is linked to cellular EGFR levels.

In Aim 3, we test the hypothesis that RTN4, TSP1 and TIMP2, identified in the RENCA macrobead secretome, inhibit growth of target tumor cells. 3.1) Validate and quantify levels of RTN4, TSP1 and TIMP2 in RENCA macrobead conditioned media. 3.2) Assess EGFR status, MEF2 reporter activity and MEF2 isoform expression in the presence or absence of identified proteins, and 3.3) determine the functional impact of individual proteins on growth of target tumor cells.

CHAPTER 2: MATERIALS AND METHODS

2.1. Cell lines

The RENCA tumor cell line used for these experiments is a renal cortical adenocarcinoma that arose spontaneously in Balb/c mice, originally obtained from the National Cancer Institute (Bethesda, MD) and now available from ATCC (American Type Culture Collection, Manassas, VA, CRL-2947). RENCA cells were maintained in RPMI 1640 (Life Technologies, Carlsbad, CA) with 10% newborn calf serum (NCS; Life Technologies). The human prostate carcinoma cell line, DU145, originally obtained from ATCC (HTB-81) was cultured in RPMI 1640 supplemented with 10% fetal bovine serum (FBS; Life Technologies). The human breast adenocarcinoma MCF7 is an adherent, epithelial luminal cell line obtained from ATCC (HTB-22) and cultured in Minimum Essential Medium (MEM) with Earle's salts (Sigma-Aldrich, St. Louis, MO) supplemented with 10% FBS, 2 mM L-glutamine (Sigma-Aldrich) and 0.01 mg/mL bovine insulin (Sigma-Aldrich). MDA-MB-231 is a highly aggressive, basal-like, triple-negative breast cancer cell line, also obtained from ATCC (HTB-26), and cultured in RPMI 1640 supplemented with 10% FBS and 2 mM L-glutamine. In Aim 3, for assays related to RENCA macrobead secreted proteins, 5% serum was used for cell culture with no impact on cell growth or viability. All cell lines were maintained in tissue culture flasks at 37 °C in 5% CO_2 + air. Cell passages were limited to no more than 20 from a frozen stock of these cells unless otherwise indicated. Routine testing for *Mycoplasma* contamination has been consistently negative (Bionique Testing Laboratories, Saranac Lake, NY).

2.2. Generation of a gefitinib-resistant cell line

Gefitinib (*N*-(3-chloro-4-fluoro-phenyl)-7-methoxy-6-(3-morpholin-4-ylpropoxy) quinazolin-4-amine) was purchased from Tocris (Minneapolis, MN). The gefitinib-resistant subline (DU145/GRS) was established by culturing parental DU145 cells with incrementally increasing gefitinib concentrations from 1 μM to 3 μM over 6 months. DU145 cells were continuously maintained in gefitinib, with treatments beginning at the initial IC_{50} of the DU145 parental line [282]. Following recovery of doubling time compared to the parental DU145 cell line, the concentration of gefitinib was increased by 0.5 μM in DU145 culture media at each incremental step until gefitinib concentration was maximal at 3 μM. A second gefitinib-resistant subline (DU145/GRC) was generated by continuously culturing parental DU145 cells in high-dose (3 μM) gefitinib. Assessment of resistance to gefitinib was performed every 4 passages for the first 12 passages and every passage thereafter. DU145/GRS and DU145/GRC exhibited a 21.4 and 6.5-fold increase, respectively, in resistance to the growth-inhibitory effect of gefitinib as determined by MTT assay (Appendix A: Supplementary Figure 1A). The resistant phenotype had been stable for at least 6 passages under drug-free conditions prior to use in experiments. Since DU145/GRS cells exhibited substantially higher resistance to gefitinib, these cells were used in subsequent studies and were hereafter designated DU145/GR. Parental DU145 cells that did not receive treatment were passaged alongside treated cells and were used at equivalent passage numbers.

2.3. RENCA macrobeads

RENCA macrobeads were prepared as previously described [85, 283]. Briefly, 1.5×10^5 RENCA cells were mixed with 100 µL of 0.8% low-viscosity agarose (HSB-LV; Lonza Copenhagen ApS, Vallensbak Strand) in MEM (Sigma-Aldrich) and expelled into mineral oil to form the core of the macrobead. Following washing with RPMI 1640, the core was rolled in approximately 1 mL of 4.5% agarose to apply an outer coat. RENCA macrobeads were cultured in 90-mm Petri dishes at 10 macrobeads per 40 mL of RPMI 1640 supplemented with 10% NCS for use with RENCA cells; RPMI 1640 supplemented with 10% FBS for assays using DU145 or DU145-derivative cells; MEM with Earle's salts supplemented with 10% FBS, 2 mM L-glutamine and 0.01 mg/mL bovine insulin for use with MCF7 cells or RPMI 1640 supplemented with 10% FBS and 2 mM L-glutamine for experiments involving MDA-MB-231 cells. As described previously, for assays related to RENCA macrobead secreted proteins, 5% serum was used for macrobead culture without significant impact on metabolic activity or functionality. Conditioned media was collected after 5 days of culture with RENCA macrobeads. Medium was refreshed weekly. RENCA macrobeads used in experiments were categorized by age as young (1-3 weeks post-encapsulation) or mature (greater than 18 weeks post-encapsulation) macrobeads.

2.4. Concentration of RENCA macrobead conditioned media

RENCA macrobead conditioned media was initially concentrated by culturing 40 macrobeads in 40 mL of RPMI 1640 supplemented with 5% NCS or FBS for 7 days. Conditioned media was further concentrated by centrifugation at 3,000 × g at 4 °C using the Macrosep Advance CFD, 3K MWCO (Pall Corporation, Michigan, ND) to convert an

initial volume of 40 mL to a final volume of 1 mL of concentrated conditioned media. For immunodepletion studies, 5 mL of naïve media containing protein eluate or conditioned media, cultured at a ratio of 4 mL media per bead, was concentrated to 0.3 mL using a Microsep Advance CFD, 3K MWCO (Pall Corporation). Concentrated media was stored at -80 °C until further analysis. Total protein levels in concentrated conditioned media was determined via Pierce BCA test (Thermo Scientific, Waltham, MA).

2.5. Enzyme-linked immunosorbent assay

The concentration of RTN4, TSP1 and TIMP2 proteins in culture media was determined using commercially available ELISAs (RayBiotech, Peachtree Corners, GA) as per the manufacturer's instructions. Briefly, duplicate aliquots (100 μL per well) of standard protein and concentrated conditioned media were added to pre-coated 96-well ELISA plates. Following a 2.5 h incubation at room temperature (RT), unbound materials were washed away, and biotinylated detection antibody (anti-RTN4, anti-TSP1, or anti-TIMP2) was added to each well. Plates were incubated for 1 h at RT, followed by a wash step and incubation with HRP-conjugated streptavidin solution for 45 min at RT. After a final wash step, color development was observed following addition of 3,3,5,5'-tetramethylbenzidine (TMB) one-step substrate solution in the dark for 30-40 minutes at RT. The reaction was stopped by adding 50 μL per well 0.2 M sulfuric acid (stop solution). Optical density (OD) was measured at 450 nm using a microplate reader (BioTek Model ELx800 or Synergy 2, Winooski,VT). Sample concentrations (ng/mL) were determined based on standard concentration curves and normalized to total protein content (ng/mg).

2.6. Depletion of RTN4, TSP1 or TIMP2 using Protein A magnetic beads

RTN4, TSP1 or TIMP2 were immunoprecipitated from RENCA macrobead conditioned media with PureProteome Protein A magnetic beads (Millipore, St. Louis, MO, LSKMAGA10) and protein specific antibodies against RTN4 (13401), TSP1 (D7E5F; 37879), TIMP2 (D18B7; 5738) (Cell Signaling Technology, Danvers, MA) or Rb IgG isotype control antibody (Abcam, Cambridge, MA, ab37415). RENCA macrobeads were cultured in RPMI 1640 supplemented with 5% NCS or FBS at a ratio of 4 mL media per bead for 5 days. Twenty-four hours prior to media collection, capture antibodies for RTN4, TSP1, TIMP2 or Rb IgG isotype control were added to RENCA macrobead culture. The following day, media containing pre-formed antibody-antigen complexes were added to 500 μL washed Protein A magnetic beads and incubated for 30 min at RT with continuous mixing. Following incubation, conical tubes were placed in a PureProteome magnetic stand (Millipore) and bead-free media was transferred to a fresh conical tube. This procedure was repeated two additional times to ensure complete removal of magnetic beads. Aliquots of conditioned media individually depleted of RTN4, TSP1 or TIMP2 were used the same day for cell growth or gene expression assays, reporter assays and in-cell western analysis or concentrated as described previously and stored at -80 °C until further analysis. Beads coupled to the antibody-antigen complex were washed 5 times with PBS containing 0.1% Tween-20 (Sigma-Aldrich) and eluted 3 times with 450 μL 0.1 M glycine (pH 2.7) (Teknova, Hollister, CA). Eluate was neutralized with 150 μL 1 M Tris (pH 8.5) (Teknova) for a final volume of 1.5 mL. Each eluate containing RTN4, TSP1 or TIMP2 was combined with RPMI 1640 supplemented with 5% NCS or FBS and aliquots were used as described above. Immunodepletion was confirmed by ELISA.

2.7. In-cell western analysis

RENCA (90,000/cm^2), DU145 (150,000/cm^2), DU145/GR (150,000/cm^2), MCF7 (120,000/cm^2), or MDA-MB-231 (120,000/cm^2) cells were seeded in 96-well black, clear-bottom tissue culture-treated microplates, allowed to attach overnight, and synchronized using serum starvation. For time course studies, cells were incubated with indicated media for 0, 5, 15, 30, 60 (1 h), 360 (6 h), 960 (16 h), or 1440 (24 h) minutes. In all other cases, indicated media was added to cells for 30 min, followed by pre-fixation in 2% paraformaldehyde (PFA; EMS, Hatfield, PA) for 10 min and fixation in 4% PFA for an additional 20 min at RT. The cells were permeabilized with 0.1% Triton X-100 in TBS (Sigma-Aldrich) followed by incubation in Odyssey Blocking Buffer™ (LI-COR Biosciences, Lincoln, NE) for 90 min at RT with gentle agitation. Cells were double stained with mouse monoclonal IgG antibody against EGFR (E-8) (SCBT, Dallas, TX) together with rabbit monoclonal IgG antibody against phosphorylated EGFR Tyr-1068 (EP774Y) (Millipore) diluted in blocking buffer at 4 °C overnight. In wells designated as no primary antibody controls, blocking buffer was added during the primary antibody incubation. Cells were washed with 0.1% Tween-20 in TBS (Sigma-Aldrich) and stained with donkey anti-mouse IgG IRDye™ 800CW and donkey anti-rabbit IgG IRDye™ 680RD (LI-COR Biosciences) for 1 h at RT protected from light. CellTag™ 700 (LI-COR Biosciences) was used for cell number normalization. Images of target molecule fluorescence were obtained using the Odyssey Infrared Imaging System (LI-COR Biosciences). Integrated intensities of fluorescence in each well were quantified following subtraction of the average IR signal from wells designated as no primary antibody controls.

2.8. Cignal MEF2 reporter assay

For the Cignal MEF2 reporter assay (Qiagen, Valencia, CA), RENCA (10,000), DU145 (40,000), DU145/GR (40,000), MCF7 (25,000), or MDA-MB-231 (25,000) cells were reverse transfected with MEF2 transcription factor-responsive luciferase reporters or control constructs using Lipofectamine 2000 or 3000 (Life Technologies). Transiently transfected cells were incubated with indicated media for 24h. Regulation of the MEF2 reporter was measured using the dual-luciferase reporter assay (Promega, Madison, WI) on a Synergy 2 microplate reader (Bio-Tek). Luminescence values for the MEF2 reporter signal (firefly luciferase, FL) and the internal control signal (Renilla luciferase, RL) were expressed as ratios (FL/RL) to correct for variations in transfection efficiency and cell number. Fold change in relative luciferase units (RLUs) was calculated based on normalized luciferase activity.

2.9. RNA isolation and qRT-PCR

Total RNA was isolated from RENCA, DU145, DU145/GR, MCF7 and MDA-MB-231 cells cultured under the indicated conditions. RNA was extracted using a RNeasy mini kit followed by genomic DNA elimination with RNase-Free DNase (Qiagen) according to manufacturer's recommendations. RNA concentration and quality were determined using the Agilent 2100 RNA Bioanalyzer with the Agilent 6000 Nano Kit (Agilent Technologies, Santa Clara, CA). To confirm RNA quality, electropherograms were evaluated where purified RNA had an RNA Integrity Number (RIN) between 9.2 and 10. For quantitative real-time PCR (qRT-PCR), RNA (500 ng) was reverse transcribed using the RT^2 First

Strand Kit (Qiagen). Synthesized cDNA (20 ng) was combined with 2X TaqMan® Gene Expression Master Mix, 250 nM 6- FAM™ dye labeled TaqMan® MGB probe, and 900 nM each of forward and reverse unlabeled primers for *MEF2a/A*, *MEF2b/B*, *MEF2c/C*, *MEF2d/D*, and the housekeeping genes, *Gapdh/GAPDH* and *Tbp/TBP* (IDT, Coralville, IA). The primer and probe sequences used in this study are included in Appendix A: Supplementary Tables 1A and 1B for samples of mouse and human origin respectively. Each reaction was initially incubated at 50 °C for 2 min and 95 °C for 10 min followed by 40 cycles of denaturation at 95 °C for 15 s, annealing and extension at 60 °C for 1 min. Real time and endpoint fluorescence data was collected with an Eppendorf Mastercycler ep realplex 4 s (Eppendorf, Hamburg, Germany). Analysis was performed using the comparative $\Delta\Delta C_t$ method [284].

2.10. Cell proliferation assays

Cell proliferation of RENCA, DU145, DU145/GR, MCF7 and MDA-MB-231 cells cultured under the indicated conditions were measured by trypan blue exclusion assay or as previously described [85, 285]. RENCA (1,560/cm^2), DU145 (3,125/cm^2), DU145/GR (3,125/cm^2), MCF7 (7,810/cm^2), or MDA-MB-231 (7,810/cm^2) cells were seeded in 6-well plates, allowed to attach overnight, and cultured with or without RENCA macrobeads suspended in cell culture inserts (BD Biosciences, Franklin Lakes, NJ). Alternatively, cells were seeded in 12-well plates at the same densities with conditioned media depleted of RTN4, TSP1, or TIMP2 or fresh media containing RTN4, TSP1, or TIMP2 eluates and related controls. Following a 5-day incubation period, cells were harvested by TrypLE™ (Gibco, Carlsbad, CA) dissociation, stained with 0.2% trypan blue solution (Sigma-

Aldrich) and counted with a hemocytometer. In an alternate technique, cells were methanol-fixed and stained with 0.33% (w/v) neutral red (Sigma-Aldrich). The stain was extracted in 1.25% (w/v) sodium dodecyl sulfate (Life Technologies) and absorbance read at 540 nm with 630 nm as the reference wavelength.

2.11. Flow cytometry analysis

To evaluate cell cycle distribution, cells were harvested by TrypLE™ (Gibco, Carlsbad, CA) dissociation, washed in cold PBS, fixed in ice-cold 66% ethanol and incubated at 4 °C for 24 h. Fixed cells were equilibrated to RT, washed in PBS and resuspended in 400 μL PBS containing 20 μg propidium iodide and 220U RNaseA (Abcam). Cells were run, gated and analyzed using an Accuri C6 flow cytometer (BD Biosciences). Histograms were generated using the FCS express 4 software (De Novo Software, Glendale, CA).

2.12. Gene silencing of MEF2 isoforms

Accell SMARTpool™ siRNA constructs for knockdown of *MEF2a/A*, *MEF2b*, *MEF2C* or *MEF2d/D*, and Accell non-targeting control siRNA were purchased from Dharmacon (Lafayette, CO). RENCA (2,000/cm^2) or DU145 (4,000/cm^2) cells were seeded in 12-well plates, allowed to attach overnight, and incubated with 1 μM siRNA in Accell delivery media for 72 h. Media and siRNA were replenished for an additional 72-h period to maximize gene knockdown. Knockdown was confirmed by qRT-PCR.

2.13. Statistical analysis

Independent-sample two-tailed *t* tests for equal variance were performed to test for significant differences between experimental groups and controls. Differences were considered statistically significant at $p < 0.05$. All data was generated from a minimum of three independent experiments and expressed as mean ± SD.

CHAPTER 3: RESULTS

3.1. Mature RENCA macrobeads modulate MEF2 transcript levels.

Since differential regulation of MEF2 isoforms during the cell cycle impacts proliferation and survival decisions [144, 145, 147, 148, 150, 151], we sought to determine whether factors released by RENCA macrobeads alter the expression of MEF2 in target tumor cells. Using qRT-PCR, we measured MEF2 isoform transcript levels in RENCA and DU145 cells cultured in naïve media or together with young or mature RENCA macrobeads. RENCA cells were used because the growth inhibitory capacity of RENCA macrobeads throughout development is routinely assessed using these cells as targets. Moreover, early mechanistic studies were performed in RENCA cells, making this cell line an ideal candidate to evaluate MEF2 involvement in RENCA macrobead-mediated growth inhibition. RENCA macrobeads have also been investigated in clinical trials as a treatment for prostate malignancies [87]. Therefore, the DU145 cell line was included in these experiments as a model of human prostate cancer. Since our previous studies have shown that RENCA macrobeads inhibit tumor cell proliferation with neither species nor tumor-type specificity, studies in both the murine RENCA and human DU145 cells will help determine whether RENCA macrobead regulation of the transcription factor MEF2 is conserved amongst species.

In RENCA cells, *MEF2a* expression was comparable between naïve media and different ages of RENCA macrobeads (Figure 3A). However, following exposure to mature but not

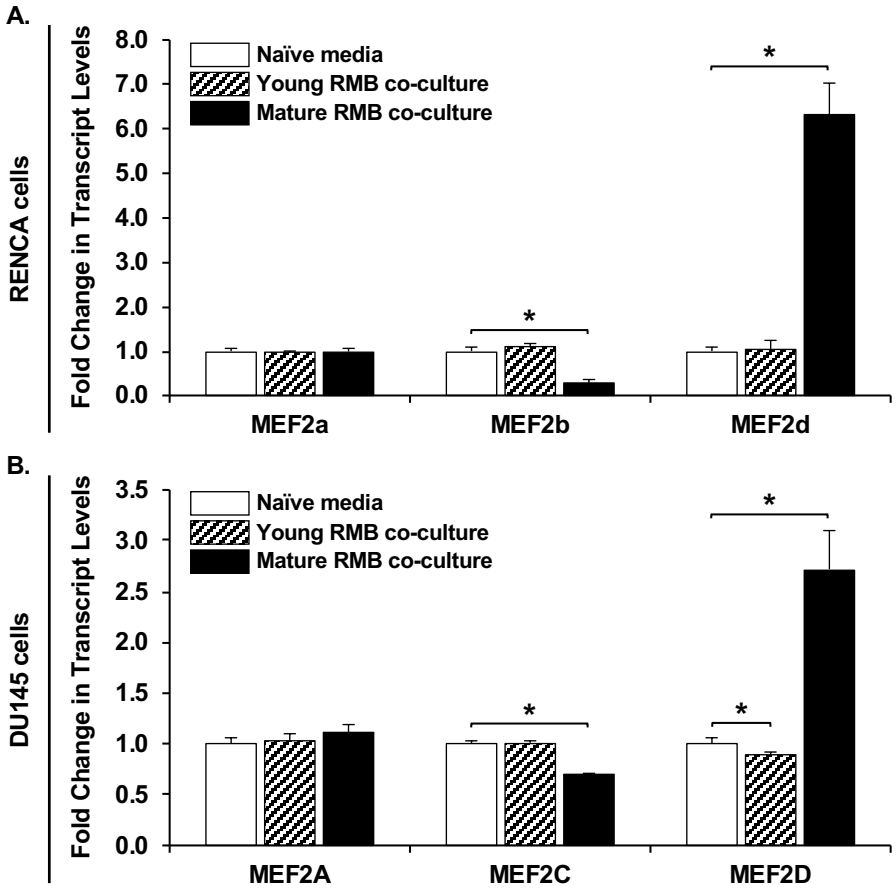

Figure 3: Mature RENCA macrobeads modulate MEF2 transcript levels. MEF2 isoform transcript levels were analyzed using Taqman based qRT-PCR in (A) RENCA, and (B) DU145 cells following culture in naïve media, or co-culture with young or mature RENCA macrobeads (RMB) for 5 days. *p-value < 0.05 relative to naïve media.

young RENCA macrobeads, *MEF2b* expression was reduced by 3.90-fold while *MEF2d* transcript levels significantly increased (6.30-fold) (Figure 3A). *MEF2c* transcripts were not detected in RENCA cells. In DU145 cells, *MEF2A* expression was also similar following culture in naïve media or different ages of RENCA macrobeads (Figure 3B). *MEF2C* transcript levels were significantly reduced (1.44-fold) in the presence of mature RENCA macrobeads but unaffected by co-culture with young RENCA macrobeads. Additionally, *MEF2D* expression was decreased by 1.13-fold with young RENCA macrobead exposure but elevated (2.72-fold) following co-culture with mature RENCA macrobeads (Figure 3B). Expression of the *MEF2B* isoform was not observed in DU145 cells. These results indicate that mature RENCA macrobeads, with the capacity to inhibit tumor growth, modulate the expression of multiple MEF2 isoforms.

3.2. MEF2D is required for RENCA macrobead-mediated growth inhibition.

RENCA macrobead regulation of MEF2 expression suggests that depletion of these isoforms might alter RENCA macrobead-mediated growth inhibition. We investigated this idea by transfecting tumor cell lines with MEF2 isoform-specific siRNA followed by exposure to naïve media or RENCA macrobeads using a co-culture insert system. As *MEF2c* and *MEF2B* were undetectable in RENCA and DU145 cells respectively, further analysis was restricted to expressed MEF2 isoforms. In addition, we included a pooled MEF2 siRNA condition, simultaneously depleting all expressed MEF2 isoforms in each cell line (MEF2a, b, d siRNA for RENCA and MEF2A, C, D siRNA for DU145), to examine the role of redundant gene family members in RENCA macrobead-induced inhibition.

Quantitative RT-PCR analysis of MEF2 expression confirmed knockdown efficiency to be greater than 80% and specific to the targeted isoform, at the beginning and at the end of the growth inhibition assay (day 0 and day 5, respectively) in RENCA (Appendix B: Supplementary Figure 2) and DU145 (Appendix B: Supplementary Figure 3) cell lines. Furthermore, there was no compensatory upregulation of MEF2 transcripts in response to acute depletion of individual MEF2 isoforms.

In naïve media or following co-culture with young RENCA macrobeads, the knockdown of MEF2a or MEF2d did not influence cell growth but gene silencing of MEF2b significantly reduced survival in RENCA cells by 27.9% or 28.3% respectively. Similarly, pooled MEF2a, MEF2b and MEF2d siRNAs significantly suppressed growth of RENCA cells in naïve media (26.6%) or when cultured together with young RENCA macrobeads (28.5%), likely due to MEF2b knockdown (Figure 4A).

Following co-culture with mature RENCA macrobeads, RENCA cells lacking siRNA treatment (untreated) exhibited 43.8% growth inhibition, similar to the growth reduction observed in RENCA cells transfected with NT siRNA (41.2%). In cells lacking MEF2a, there was a significant decrease in inhibition when compared to NT siRNA (22.3% vs. 41.2%). Silencing of MEF2b in combination with mature RENCA macrobead exposure also reduced inhibition as compared to NT siRNA treated cells but did not reveal a substantial difference in the inhibitory response (5.1%) as compared to MEF2b knockdown alone. However, MEF2d knockdown promoted survival in response to factors secreted by

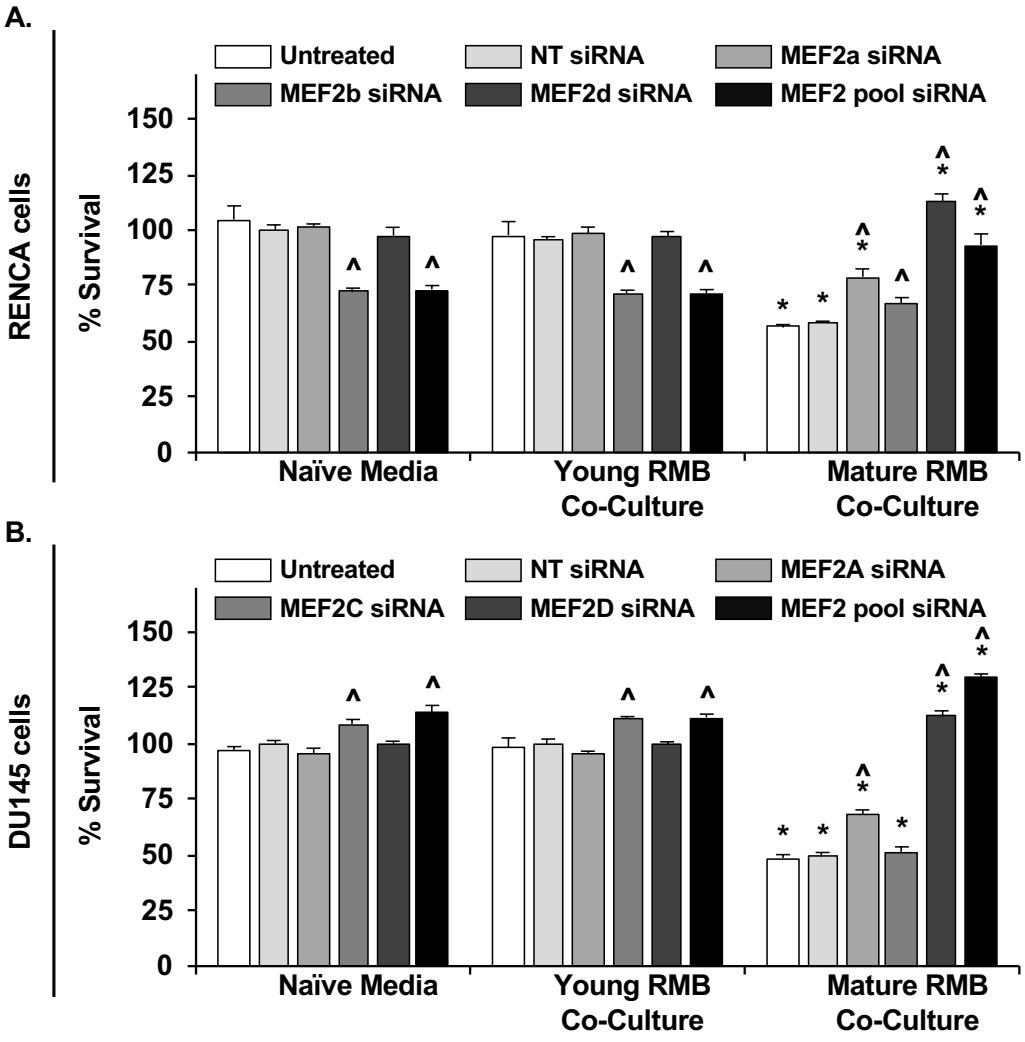

Figure 4: MEF2D is required for RENCA macrobead-mediated growth inhibition. (A) RENCA and (B) DU145 cells were transfected with MEF2 isoform-specific siRNA followed by exposure to naïve media, young or mature RENCA macrobeads for 5 days. Cell proliferation was quantified by neutral red staining and confirmed using trypan blue exclusion assay. Y-axis represents the percent survival relative to naïve cultures treated with NT siRNA. p-value < 0.05 relative to NT siRNA within a culture condition (^) or relative to naïve media with the same siRNA knockdown (*).

mature RENCA macrobeads, increasing cell proliferation by 15.8% over baseline growth of cells exposed to naïve media, corresponding to a 57.0% (NT siRNA 41.2% + MEF2d siRNA 15.8%) growth increase over cells treated with NT siRNA together with mature RENCA macrobeads. Combined siRNA-mediated knockdown (MEF2 pool) in RENCA cells also resulted in significantly enhanced cell survival (61.2%; NT siRNA 41.2% + MEF2 pool 20.0%) following co-culture with mature RENCA macrobeads (Figure 4A). These results indicate that expressed MEF2 isoforms contribute to RENCA macrobead-mediated growth inhibition of RENCA cells.

Analogous to RENCA cells, MEF2A deficiency in DU145 cells did not impact growth in naïve media or in the presence of young RENCA macrobeads but loss of MEF2A when cultured together with mature RENCA macrobeads decreased inhibition relative to NT siRNA (28.2% vs. 50.8%), suggesting that MEF2A partially contributes to the anti-proliferative effect in this cell line (Figure 4B). In contrast, MEF2C knockdown increased DU145 cell survival in naïve media or following co-culture with young RENCA macrobeads but mature RENCA macrobeads restored inhibition of MEF2C-deficient DU145 cells to levels similar to untreated cells, indicating that RENCA macrobead-mediated inhibition is MEF2C-dispensable. MEF2D depletion also resulted in a significant increase in cell proliferation (63.0%; NT siRNA 50.8% + MEF2D 12.2%) following co-culture with mature RENCA macrobeads while having no discernable effect on growth in naïve media or in the presence of young RENCA macrobeads. Likewise, pooled MEF2 knockdown promoted survival in the presence of mature RENCA macrobeads, increasing proliferation by 14.5% over cells cultured in naïve media which corresponded to a 65.3%

(NT siRNA 50.8% + MEF2 pool siRNA 14.5%) growth increase over cells treated with NT siRNA (Figure 4B). These data suggest that MEF2D is required for RENCA macrobead induced growth inhibition of DU145 cells.

Overall, these results reveal that MEF2 family members, most notably MEF2d/D, have distinct transcriptional functions in RENCA and DU145 cells in response to RENCA macrobeads and suggest that these differences are critical for tumor growth control.

3.3. MEF2 depletion abrogates RENCA macrobead induced S-phase arrest.

MEF2 isoforms, specifically MEF2C and MEF2D, have been described to inhibit proliferation by inducing p21 expression [148] which can lead to accumulation of cells in S-phase [286]. Since mature RENCA macrobeads suppress proliferation of freely growing cancer cells by inducing S-phase arrest [85] and RENCA macrobeads modulate MEF2 isoform expression, we sought to determine whether the depletion of MEF2 isoforms in target tumor cells alters cell-cycle distribution in the presence of RENCA macrobeads.

In naïve media or following co-culture with young RENCA macrobeads, knockdown of MEF2b or combined silencing of expressed MEF2 isoforms in RENCA cells increased S-phase accumulation with an associated decrease in the percentage of cells in G1 phase (Figure 5). Consistent with previous observations [85], culture of RENCA cells with mature RENCA macrobeads impaired progression through S-phase (23.7% vs. 8.0% for cells cultured in naïve media) with a corresponding decrease in G1 (31.7% vs. 43.8%) and G2/M phases (44.6% vs. 48.1%). A similar pattern of cell-cycle distribution was observed

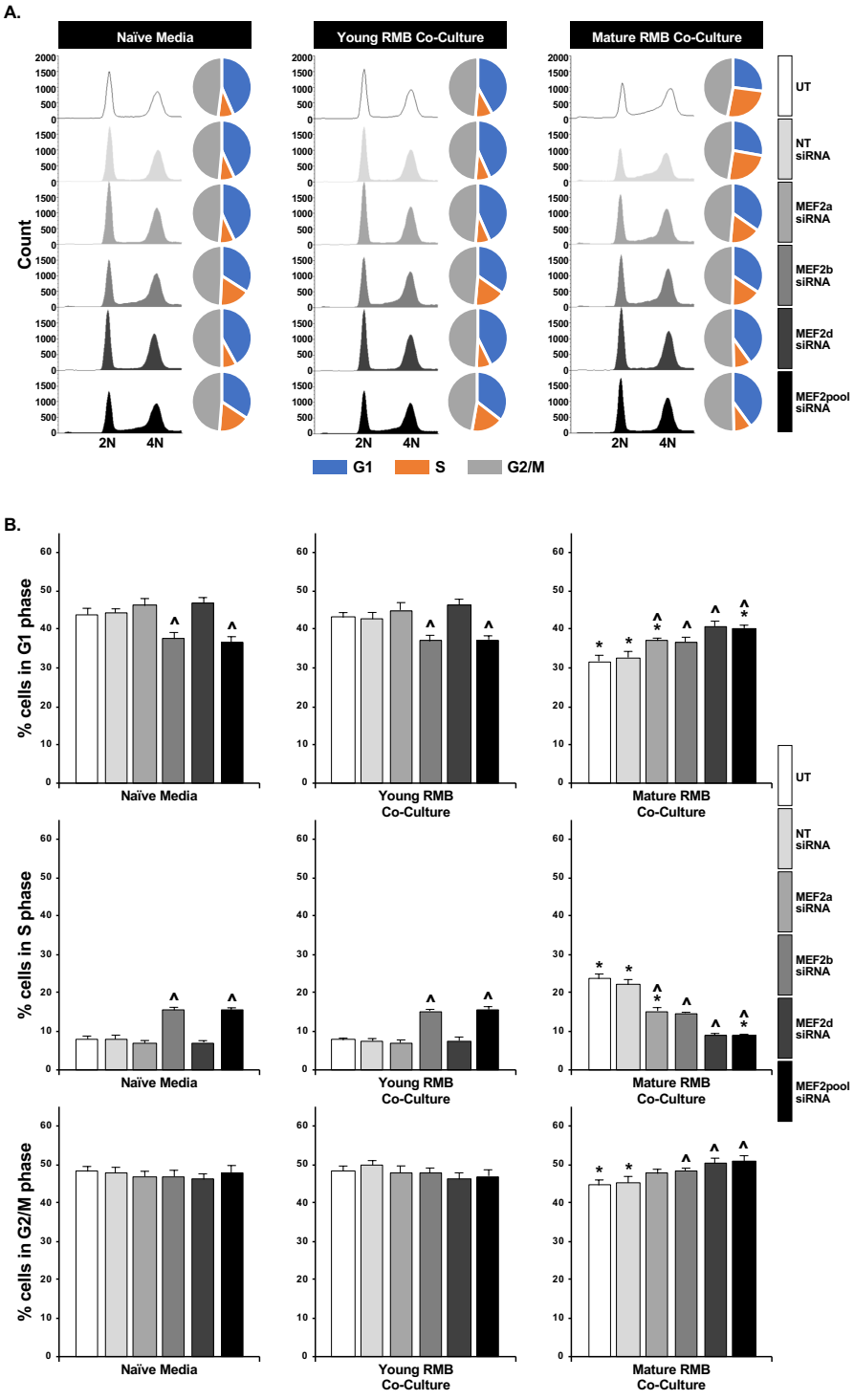

Figure 5: MEF depletion abrogates RENCA macrobead induced S-phase arrest in RENCA cells. (A) Cell cycle profiles with pie charts and (B) the percentage of the cell population in each phase of the cell cycle in RENCA cells transfected with MEF2 isoform-specific siRNA followed by exposure to naïve media, young or mature RENCA macrobeads after 5 days. p-value < 0.05 relative to NT siRNA within a culture condition (^) or relative to naïve media with the same siRNA knockdown (*).

for cells transfected with NT siRNA in the presence of RENCA macrobeads (G1: 32.7%; S: 22.1%; G2/M: 45.2%).

Depletion of MEF2 isoforms abrogated RENCA macrobead-induced S-phase arrest (Figure 5). In cells lacking MEF2a, there was a significant decrease in the percentage of cells in S-phase (15.4% vs. 22.1%) accompanied by an increase in G1 phase (37.1% vs. 32.7%). Silencing of MEF2b also reduced S-phase accumulation (14.8%) and increased G1 (36.7%) and G2/M (48.4%) phase populations as compared to NT siRNA treated cells but did not reveal a significant difference in cell cycle distribution when compared to MEF2b knockdown alone. Loss of MEF2d completely abolished S-phase accumulation to levels comparable to naïve media, supporting a critical role for this isoform in inducing RENCA macrobead-mediated S-phase arrest (Figure 5). Combined siRNA-mediated knockdown in RENCA cells also resulted in significantly reduced S-phase accumulation (9.0%) following co-culture with mature RENCA macrobeads. These results indicate that MEF2a, MEF2b and particularly, the MEF2d isoform contribute to RENCA macrobead-mediated S-phase accumulation of RENCA cells.

In the DU145 cell line, depletion of MEF2 isoforms did not influence cell cycle profiles when cultured in naïve media or following co-culture with young RENCA macrobeads; however, the presence of mature RENCA macrobeads significantly altered cell cycle phase distribution (Figure 6). Following co-culture with mature RENCA macrobeads, untreated DU145 cells accumulated in S-phase (24.8% vs. 14.4% for cells cultured in naïve media) along with a significant decrease in G1 (44.1% vs. 48.0%) and G2/M phases (31.1% vs.

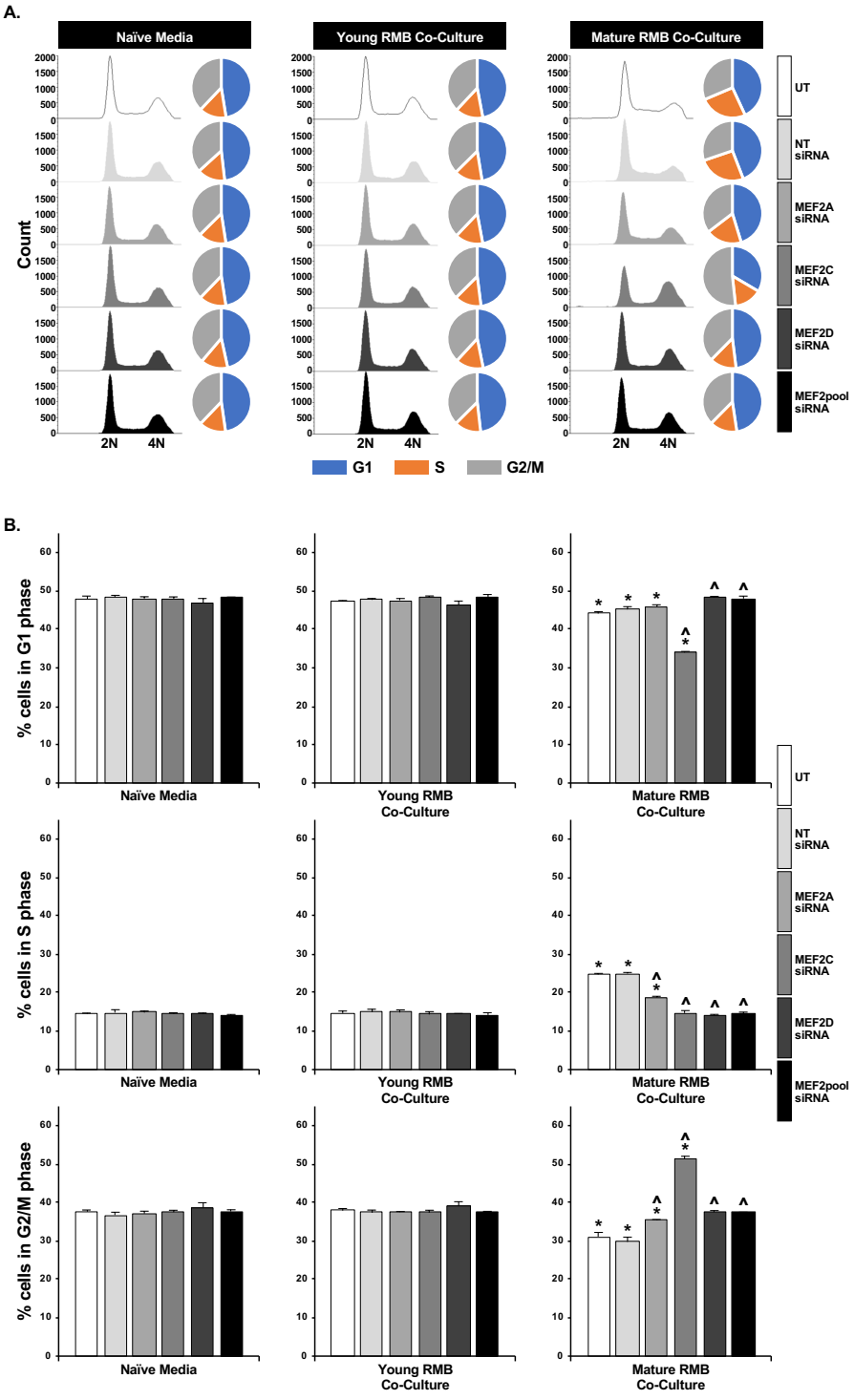

Figure 6: MEF depletion abrogates RENCA macrobead induced S-phase arrest in DU145 cells. (A) Cell cycle profiles with pie charts and (B) the percentage of the cell population in each phase of the cell cycle in DU145 cells transfected with MEF2 isoform-specific siRNA followed by exposure to naïve media, young or mature RENCA macrobeads after 5 days. p-value < 0.05 relative to NT siRNA within a culture condition (^) or relative to naïve media with the same siRNA knockdown (*).

37.6%), similar to the cell cycle distribution profiles of DU145 cells transfected with NT siRNA (G1: 45.2%; S: 25.0%; G2/M: 29.8%).

Loss of MEF2A decreased S-phase arrest (18.8%) with a moderate increase in G2/M phase (35.4%) (Figure 6). MEF2C knockdown also reduced S-phase accumulation (14.7%) in comparison to NT siRNA but surprisingly, a large proportion of MEF2C depleted DU145 cells accumulated in G2/M phase (51.3%) (Figure 6), suggesting an alternative mechanism for RENCA macrobead-induced growth arrest in the absence of MEF2C for this cell line. Analogous to RENCA cells, silencing of MEF2D or combined knockdown of MEF2 isoforms in DU145 cells abrogated S-phase accumulation, suggesting a conserved role for MEF2D in mediating RENCA macrobead-induced S-phase arrest (Figure 6). Overall, these results demonstrate a critical role for MEF2 isoforms in RENCA macrobead-induced cell-cycle regulation of DU145 cells *in vitro*, similar to the role of MEF2 in RENCA cells as shown above.

3.4. Mature RENCA macrobead-induced upregulation of EGFR activity correlates with levels of functional EGFR expression.

Regulation of transcriptional programs that control cell fate can occur in response to extracellular signals acting through cell surface receptors. Our preliminary studies indicated that mature RENCA macrobeads increase the levels of total and phosphorylated EGFR in RENCA cells. Overexpression of EGF receptor and activation of EGFR-tyrosine kinase induces growth inhibition, cell cycle arrest and apoptosis in specific contexts [165, 166, 169, 170, 175, 287], suggesting a possible signaling link that translates RENCA

macrobead-released signals into an inhibitory response. Therefore, we evaluated the association between EGFR expression or tyrosine kinase responsiveness and RENCA macrobead-mediated growth suppression using a panel of four cell lines: DU145, DU145/GR, MDA-MB-231 and MCF7. The human prostate cancer cell line DU145 harbors wild-type EGFR gene amplification with an estimated $2.4 – 4\times10^5$ EGFRs per cell [288-290]. DU145/GR cells, as described in Chapter 2, are a gefitinib-resistant subline generated through chronic adaptation with the tyrosine kinase inhibitor, gefitinib. These cells exhibit weak tyrosine kinase activity in the presence of EGF as compared to the parental DU145 cell line (Appendix A: Supplementary Figure 1). MDA-MB-231 is an epithelial-derived basal breast cancer cell line reported to express EGFR at high levels ($\sim7\times10^5$ EGFRs/cell) [291] while MCF7, an epithelial-derived luminal A breast cancer cell line has substantially lower levels of EGFR expression ($\sim8\times10^2$ EGFRs/cell) [291, 292].

To better understand whether the relative levels of EGF receptor correlate with the ability of RENCA macrobeads to inhibit cell growth, we used in-cell western analysis to assess the relative expression and activation (pY1068) of EGFR in response to RENCA macrobead-released signals in each cell line. Whereas young RENCA macrobead conditioned media had a negligible effect on EGFR abundance and activity as compared to cells cultured in naïve media, mature RENCA macrobead conditioned media significantly increased EGFR expression (3.9-fold) and activation (2.3-fold) in DU145 cells (Figure 7A). In contrast, DU145/GR cells, demonstrated a moderate upregulation of total (1.8-fold) and phosphorylated EGFR (1.5-fold) (Figure 7B) despite having similar

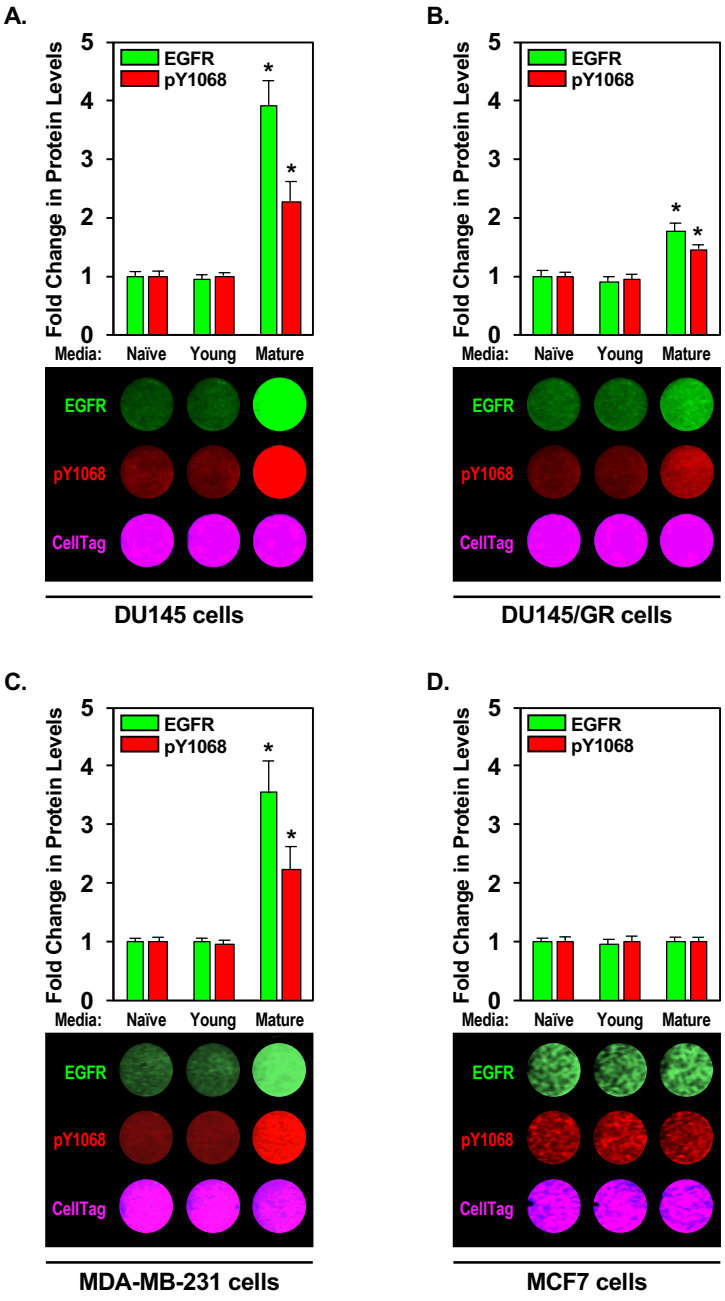

Figure 7: Mature RENCA macrobead-induced upregulation of EGFR activity correlates with levels of functional EGFR expression. The relative expression of EGFR and pY1068 was detected via in-cell western analysis 30-minutes following exposure to naïve media or conditioned media from young or mature RENCA macrobeads in (A) DU145, (B) DU145/GR, (C) MDA-MB-231, and (D) MCF7 cells. CellTag 700 stain was used for normalization to cell number. Y-axis represents the fold change in protein levels relative to naïve cultures. *p-value < 0.05 relative to naïve media within the cell type.

basal receptor expression and pY1068 levels as the parental DU145 cell line (Appendix A: Supplementary Figure 1B). MDA-MB-231 cells also exhibited elevated EGFR (3.5-fold) and pY1068 (2.2-fold) (Figure 7C); however, no changes in total EGFR or pY1068 levels were observed in MCF7 cells (Figure 7D). These data demonstrate that mature RENCA macrobead-induced upregulation of EGFR expression and activity correlates with levels of functional EGFR.

3.5. Mature RENCA macrobeads sustain activated EGFR signaling in cells with high levels of functional EGF receptor.

Experiments in multiple cell types have shown that the specificity of cellular responses depends on EGFR signal duration (e.g., whether EGFR activation is transient or sustained) [287, 293, 294]. Therefore, signaling through the same pathway may result in entirely different outputs depending on the amplitude and persistence of receptor activation. To explore the temporal regulation of EGFR in response to RENCA macrobeads, EGFR expression and phosphorylation was assessed in cell lines exposed to naïve or conditioned media from varied ages of RENCA macrobeads over a 24-hour period. Naïve media or young RENCA macrobead-treated DU145 cells demonstrated an early, transient increase in EGFR phosphorylation accompanied by a modest upregulation of EGFR expression. In contrast, exposure of DU145 cells to conditioned media from mature RENCA macrobeads prompted a rapid and sustained increase in total and activated EGFR that remained relatively stable for 24 hours following initial stimulation (Figure 8A). A comparable pattern of EGFR expression and activation kinetics was observed in the MDA-MB-231 cell line (Figure 8C). Although DU145/GR cells in naïve or young RENCA macrobead

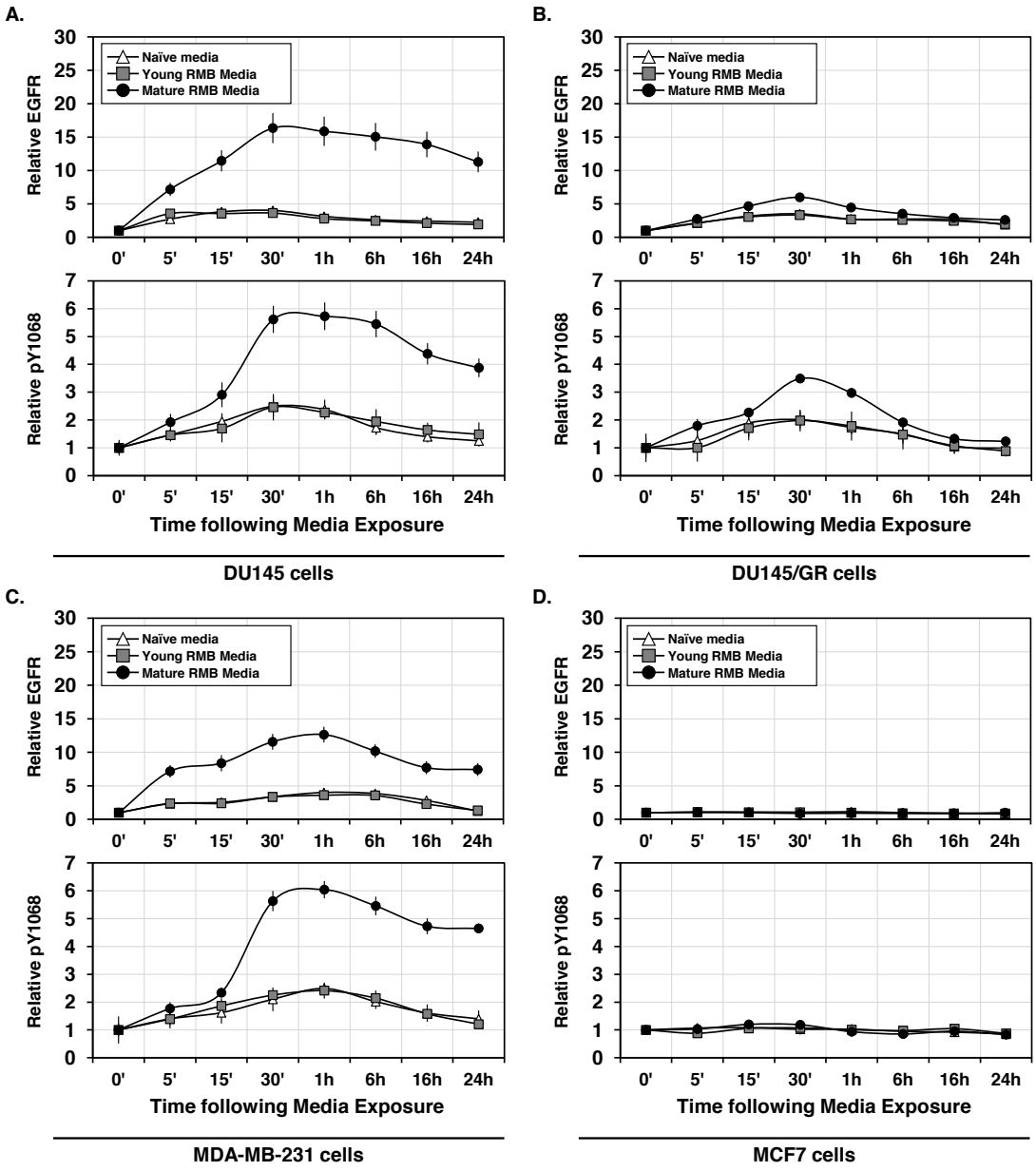

Figure 8: Mature RENCA macrobeads sustain activated EGFR signaling in cells with high levels of functional EGF receptor. Time course of EGFR (top panel) and pY1068 (bottom panel) expression in (A) DU145, (B) DU145/GR, (C) MDA-MB-231, and (D) MCF7 cells following exposure to naïve media or conditioned media from young or mature RENCA macrobeads. Each datapoint represents protein expression relative to time = 0.

conditioned media exhibited similar activation kinetics to the parental DU145 cell line, mature RENCA macrobead treatment induced only moderately elevated total and pY1068 levels, returning to baseline within 1-6 hours following initial stimulation (Figure 8B). Comparatively, MCF7 cells exhibited a complete lack of response in activity throughout the time course regardless of the type of media exposure (Figure 8D). This demonstrates that mature RENCA macrobead-released signals extend EGFR engagement in cells overexpressing functional EGFR.

3.6. Association between levels of functional EGFR and RENCA macrobead-induced MEF2 activity and expression.

Downstream effectors of EGFR signaling, such as BMK1, ERK5 and p38, influence MEF2 transcriptional activity [295, 296]. Therefore, we sought to examine the extent to which RENCA macrobead-induced EGFR signaling is associated with MEF2 reporter activity. In all cell lines tested, mature but not young RENCA macrobeads increased MEF2 reporter activity as compared to cells cultured in naïve media (DU145: 35.1-fold; DU145/GR; 10.4-fold; MDA-MB-231: 15.5-fold; MCF7: 3.4-fold) (Figure 9A-D). However, mature RENCA macrobead-induced MEF2 activity was significantly greater in cell lines with higher expression of functional EGFR.

Components of MEF2 transcriptional regulation are also dependent on ERK and Ras signaling, likely downstream of EGFR [295, 296]. Since mature RENCA macrobeads modulate MEF2 transcript levels, we determined whether signaling through EGFR correlated with MEF2 isoform expression in the presence of RENCA macrobeads.

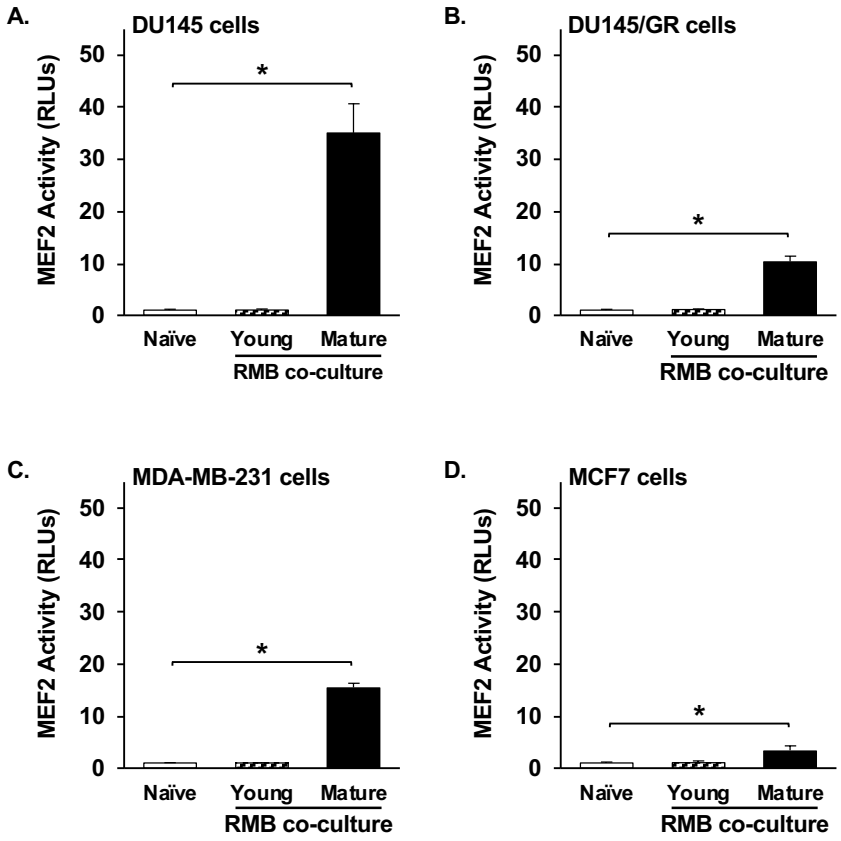

Figure 9: Association between levels of functional EGFR and RENCA macrobead-induced MEF2 activity. (A) DU145, (B) DU145/GR, (C) MDA-MB-231, and (D) MCF7 cells transiently transfected with the MEF2 reporter were exposed to naïve media or conditioned media from young or mature RENCA macrobeads for 24 hours. Luminescence values for the MEF2 reporter signal was measured using a dual-luciferase reporter assay and normalized to the internal control signal, Renilla. Y-axis represents the fold change in MEF2 activity relative to naïve cultures. *p-value < 0.05.

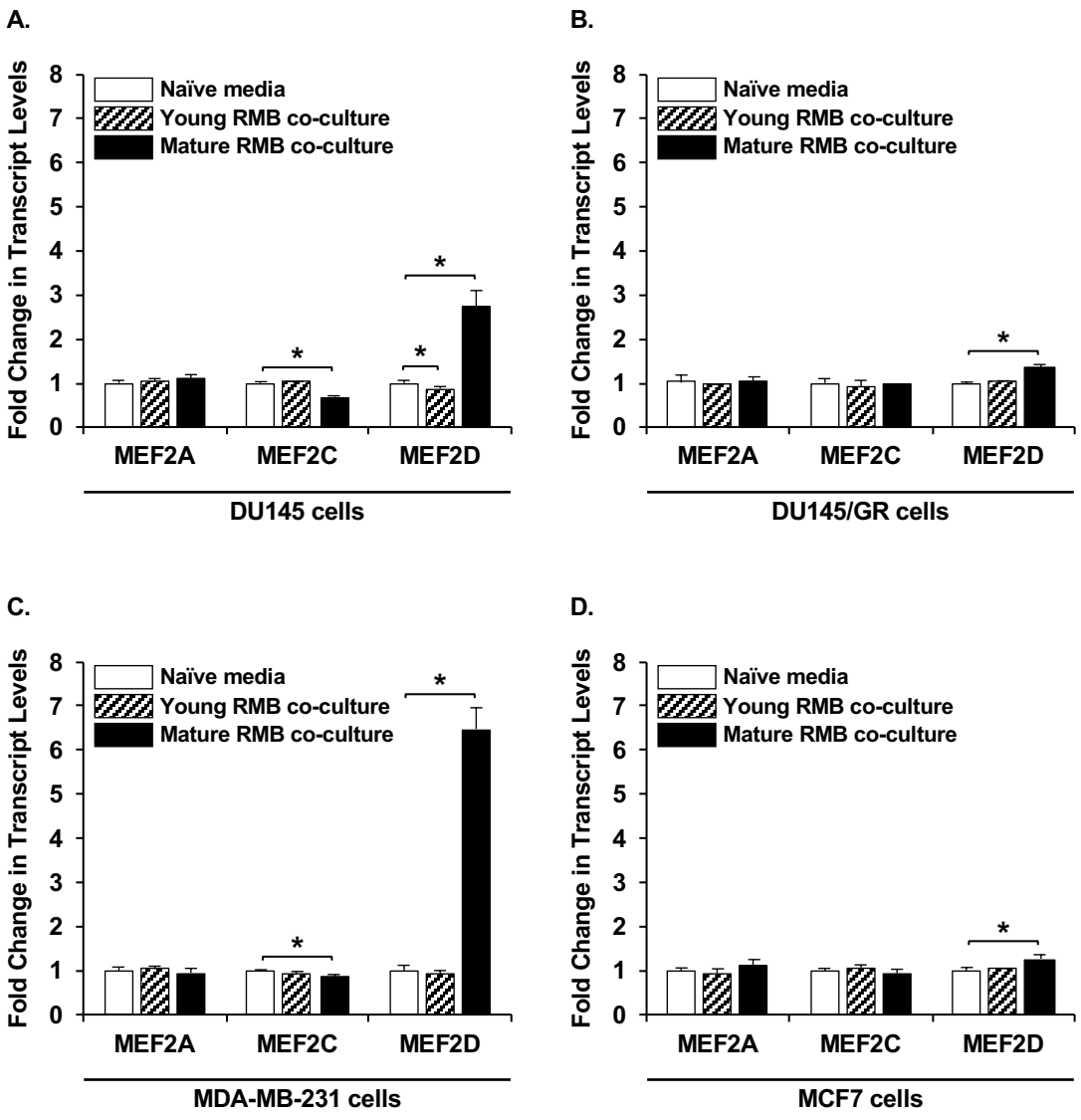

Figure 10: Association between levels of functional EGFR and RENCA macrobead-induced MEF2 expression. MEF2 isoform transcript levels were analyzed using Taqman based qRT-PCR in (A) DU145, (B) DU145/GR, (C) MDA-MB-231, and (D) MCF7 cells following culture in naïve media, or co-culture with young or mature RENCA macrobeads (RMB) for 5 days. *p-value < 0.05 relative to naïve media.

Following exposure to mature RENCA macrobeads, *MEF2C* transcript levels were reduced in cells overexpressing EGFR, specifically 1.44-fold in DU145 cells (Figure 10A) and 1.18-fold in MDA-MB-231 cells (Figure 10C) but *MEF2C* mRNA was comparable to naïve media in DU145/GR (Figure 10B) and MCF7 cells (Figure 10D). Additionally, *MEF2D* expression was significantly increased in all cell lines (DU145: 2.72-fold; DU145/GR; 1.34-fold; MDA-MB-231: 6.49-fold; MCF7: 1.27-fold) in response to mature RENCA macrobeads (Figure 10). However, it is noted that RENCA macrobead-induced mRNA levels of *MEF2D* were greater in cells with EGFR overexpression. Overall, these data demonstrate that the level of MEF2 activity and isoform-specific expression induced by mature RENCA macrobead exposure is associated with the level of EGFR expression in the tested cell lines.

3.7. EGFR overexpression correlates with sensitivity to growth inhibition by mature RENCA macrobeads.

To investigate whether the extent of RENCA macrobead-mediated growth inhibition depended on EGFR expression levels or responsiveness, cells cultured in naïve media or together with RENCA macrobeads were stained with neutral red and percent survival was calculated based on naïve cultures. Results were confirmed using the trypan blue exclusion assay. Young RENCA macrobeads did not significantly impact cell survival in any of the tested cell lines as compared to cells cultured in naïve media. However, mature RENCA macrobeads inhibited proliferation of DU145 (Figure 11A), DU145/GR (Figure 11B), MDA-MB-231 (Figure 11C) and MCF7 (Figure 11D) cells by 40.8% (DU145), 16.0%

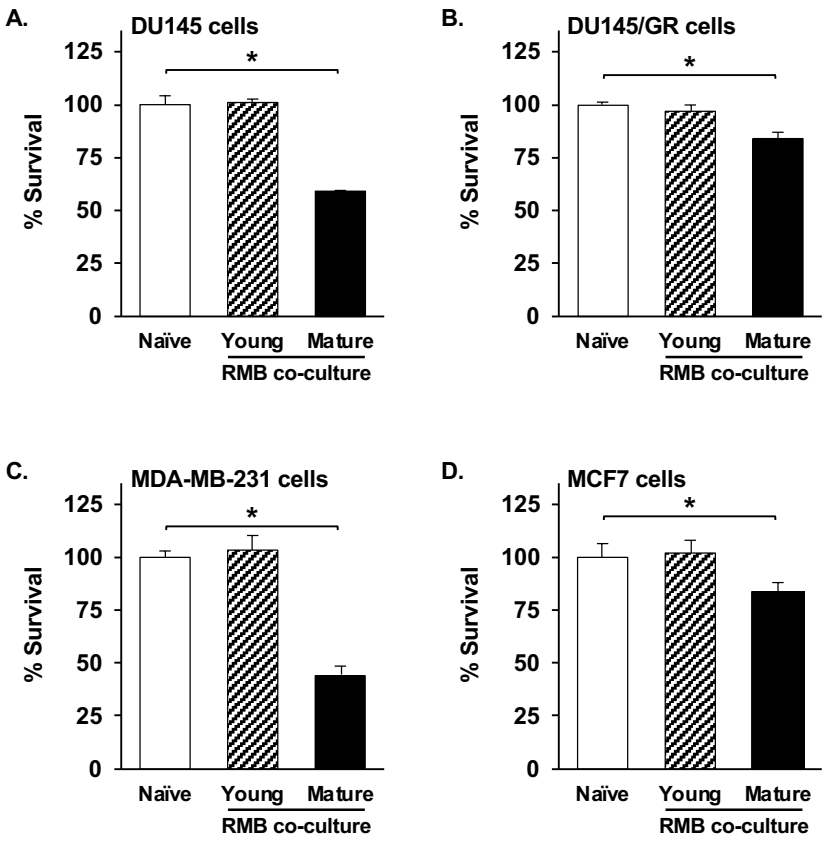

Figure 11: EGFR overexpression correlates with sensitivity to growth inhibition by mature RENCA macrobeads. Growth of (A) DU145, (B) DU145/GR, (C) MDA-MB-231, and (D) MCF7 cells following exposure to naïve media or co-culture with young or mature RENCA macrobeads for 5 days. Cells were fixed and stained with neutral red. Y-axis represents the percent survival relative to naïve cultures. *p-value < 0.05.

(DU145/GR), 55.3% (MDA-MB-231) and 16.4% (MCF7), as compared to naïve media. These results demonstrate that sensitivity to growth inhibition induced by mature RENCA macrobeads is correlated with the level of functional EGFR expression.

3.8. RENCA macrobead-induced S-phase accumulation correlates with levels of functional EGFR expression.

As S-phase accumulation is a prominent feature of RENCA macrobead-mediated suppression of freely growing cancer cells [85] and regulation of EGFR modulates cell cycle progression [297], we sought to examine whether EGFR status is associated with RENCA macrobead-induced cell cycle inhibition. Co-culturing DU145 cells with mature RENCA macrobeads significantly increased S-phase accumulation (24.8% vs. 14.4%), thereby reducing the proportion of cells in G1 (44.1% vs. 48.0%) and G2/M phases (31.1% vs. 37.6%), compared to cells cultured in naïve media (Figure 12A). Contrastingly, comparable numbers of DU145/GR cells were identified in S-phase regardless of culture medium (Figure 12B), supporting a central role for functionally active EGFR in transducing RENCA macrobead-released signals into intracellular growth inhibitory responses that promote S-phase arrest. Interestingly, in DU145/GR cells, a significant increase in the proportion of cells that accumulated in G2/M phase and a concomitant decrease in G1 phase was observed in the presence of mature but not young RENCA macrobeads (Figure 12B), suggesting a secondary mechanism by which RENCA macrobeads could inhibit growth in the absence of functionally active EGFR. Furthermore, this supports the notion that RENCA macrobeads impede multiple processes essential for

Figure 12: RENCA macrobead-induced S-phase accumulation correlates with levels of functional EGFR expression. Cell cycle profiles with pie charts (top) and graphs (bottom) showing the percentage of the cell population in each phase of the cell cycle in (A) DU145, (B) DU145/GR, (C) MDA-MB-231, and (D) MCF7 cells following exposure to naïve media, young or mature RENCA macrobeads for 5 days. *p-value < 0.05 relative to naïve cultures.

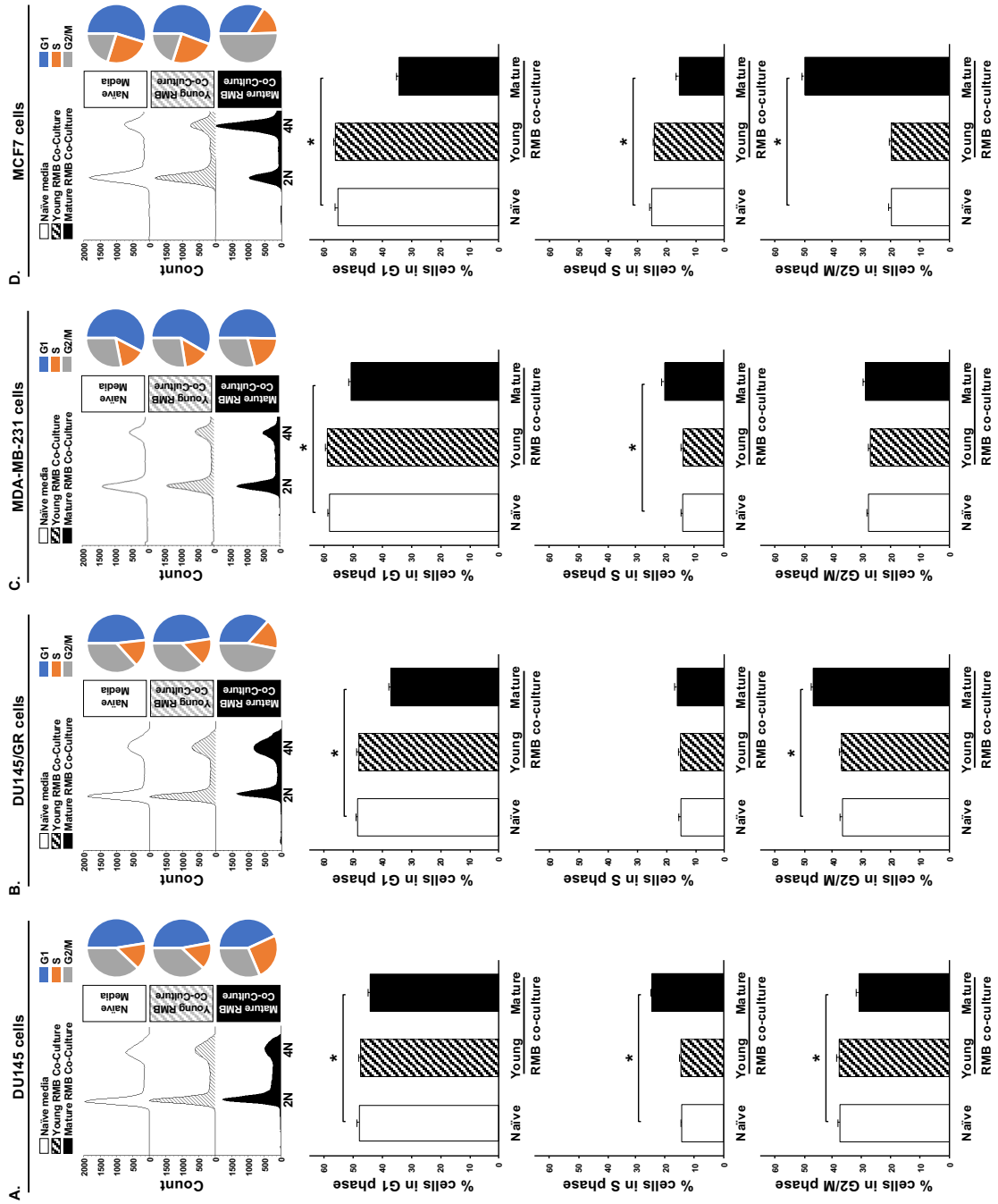

tumor cell proliferation. Analogous to DU145 cells, significantly more MDA-MB-231 cells accumulated in S-phase when cultured with mature RENCA macrobeads (20.5%) with an associated decrease in G1 phase as compared to naïve media (14.1%) or co-culture with young RENCA macrobeads (14.0%) (Figure 12C). MCF7 cells cultured in naïve media or together with young RENCA macrobeads aggregated in G1 phase and had a relatively even distribution of S and G2/M populations. However, exposure to mature RENCA macrobeads caused a cell cycle shift, with significantly fewer cells accumulating in S-phase (15.6% vs. 24.9%) while a large proportion collected in the G2/M phase (50.0% vs. 19.9%) (Figure 12D). These results demonstrate that signaling through EGFR correlates with RENCA macrobead-induced S-phase cell accumulation.

3.9. RTN4, TSP1 and TIMP2 are present in the RENCA macrobead secretome.

Data presented thus far supports the idea that EGFR overexpression and activation correlates with sensitivity to RENCA macrobead-induced inhibition. EGF-like ligands, such as RTN4, TSP1 and TIMP2, identified by mass spectrometry in conditioned media of RENCA macrobeads at different stages of development, have reported tumor suppressive functions [218, 223, 224, 243, 244, 246, 249, 252, 266, 272, 273] and consequently, may participate in RENCA macrobead-mediated growth inhibition of target tumor cells. Thus, we sought to confirm the presence of these proteins in conditioned media collected from RENCA macrobeads followed by characterizing their roles in growth inhibition.

Using an ELISA, we quantified levels of RTN4, TSP1 and TIMP2 in RENCA macrobead conditioned media. Each target protein was detected (~540 pg – 15 ng/mg total protein) in

		RTN4 (ng/mg)	TSP1 (ng/mg)	TIMP2 (ng/mg)
5% NCS	Naïve Media	ND	ND	ND
	Young RMB Media	ND	ND	0.031 ± 0.011
	Mature RMB Media	0.546 ± 0.073	11.644 ± 1.676	1.533 ± 0.259
5% FBS	Naïve Media	ND	ND	ND
	Young RMB Media	ND	ND	0.058 ± 0.008
	Mature RMB Media	0.611 ± 0.089	14.381 ± 2.174	1.629 ± 0.317

Table 1: RTN4, TSP1 and TIMP2 levels in naïve and RENCA macrobead conditioned media. Concentrated naïve and conditioned media from young or mature RENCA macrobeads was analyzed by ELISA for RTN4, TSP1 and TIMP2. NCS and FBS cultures were concentrated and quantified separately to establish baseline measurements for comparison with future tests involving RENCA and DU145 cells respectively. ND, not detected in tested media with the following detection limits: RTN4 ≤ 0.012 ng/mg; TSP1 ≤ 0.165 ng/mg; TIMP2 ≤ 0.002 ng/mg. Values represent quantity (ng) of detected protein relative to total protein (mg).

concentrated conditioned media from mature RENCA macrobeads but none were identified in concentrated naïve cultures. In young RENCA macrobead concentrated conditioned media, RTN4 and TSP1, if present, were below the detection limit of the assay and TIMP2, although detected, was present at a lower abundance (~25-50-fold) as compared to concentrated conditioned media from mature RENCA macrobeads (Table 1).

3.10. RTN4, TSP1 and TIMP2 partially contribute to RENCA macrobead-induced EGFR activation.

To confirm whether RTN4, TSP1 and TIMP2, present at expressed levels in RENCA macrobead conditioned media, influence EGFR status in RENCA, DU145, and DU145/GR cells, we assessed the relative expression of EGFR and levels of pY1068 using (1) media individually immunodepleted of each of the detected proteins or (2) naïve media to which protein eluate, recovered from the immunodepletion process, were added.

RTN4, TSP1 and TIMP2 were not detected following precipitation from mature RENCA macrobead conditioned media, suggesting effective depletion using Protein A magnetic beads. Furthermore, similar levels of each protein were observed in the eluate fraction as compared to mock depletion (Rb IgG), confirming successful recovery of depleted proteins (Appendix B: Supplementary Table 2). TIMP2 was not detected in the eluate recovered from immunodepleted young RENCA macrobead conditioned media (data not shown) likely because levels were below the detection limit of the ELISA. As such, further analysis was restricted to proteins depleted from mature RENCA macrobead conditioned media.

RTN4-depleted mature RENCA macrobead conditioned media significantly decreased total and phosphorylated EGFR levels in both RENCA and DU145 cells but had no effect in DU145/GR cells (Figure 13A-C). However, addition of RTN4 eluate to naïve media enhanced EGFR activation in RENCA and DU145 cells with no impact on total EGFR levels (Figure 13D-E). No changes in EGFR status were observed in DU145/GR cells upon treatment with RTN4 eluate (Figure 13F). Similar to RTN4, depletion of TSP1 reduced total and phosphorylated EGFR levels in both RENCA and DU145 cells but not DU145/GR cells (Figure 14A-C). In comparison, TSP1 eluate increased total and phosphorylated levels in RENCA (Figure 14D) but only altered pY1068 in DU145 cells (Figure 14E) with a lack of effect in DU145/GR cells (Figure 14F). TIMP2 depletion reduced total EGFR in RENCA and DU145 cells with a negligible impact on pY1068 levels (Figure 15A-B). Supplementation of naïve media with TIMP2 eluate also increased total EGFR expression in RENCA and DU145 cells (Figure 15D-E). TIMP2, whether depleted from mature RENCA macrobead conditioned media or added to naive media, had no effect on EGFR status in the DU145/GR cell line (Figure 15C, F). These data suggest that while each protein partially contributes to the observed increase in mature RENCA macrobead-induced EGFR expression, RTN4 and TSP1 are required for maximal EGFR phosphorylation. These studies also demonstrate that individual macrobead-released proteins independently influence EGFR status. However, the fractional contribution of each protein to the observed increase in mature RENCA macrobead-induced EGFR expression and activation suggests that these proteins act in concert with additional proteins to elicit the maximal response.

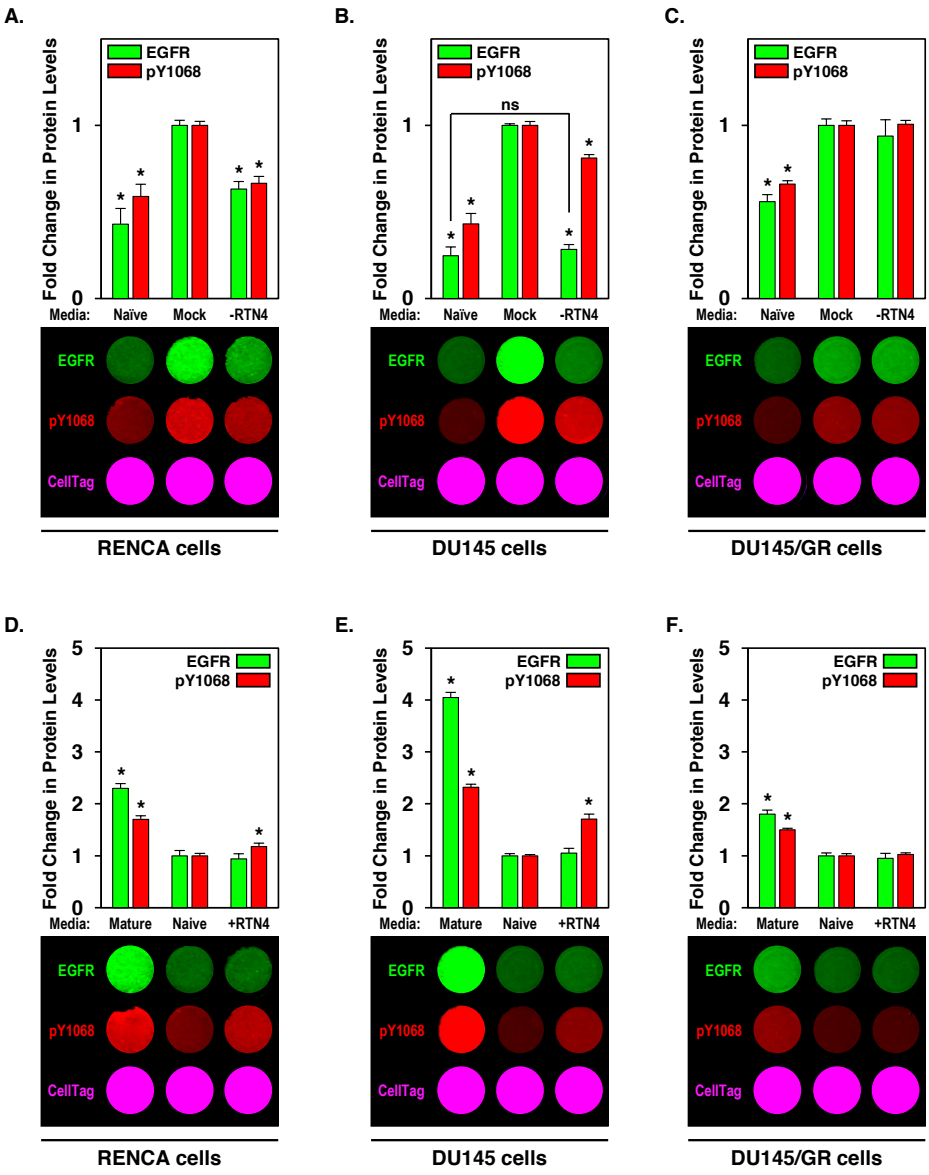

Figure 13: Mature RENCA macrobead-released RTN4 partially contributes to EGFR activation. The relative expression of EGFR and pY1068 was detected via in-cell western analysis 30-minutes following exposure to RTN4-depleted mature RENCA macrobead conditioned media (A-C) or naïve media to which RTN4, eluted from immunodepleted media, was added (D-F) in (A, D) RENCA, (B, E) DU145, and (C, F) DU145/GR cells. CellTag 700 stain was used for normalization to cell number. X-axis includes (A-C) naïve media (Naïve), Rb IgG depleted (Mock), or protein-specific depletion (-RTN4) from mature RENCA macrobead conditioned media and (D-F) mature RENCA macrobead conditioned media (Mature), Rb IgG added (Naïve), or protein-specific addition (+RTN4) to naïve media. Y-axis represents the fold change in protein levels relative to Rb IgG (Mock) depleted mature RENCA macrobead conditioned media (A-C) or Rb IgG added to naïve media (Naïve) (D-F). *p-value < 0.05 relative to Mock in A-C or Naïve in D-F.

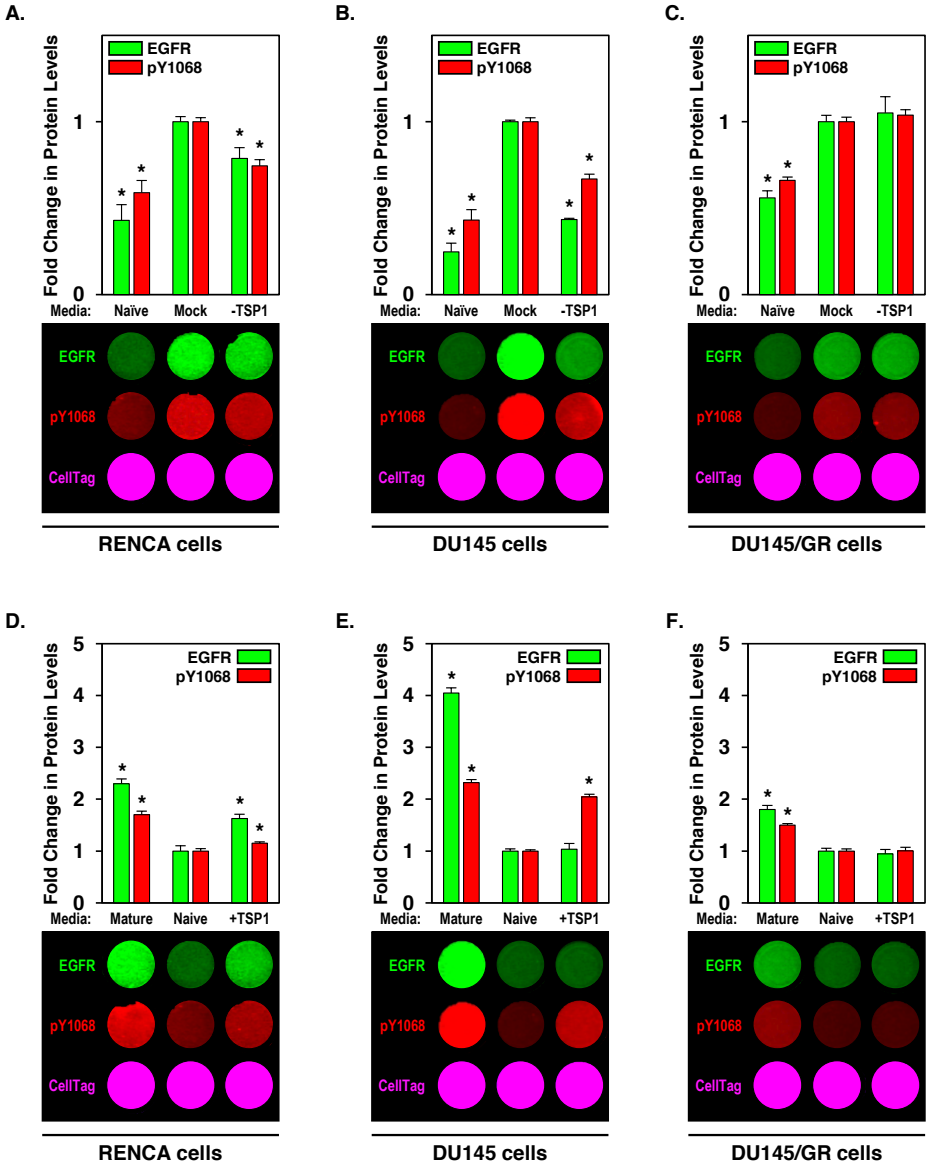

Figure 14: Mature RENCA macrobead-released TSP1 partially contributes to EGFR activation. The relative expression of EGFR and pY1068 was detected via in-cell western analysis 30-minutes following exposure to TSP1-depleted mature RENCA macrobead conditioned media (A-C) or naïve media to which RTN4, eluted from immunodepleted media, was added (D-F) in (A, D) RENCA, (B, E) DU145, and (C, F) DU145/GR cells. CellTag 700 stain was used for normalization to cell number. X-axis includes (A-C) naïve media (Naïve), Rb IgG depleted (Mock), or protein-specific depletion (-TSP1) from mature RENCA macrobead conditioned media and (D-F) mature RENCA macrobead conditioned media (Mature), Rb IgG added (Naïve), or protein-specific addition (+TSP1) to naïve media. Y-axis represents the fold change in protein levels relative to Rb IgG (Mock) depleted mature RENCA macrobead conditioned media (A-C) or Rb IgG added to naïve media (Naïve) (D-F). *p-value < 0.05 relative to Mock in A-C or Naïve in D-F.

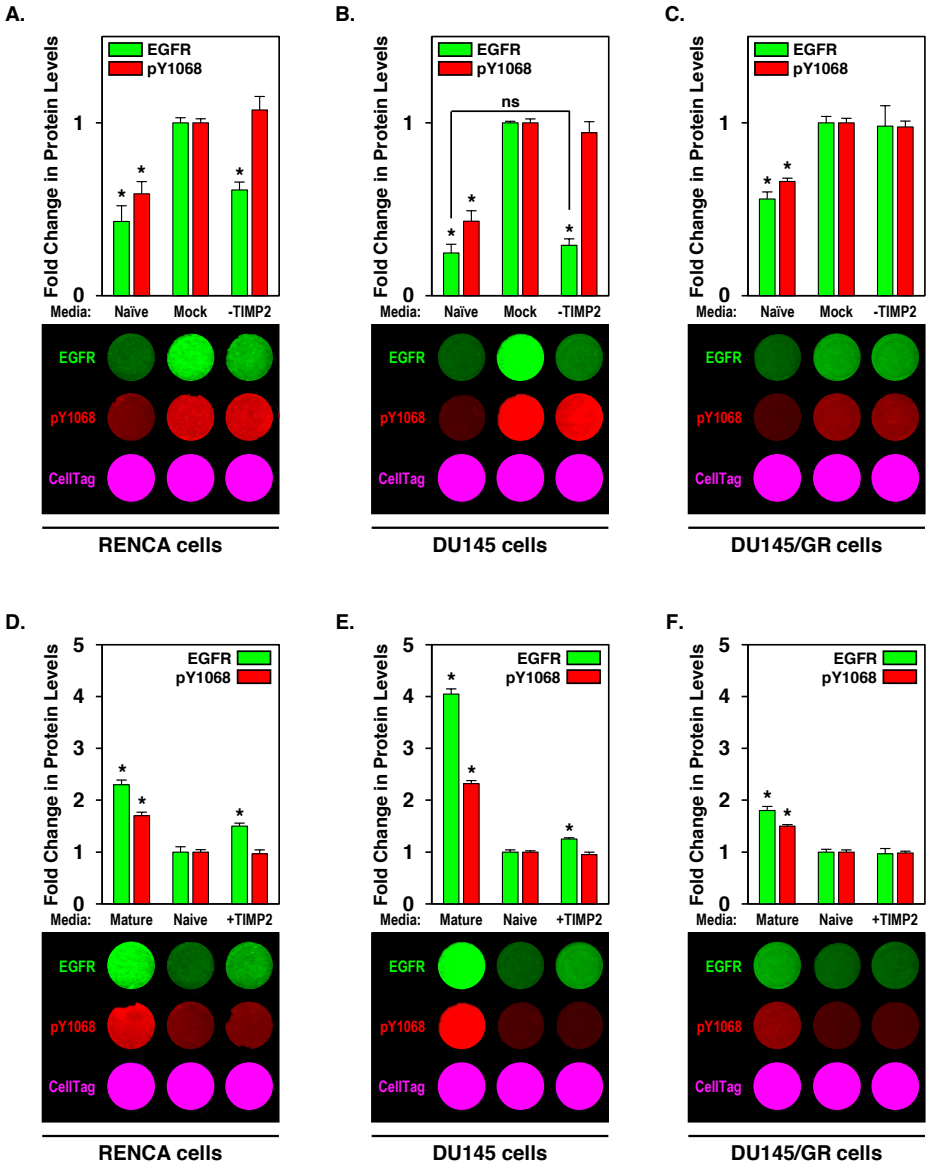

Figure 15: Mature RENCA macrobead-released TIMP2 partially contributes to EGFR activation. The relative expression of EGFR and pY1068 was detected via in-cell western analysis 30-minutes following exposure to TIMP2-depleted mature RENCA macrobead conditioned media (A-C) or naïve media to which RTN4, eluted from immunodepleted media, was added (D-F) in (A, D) RENCA, (B, E) DU145, and (C, F) DU145/GR cells. CellTag 700 stain was used for normalization to cell number. X-axis includes (A-C) naïve media (Naïve), Rb IgG depleted (Mock), or protein-specific depletion (-TIMP2) from mature RENCA macrobead conditioned media and (D-F) mature RENCA macrobead conditioned media (Mature), Rb IgG added (Naïve), or protein-specific addition (+TIMP2) to naïve media. Y-axis represents the fold change in protein levels relative to Rb IgG (Mock) depleted mature RENCA macrobead conditioned media (A-C) or Rb IgG added to naïve media (Naïve) (D-F). *p-value < 0.05 relative to Mock in A-C or Naïve in D-F.

3.11. RTN4, TSP1 and TIMP2 differentially regulate MEF2 activity and expression.

Next, we determined the extent to which RENCA macrobead-secreted RTN4, TSP1 or TIMP2 contributes to MEF2 activity. Depletion of RTN4 from conditioned media of mature macrobeads resulted in decreased MEF2 activity in both RENCA and DU145 cells (1.89-fold and 1.48-fold, respectively), but not DU145/GR cells (Figure 16A-C). Addition of the RTN4 eluate significantly increased MEF2 activity in RENCA and DU145 cells (1.97-fold and 3.96-fold, respectively) with no impact on DU145/GR cells (Figure 16D-F). TSP1 depletion also reduced MEF2 activity in DU145 cells (1.94-fold) but had no effect on RENCA or DU145/GR cells (Figure 17A-C). Introduction of TSP1 to naïve media increased activity in the DU145 cell line (4.94-fold) with no impact on RENCA or DU145/GR cells (Figure 17D-F). Comparable to RTN4, TIMP2-depletion decreased MEF2 activity in both RENCA and DU145 cells (1.50-fold and 1.51-fold, respectively) (Figure 18A-B) while addition of TIMP2 significantly increased MEF2 activity (3.45-fold and 6.38-fold, respectively) (Figure 18D-E). Altering TIMP2 levels in media (i.e. depletion from mature RENCA macrobead conditioned media or addition to naïve media) had no effect on MEF2 activity in the DU145/GR cell line (Figure 18C, F). These studies demonstrate that although tumor target cell-specific differences exist, individual proteins present in mature RENCA macrobead conditioned media can independently influence MEF2 reporter activity.

To determine whether RTN4, TSP1 or TIMP2 from mature RENCA macrobeads modulate MEF2 transcript levels in target tumor cells, we measured MEF2 isoform mRNA using qRT-PCR. While mock depletion has no effect on MEF2 isoform expression in any of the

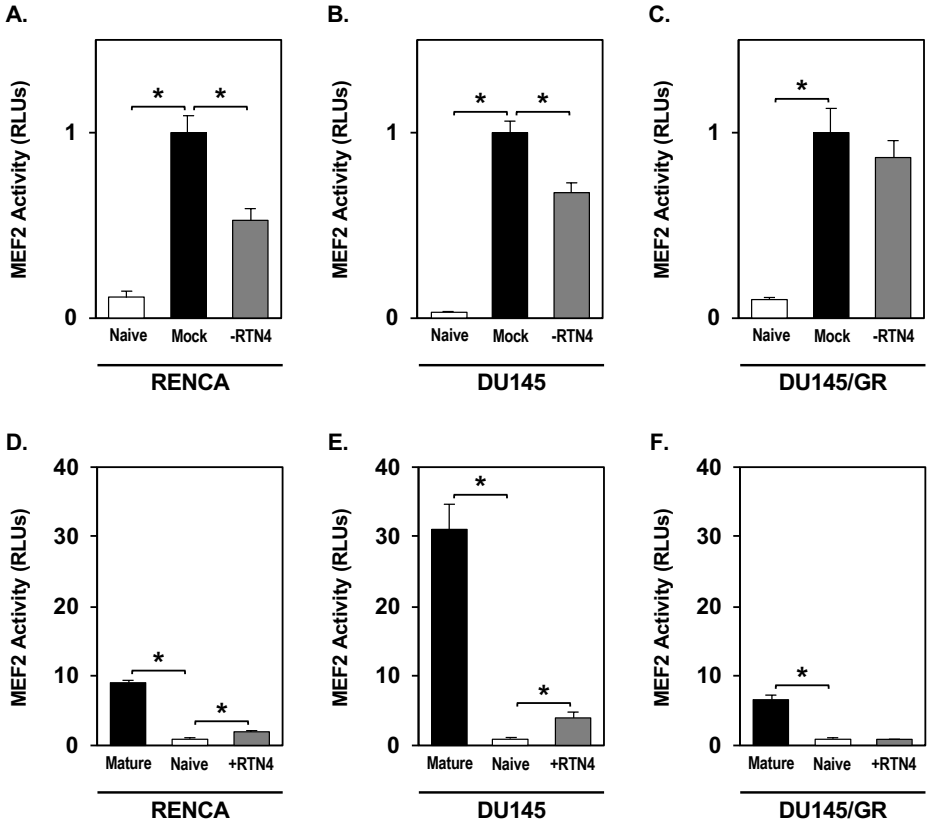

Figure 16: Cell-specific induction of MEF2 activity by mature RENCA macrobead- secreted RTN4. (A, D) RENCA, (B, E) DU145, and (C, F) DU145/GR cells transiently transfected with the MEF2 reporter were exposed to (A-C) RTN4-depleted mature RENCA macrobead conditioned media or (D-F) naïve media to which RTN4, eluted from immunodepleted media, was added. Luminescence values for the MEF2 reporter signal was measured using a dual-luciferase reporter assay and normalized to the internal control signal, Renilla. X-axis includes (A-C) naïve media (Naïve), Rb IgG depleted (Mock), or protein-specific depletion (-RTN4) from mature RENCA macrobead conditioned media and (D-F) mature RENCA macrobead conditioned media (Mature), Rb IgG added (Naïve), or protein-specific addition (+RTN4) to naïve media. Y-axis represents the fold change in MEF2 activity relative to Rb IgG (Mock) depleted mature RENCA macrobead conditioned media (A-C) or Rb IgG added to naïve media (Naïve) (D-F). *p-value < 0.05 relative to Mock in A-C or Naïve in D-F.

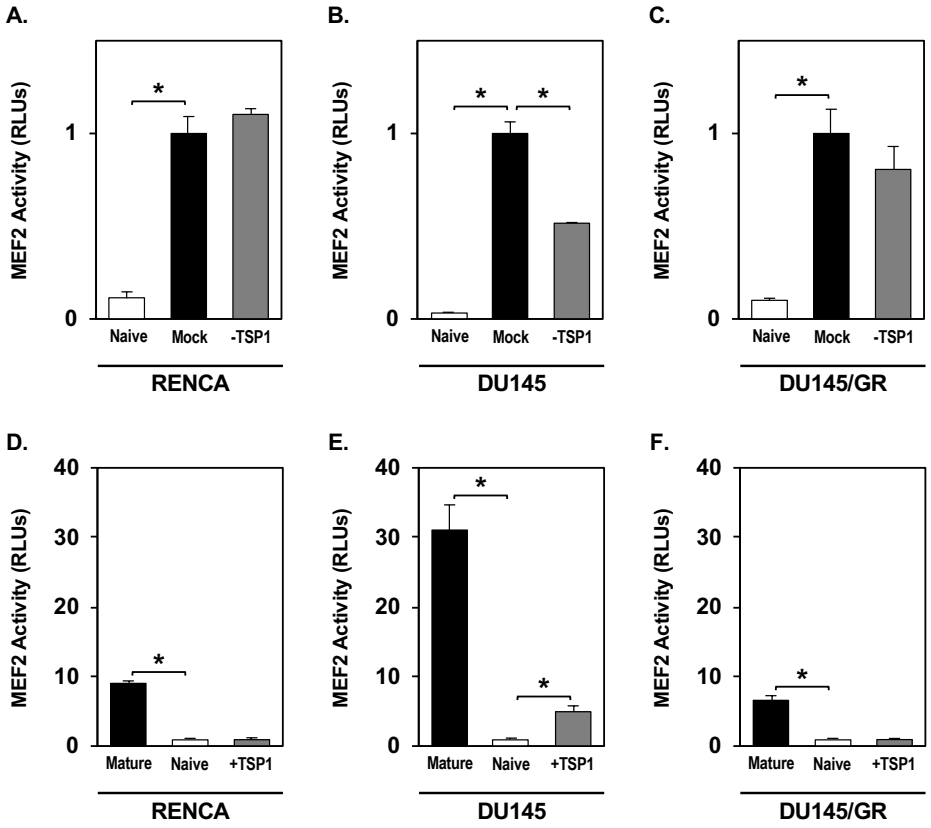

Figure 17: Cell-specific induction of MEF2 activity by mature RENCA macrobead- secreted TSP1. (A, D) RENCA, (B, E) DU145, and (C, F) DU145/GR cells transiently transfected with the MEF2 reporter were exposed to (A-C) TSP1-depleted mature RENCA macrobead conditioned media or (D-F) naïve media to which TSP1, eluted from immunodepleted media, was added. Luminescence values for the MEF2 reporter signal was measured using a dual-luciferase reporter assay and normalized to the internal control signal, Renilla. X-axis includes (A-C) naïve media (Naïve), Rb IgG depleted (Mock), or protein-specific depletion (-TSP1) from mature RENCA macrobead conditioned media and (D-F) mature RENCA macrobead conditioned media (Mature), Rb IgG added (Naïve), or protein-specific addition (+TSP1) to naïve media. Y-axis represents the fold change in MEF2 activity relative to Rb IgG (Mock) depleted mature RENCA macrobead conditioned media (A-C) or Rb IgG added to naïve media (Naïve) (D-F). *p-value < 0.05 relative to Mock in A-C or Naïve in D-F.

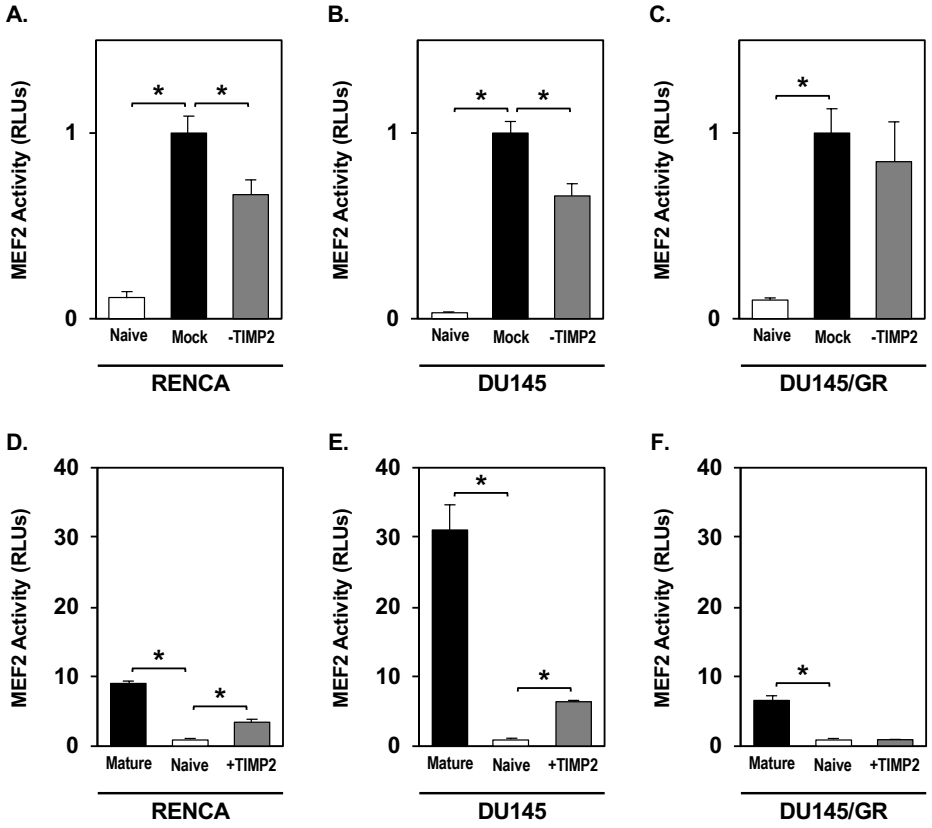

Figure 18: Cell-specific induction of MEF2 activity by mature RENCA macrobead- secreted TIMP2. (A, D) RENCA, (B, E) DU145, and (C, F) DU145/GR cells transiently transfected with the MEF2 reporter were exposed to (A-C) TIMP2-depleted mature RENCA macrobead conditioned media or (D-F) naïve media to which TIMP2, eluted from immunodepleted media, was added. Luminescence values for the MEF2 reporter signal was measured using a dual-luciferase reporter assay and normalized to the internal control signal, Renilla. X-axis includes (A-C) naïve media (Naïve), Rb IgG depleted (Mock), or protein-specific depletion (-TIMP2) from mature RENCA macrobead conditioned media and (D-F) mature RENCA macrobead conditioned media (Mature), Rb IgG added (Naïve), or protein-specific addition (+TIMP2) to naïve media. Y-axis represents the fold change in MEF2 activity relative to Rb IgG (Mock) depleted mature RENCA macrobead conditioned media (A-C) or Rb IgG added to naïve media (Naïve) (D-F). *p-value < 0.05 relative to Mock in A-C or Naïve in D-F.

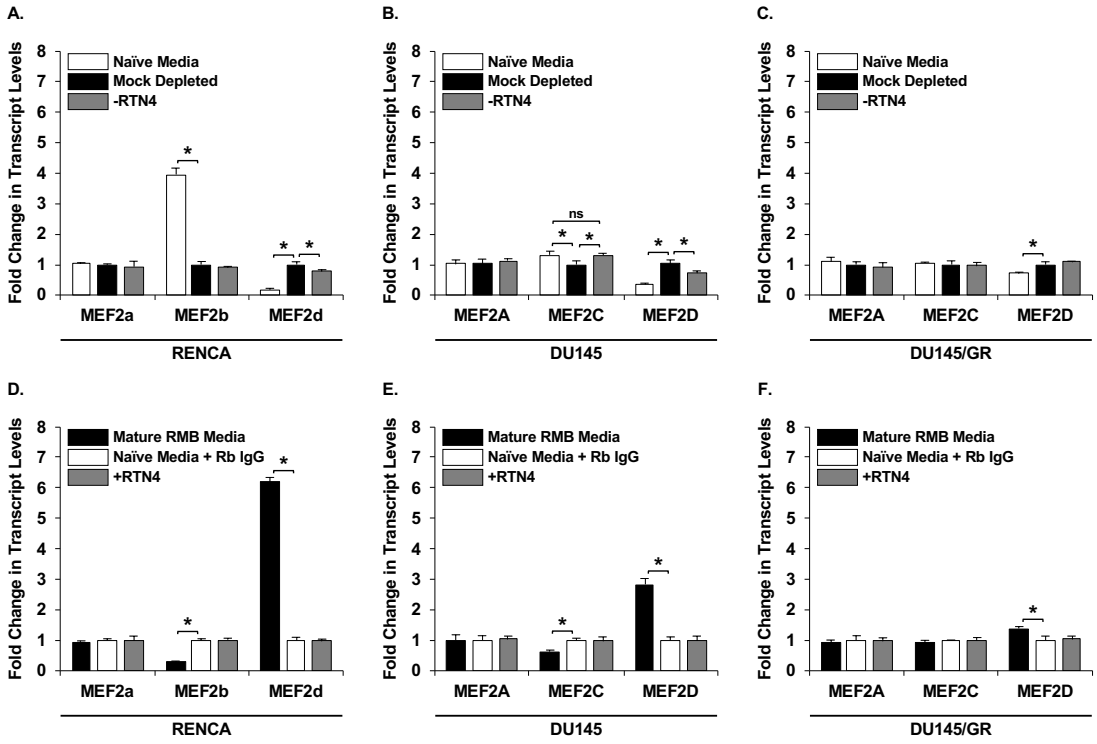

Figure 19: Mature RENCA macrobead-released RTN4 differentially regulates MEF2 expression. MEF2 isoform transcript levels were analyzed using Taqman based qRT-PCR in (A, D) RENCA, (B, E) DU145, and (C, F) DU145/GR cells 5 days following exposure to (A-C) RTN4-depleted mature RENCA macrobead conditioned media or (D-F) naïve media to which RTN4, eluted from immunodepleted media, was added. (A-C) naïve media, Rb IgG depleted (Mock Depleted), or protein-specific depletion (-RTN4) from mature RENCA macrobead conditioned media and (D-F) mature RENCA macrobead conditioned media, Rb IgG added, or protein-specific addition (+RTN4) to naïve media were included. Y-axis represents the fold change in transcript levels relative to Mock depleted mature RENCA macrobead conditioned media (A-C) or Rb IgG added to naïve media (D-F). *p-value < 0.05 relative to Mock Depleted in A-C or Naïve Media + Rb IgG in D-F.

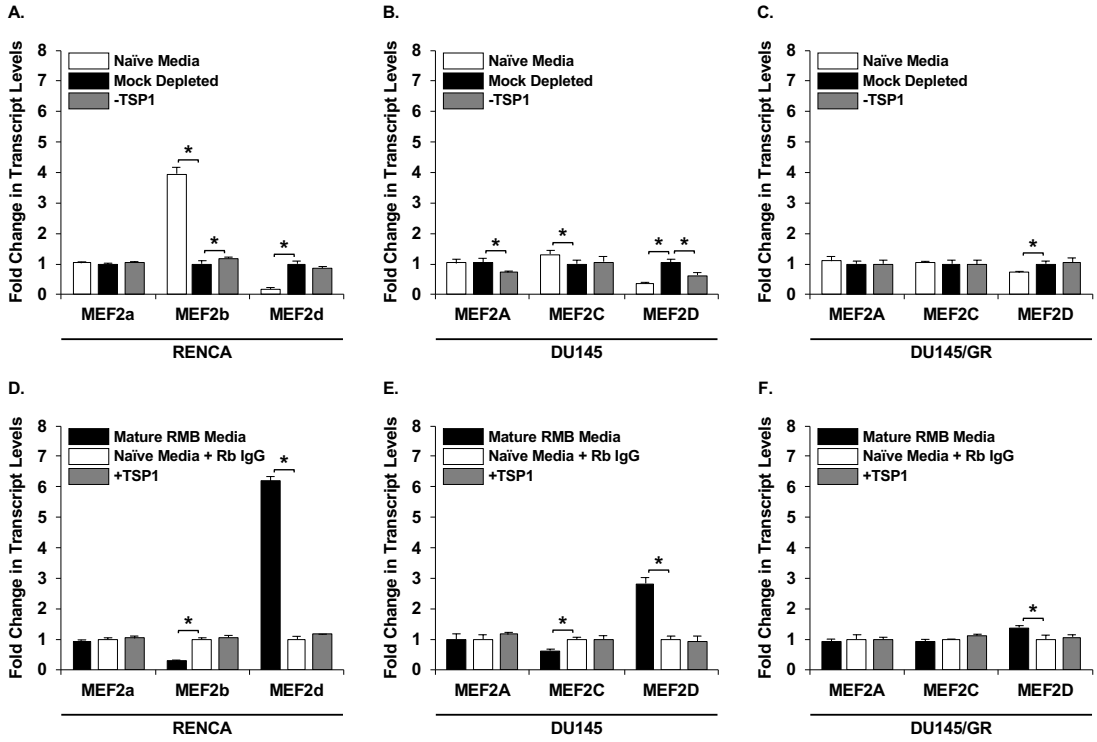

Figure 20: Mature RENCA macrobead-released TSP1 differentially regulates MEF2 expression. MEF2 isoform transcript levels were analyzed using Taqman based qRT-PCR in (A, D) RENCA, (B, E) DU145, and (C, F) DU145/GR cells 5 days following exposure to (A-C) TSP1-depleted mature RENCA macrobead conditioned media or (D-F) naïve media to which TSP1, eluted from immunodepleted media, was added. (A-C) naïve media, Rb IgG depleted (Mock Depleted), or protein-specific depletion (-TSP1) from mature RENCA macrobead conditioned media and (D-F) mature RENCA macrobead conditioned media, Rb IgG added, or protein-specific addition (+TSP1) to naïve media were included. Y-axis represents the fold change in transcript levels relative to Mock depleted mature RENCA macrobead conditioned media (A-C) or Rb IgG added to naïve media (D-F). *p-value < 0.05 relative to Mock Depleted in A-C or Naïve Media + Rb IgG in D-F.

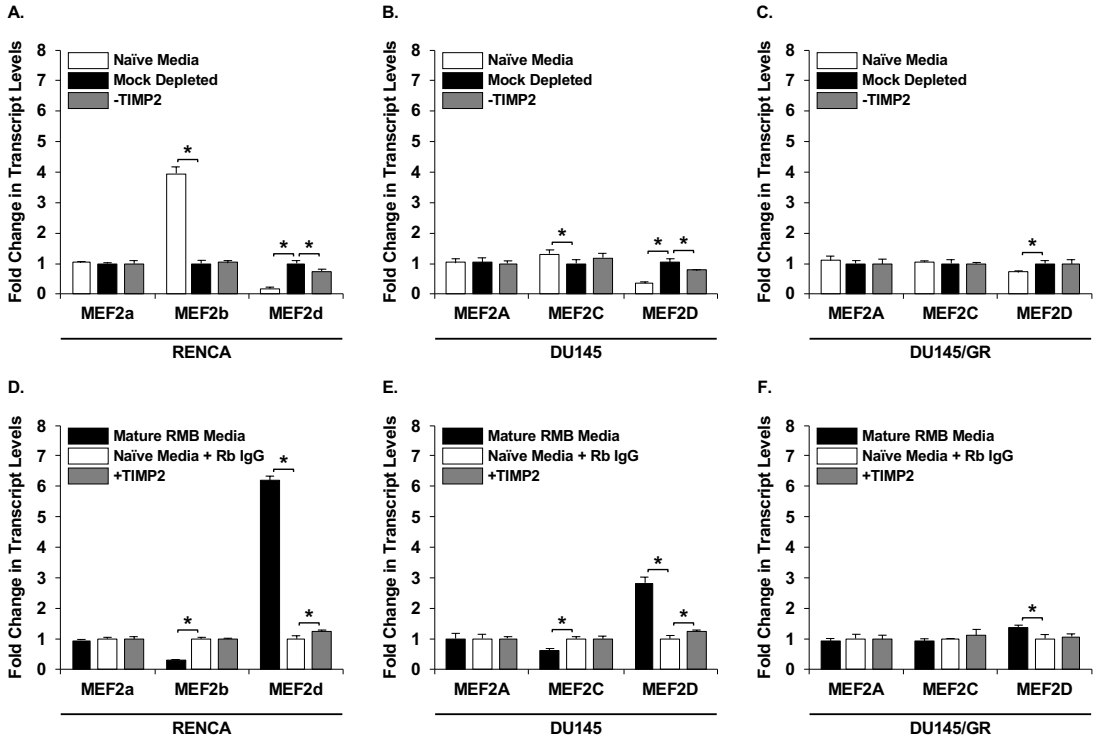

Figure 21: Mature RENCA macrobead-released TIMP2 differentially regulates MEF2 expression. MEF2 isoform transcript levels were analyzed using Taqman based qRT-PCR in (A, D) RENCA, (B, E) DU145, and (C, F) DU145/GR cells 5 days following exposure to (A-C) TIMP2-depleted mature RENCA macrobead conditioned media or (D-F) naïve media to which TIMP2, eluted from immunodepleted media, was added. (A-C) naïve media, Rb IgG depleted (Mock Depleted), or protein-specific depletion (-TIMP2) from mature RENCA macrobead conditioned media and (D-F) mature RENCA macrobead conditioned media, Rb IgG added, or protein-specific addition (+TIMP2) to naïve media were included. Y-axis represents the fold change in transcript levels relative to Mock depleted mature RENCA macrobead conditioned media (A-C) or Rb IgG added to naïve media (D-F). *p-value < 0.05 relative to Mock Depleted in A-C or Naïve Media + Rb IgG in D-F.

studied cell lines (data not shown), RTN4-depleted mature RENCA macrobead conditioned media significantly decreased *MEF2d* expression in RENCA and DU145 cells (Figure 19A-B). Removal of RTN4 also restored *MEF2C* expression in DU145 cells to levels present in naïve media (Figure 19B) while addition of this protein to naïve media had no effect on MEF2 isoform expression (Figure 19D-F). Depletion of TSP1 increased *MEF2b* transcripts in RENCA cells and although not significant, displayed a tendency towards decreased expression of *MEF2d* gene transcripts (Figure 20A). In the DU145 cell line, removal of TSP1 protein from mature RENCA macrobead conditioned media reduced *MEF2A* and *MEF2D* expression (Figure 20B). Similar to RTN4, addition of TSP1 to naïve media had a negligible impact on MEF2 isoform expression in any of the assessed cell lines (Figure 20D-F). TIMP2-depletion also reduced the *MEF2d/D* isoform in RENCA and DU145 cells (Figure 21A-B). Furthermore, supplementation of naïve media with TIMP2 eluate increased *MEF2d/D* transcripts in RENCA and DU145 (Figure 21D-E) cells. As observed in other contexts, depletion or addition of RTN4 (Figure 19C, F), TSP1 (Figure 20C, F) or TIMP2 (Figure 21C, F) had no effect on MEF2 isoform expression in DU145/GR cells.

3.12. RTN4, TSP1 and TIMP2 are necessary, but not individually sufficient, to achieve the full inhibitory capacity of RENCA macrobeads.

Finally, we investigated the functional relevance of protein depletion on growth of target cells. Culture of cell lines in Rb IgG depleted media did not have an appreciable effect on growth as compared to non-manipulated mature RENCA macrobead conditioned media (data not shown). Depletion of RTN4, TSP1 or TIMP2 from mature RENCA macrobead

conditioned media significantly increased survival of RENCA (Figure 22-24A) and DU145 cells (Figure 22-24B) relative to mock (Rb IgG) depleted media, suggesting that these proteins partially contribute to mature RENCA macrobead-mediated growth inhibition. However, individual depletion of these proteins from mature RENCA macrobead conditioned media had no impact on survival of DU145/GR cells (Figure 22-24C). This supports the notion that although these proteins may not be individually involved, other RENCA macrobead-secreted factors contribute to the observed inhibition of DU145/GR cells.

Addition of RTN4 eluate to naïve media did not influence survival of RENCA, DU145 or DU145/GR cells (Figure 22D-F). In contrast, naïve media supplemented with TSP1, recovered from mature RENCA macrobead conditioned media, decreased RENCA cell survival with a negligible effect on DU145 or DU145/GR cells (Figure 23D-F). Likewise, addition of TIMP2 eluate to naïve media decreased RENCA and DU145 but not DU145/GR cell (Figure 24D-F) survival. It is noted that although TSP1 and TIMP2 can induce cell-specific growth inhibition, each protein was not able to suppress growth of target cells to the extent of mature RENCA macrobeads. Therefore, the increased tumor growth observed following the depletion of the above specific proteins from the conditioned media of mature RENCA macrobeads and the decreased tumor growth in the presence of these proteins (especially TIMP2 for both DU145 and RENCA cells) supports the notion that individual proteins present in the mature RENCA macrobead secretome are necessary, but not individually sufficient, to achieve maximal growth inhibition of target tumor cells.

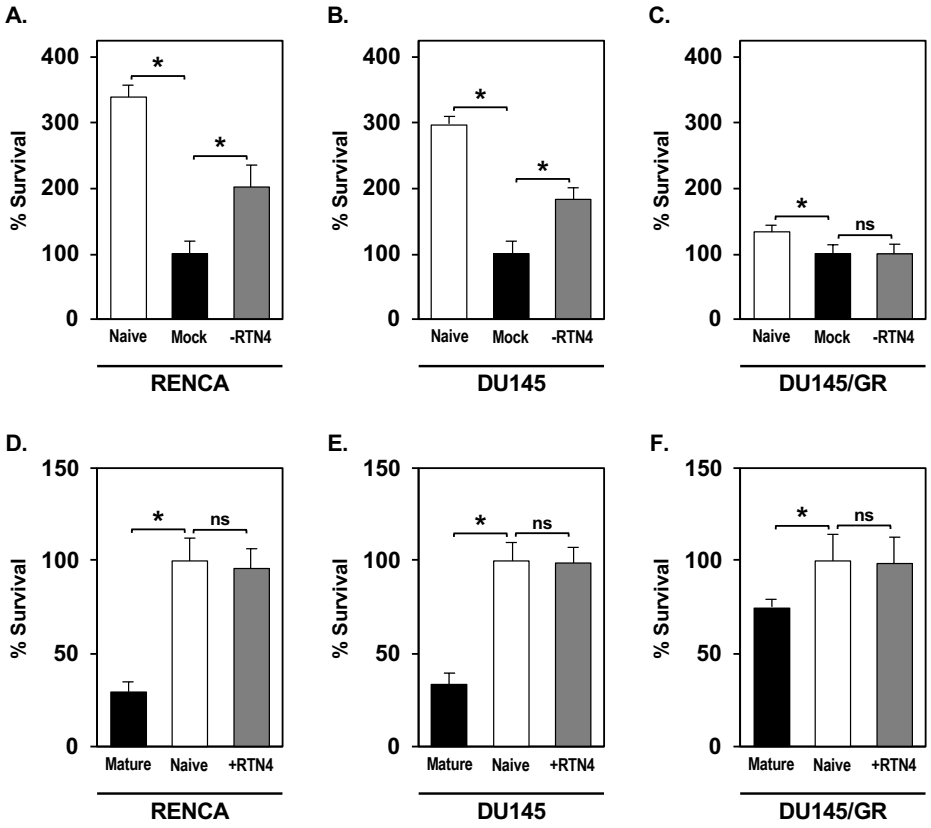

Figure 22: Mature RENCA macrobead-released RTN4 is necessary, but not individually sufficient, to achieve the full inhibitory capacity of RENCA macrobeads. (A, D) RENCA, (B, E) DU145, and (C, F) DU145/GR cells were exposed to (A-C) RTN4-depleted mature RENCA macrobead conditioned media or (D-F) naïve media to which RTN4, eluted from immunodepleted media, was added. Surviving cells were quantified 5 days following incubation with the indicated media by neutral red assay. X-axis includes (A-C) naïve media (Naïve), Rb IgG depleted (Mock), or protein-specific depletion (-RTN4) from mature RENCA macrobead conditioned media and (D-F) mature RENCA macrobead conditioned media (Mature), Rb IgG added (Naïve), or protein-specific addition (+RTN4) to naïve media. Y-axis represents the percent survival relative to Rb IgG (Mock) depleted mature RENCA macrobead conditioned media (A-C) or Rb IgG added to naïve media (Naïve) (D-F). *p-value < 0.05 relative to Mock in A-C or Naïve in D-F.

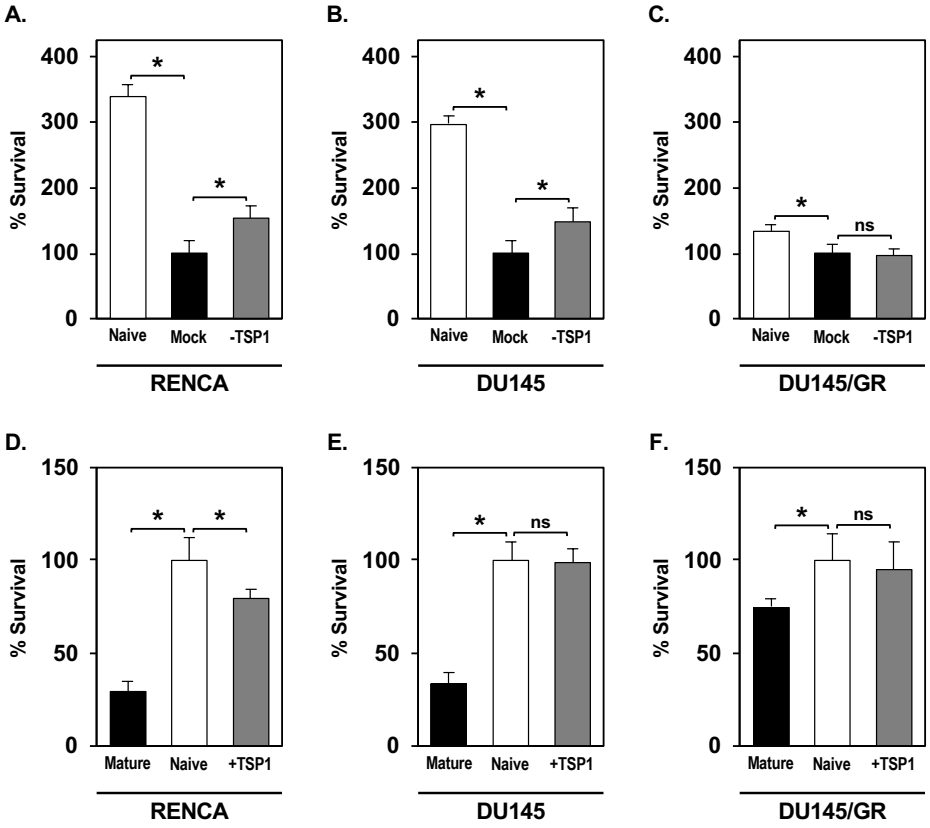

Figure 23: Mature RENCA macrobead-released TSP1 is necessary, but not individually sufficient, to achieve the full inhibitory capacity of RENCA macrobeads. (A, D) RENCA, (B, E) DU145, and (C, F) DU145/GR cells were exposed to (A-C) TSP1-depleted mature RENCA macrobead conditioned media or (D-F) naïve media to which TSP1, eluted from immunodepleted media, was added. Surviving cells were quantified 5 days following incubation with the indicated media by neutral red assay. X-axis includes (A-C) naïve media (Naïve), Rb IgG depleted (Mock), or protein-specific depletion (-TSP1) from mature RENCA macrobead conditioned media and (D-F) mature RENCA macrobead conditioned media (Mature), Rb IgG added (Naïve), or protein-specific addition (+TSP1) to naïve media. Y-axis represents the percent survival relative to Rb IgG (Mock) depleted mature RENCA macrobead conditioned media (A-C) or Rb IgG added to naïve media (Naïve) (D-F). *p-value < 0.05 relative to Mock in A-C or Naïve in D-F.

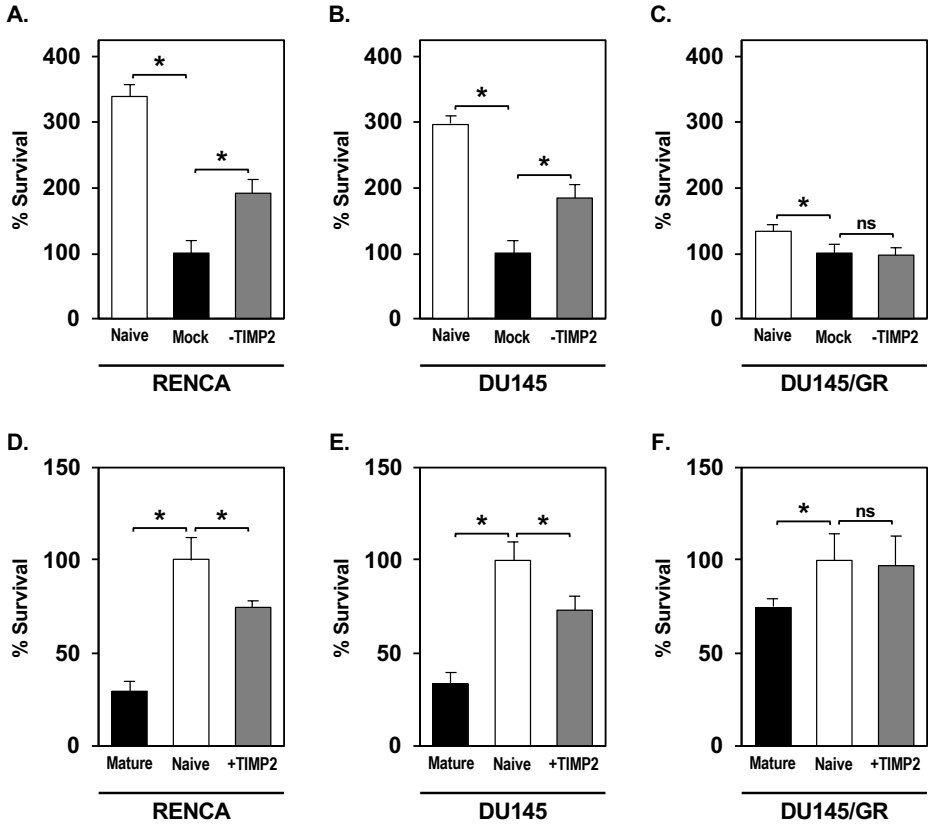

Figure 24: Mature RENCA macrobead-released TIMP2 is necessary, but not individually sufficient, to achieve the full inhibitory capacity of RENCA macrobeads. (A, D) RENCA, (B, E) DU145, and (C, F) DU145/GR cells were exposed to (A-C) TIMP2-depleted mature RENCA macrobead conditioned media or (D-F) naïve media to which TIMP2, eluted from immunodepleted media, was added. Surviving cells were quantified 5 days following incubation with the indicated media by neutral red assay. X-axis includes (A-C) naïve media (Naïve), Rb IgG depleted (Mock), or protein-specific depletion (-TIMP2) from mature RENCA macrobead conditioned media and (D-F) mature RENCA macrobead conditioned media (Mature), Rb IgG added (Naïve), or protein-specific addition (+TIMP2) to naïve media. Y-axis represents the percent survival relative to Rb IgG (Mock) depleted mature RENCA macrobead conditioned media (A-C) or Rb IgG added to naïve media (Naïve) (D-F). *p-value < 0.05 relative to Mock in A-C or Naïve in D-F.

CHAPTER 4: DISCUSSION

In this work, we provide evidence linking RTN4, TSP1, and TIMP2 with EGF receptor and MEF2 transcriptional regulation to the cell growth-inhibitory response elicited by RENCA macrobeads. Taken together, our data supports the idea that factors secreted by mature RENCA macrobeads activate EGFR and modulate MEF2 expression, particularly MEF2D, to inhibit cellular proliferation. The data also suggests that RENCA macrobeads exert their full growth inhibitory effects through additional signaling pathways or other cell communication mechanisms working in concert.

We used acute isoform-specific knockdown of the mammalian MEF2 gene to demonstrate that isoforms of this evolutionarily conserved transcription factor, deregulated in various cancer models, have distinct roles in mediating RENCA macrobead-induced inhibition. Our results show that exposure of target cells to RENCA macrobeads led to the upregulation of *MEF2D* (Figure 3). Moreover, *MEF2D*-silencing completely abolished the inhibitory activity of RENCA macrobeads (Figure 4), supporting a tumor suppressive role for this isoform in RENCA and DU145 cell lines. These results are consistent with data from other groups indicating that high expression of MEF2D is prognostic of survival in patients with renal carcinoma [298, 299]. Additionally, copy number loss of this MEF2 isoform was associated with prostate cancer progression [300], supporting the notion that intentional overexpression of MEF2D could reimpose growth control. In agreement with this idea, a previous study has demonstrated that exogenous MEF2D expression inhibited

cell proliferation in a panel of rhabdomyosarcoma cell lines [145]. Furthermore, in our study, we demonstrated that knockdown of MEF2D in the presence of RENCA macrobeads restored cell cycle distribution to levels present in actively proliferating cells (naïve media) (Figure 5-6). This data is in line with previous observations that inhibition of MEF2D upregulates cell cycle genes, leading to cell cycle reentry [151]. Upstream of the transcription start site, genes encoding GADD45 and CDKN1A/p21 contain putative MEF2 recognition elements [139, 144]. We have previously shown that *Gadd45* expression was elevated in RENCA cells treated with RENCA macrobeads [85], identifying a potential downstream component of RENCA macrobead-induced MEF2D signaling that regulates cell cycle progression. Moreover, ectopically expressed MEF2D increased p21 expression which correlated with cell cycle arrest [145, 301, 302].

We also observed that RENCA macrobeads repress the endogenous expression of *MEF2b* in target RENCA cells. Knockdown of *MEF2b* in this cell line reduced cell proliferation and independently promoted S-phase arrest, indicating that *MEF2b* may have oncogenic activity in this model system. Recently, MEF2B mutations have been described in multiple renal cancer subtypes [303] but the impact of these mutations on cancer pathogenesis and progression has not been studied. Mutations affecting the *MEF2B* gene have been noted in ~11% of diffuse large B-cell lymphomas (DLBCLs) [126]. In cell lines representing DLBCL, aberrant activity of MEF2B directly contributed to lymphomagenesis [122]. Subsequent knockdown of *MEF2B* downregulated the expression of the proto-oncogene BCL6 and repressed cell growth [122].

Although a direct effect on *MEF2A* expression was not observed in RENCA or DU145 cells following culture with RENCA macrobeads, knockdown of *MEF2A* limited the ability of RENCA macrobeads to inhibit the growth of both RENCA and DU145 cells as well as reduced the percentage of cells accumulating in S-phase, supporting a functional role for MEF2A in RENCA macrobead-induced inhibition. MEF2A influences the expression of cell cycle progression and DNA damage response genes in cooperation with other transcription factors [95]. Members of the MEF2 family bind as homo- and heterodimers to the appropriate DNA consensus sequence [97]. As a heterodimer, MEF2A preferentially interacts with MEF2D [304, 305]. As such, the loss of MEF2A could be at least partly responsible for the observed growth inhibition. Alternatively, RENCA macrobead regulation of target cell growth could be influenced by MEF2A DNA-binding activity or protein stability without impacting *MEF2A* mRNA levels. Previous work has suggested that post-translational modifications of MEF2A affect DNA-binding [306, 307] and disrupt MEF2A degradation [308]. Constitutively active MEF2A is associated with increased expression of the ER stress-induced apoptotic protein, CHOP [152], whose expression was upregulated in target RENCA cells in response to RENCA macrobeads [85]. Considering the significance of this isoform to the overall growth inhibitory effect of RENCA macrobeads, further research is necessary to understand the details by which MEF2A contributes to growth inhibition.

RENCA macrobead-induced growth regulation is also associated with decreased *MEF2C* transcripts in DU145 cells, yet *MEF2C*-silencing promoted cell growth. Based on TCGA datasets, MEF2C deletion occurs in a minority of high-grade prostate cancers [309].

MEF2C degradation has also been described to be necessary for cell proliferation and efficient progression of the cell cycle through mitosis [147]. Therefore, modulation of MEF2C expression might not be a mechanism by which RENCA macrobeads regulate cell proliferation. Since RENCA macrobeads release a large number of proteins and other signals, it is perhaps not unexpected that some of these factors may contribute to a proliferative phenotype. However, it is apparent that the activity of such factors, when present, are offset by antiproliferative signals to net an inhibitory response. Interestingly, RENCA macrobeads were able to restore inhibition of MEF2C-deficient DU145 cells to levels similar to NT siRNA treated cells with evidence of cell accumulation in G2/M phase. This supports the idea that RENCA macrobeads utilize an alternative mechanism to restrict cell proliferation in the absence of MEF2C, which remains to be explored.

Our studies also support mechanisms of cancer growth regulation that extend beyond the prevalent notion of inhibiting oncogenic signals to achieve tumor inhibition. Excessive activation of EGFR is associated with tumor progression and therefore, regulation of this receptor has been considered a major therapeutic target for cancer treatment. Two classes of therapeutic agents have been developed: monoclonal antibodies that block the binding of EGFR activating ligands, and tyrosine kinase inhibitors (TKIs) that reversibly or irreversibly occupy the ATP binding pocket of EGFR. However, the therapeutic efficacy of these EGFR inhibitors has been discouraging. Most cancers of epithelial origin express or overexpress EGFR [310, 311]; yet, only a few types of cancer, such as non-small cell lung cancer (NSCLC) and KRAS wild-type colorectal cancer, exhibit significant, albeit transient, effectiveness with these inhibitors of EGFR [312]. Our current study illustrates

that RENCA macrobeads, despite increasing EGFR expression and phosphorylation, effectively inhibit the growth of DU145, DU145/GR and MDA-MB-231 cells (Figure 7 and Figure 11). As a cell-based therapy, RENCA macrobeads allow for continuous delivery of numerous signals into the target cell environment, of which several have been previously reported to stimulate EGFR [85]. In contrast, studies with EGFR have largely been performed using fixed concentrations of common EGFR agonists, studied individually, for a short period of time [313-315], resembling a pulsatile or oscillatory pattern of signaling dynamics. The intensity and duration of EGFR signaling is critical for the cellular response and is influenced by multiple factors, including the ligand, ligand concentration, receptor density, docking state etc. In fact, an early paper that evaluated outcomes in cells that overexpress EGFR suggested that a continuum of receptor activation dictates growth responses wherein growth stimulation is associated with intermediate levels of activity while high activity levels contribute to growth inhibition [169]. Consistent with this notion and in accordance with our study, Gulli and coauthors demonstrated that physiological concentrations of EGF, accompanied by a 2-fold increase in EGFR activation, is associated with cell proliferation while supraphysiological doses of EGF, marked by a 15-fold upregulation in phosphorylated EGFR inhibited proliferation and biased cells towards death [167].

Furthermore, increased RENCA macrobead-induced inhibition corresponded with a sustained increase in EGFR expression and activation, at least in DU145 and MDA-MB-231 cells (Figure 8). This is consistent with mechanistic studies of a chemical compound of marine origin with cytotoxic properties, Aplidin™, which has been evaluated in breast

cancer cell lines [293] and has been tested as a treatment for unresectable renal cell carcinoma (APL-B-001-01) [316] and advanced prostate cancer (NCT00780975). Prolonged activation and delayed down-regulation of EGFR was shown to be necessary for Aplidin™ to be effective as an anti-tumor agent [293]. Putative negative feedback normally responsible for the transient nature of EGF-induced EGFR activation, involving receptor internalization and dephosphorylation, may be lost or impaired with RENCA macrobeads. Since EGFR agonists induce receptor internalization, variations in receptor ubiquitination, recycling or degradation of endocytosed receptors could contribute to the sustained signaling observed in the presence of RENCA macrobeads. In fact, differences in these aspects of EGFR processing have been reported for a variety of EGFR ligands [190, 317]. Alternatively, RENCA macrobead signals could reduce recruitment of tyrosine phosphatases responsible for receptor inactivation. In one such study, depletion of the protein tyrosine phosphatase, PTP1B, caused transient EGF-induced EGFR phosphorylation to become sustained [318]. In the same manner, signals that stabilize adaptor molecules, such as Grb2, to prevent dephosphorylation of tyrosines on the cytoplasmic tail of EGFR could dictate the extent to which EGFR signaling is preserved [319]. Importantly, sustained signaling has been associated with growth control while transient activation has been linked to proliferation [320-322]. In our studies, RENCA macrobeads were shown to induce sustained activation of EGFR in both DU145 and MDA-MB-231 cells, which was accompanied by growth inhibition and cell accumulation in S-phase (Figure 12).

Although not as robust as in DU145 or MDA-MB-231 cells, growth inhibition is also observed in DU145/GR and MCF7 cells, which have either reduced kinase activity or low levels of EGFR, indicating that the anti-proliferative effects of RENCA macrobeads are not necessarily unique to cells expressing high levels of functional EGFR, but signaling through EGFR partially contributes to RENCA macrobead-induced growth inhibition. RENCA macrobead-induced EGFR activation was transient in DU145/GR cells and non-existent in MCF7 cells. These cell lines accumulate in G2/M phase, indicating that RENCA macrobeads can arrest cells at two distinct parts of the cell cycle. Given the variety of signals released by RENCA macrobeads, the notion of restricting growth through multiple mechanisms is plausible, but further research is needed to explore RENCA macrobead-mediated growth inhibitory mechanisms in these cell lines. Signaling partners of the p21 gene may be interesting candidates for further evaluation. p21, an inhibitor of cyclin dependent kinases (CDKs), directly regulates CDK1, CDK2, CDK3, CDK4 and CDK6 activity [323]. Overexpression of p21 usually leads to G1 or G2 arrest by inhibiting CDK activity [324]. p21 can also directly inhibit DNA synthesis by binding to proliferating cell nuclear antigen (PCNA), causing cells to arrest in S phase [286]. The expression of p21 can be regulated at the transcriptional, post-transcriptional or post-translational levels by p53-dependent and p53-independent mechanisms [325]. Insults that damage DNA lead to activation of p53 and p53-dependent induction of the p21 gene. Expression of p21 can also be induced by DNA-damaging agents via the ATM/ATR-ERK pathway. In these instances, activated ERK-induces p21 expression in a p53-independent manner [326]. Interestingly, both DU145 and MDA-MB-231 cells have mutant *TP53* genes [327, 328] and appear to respond to RENCA macrobeads through activation of EGFR upstream of ERK activity. In

contrast, MCF7 cells with functional p53 [327] exhibit no EGFR activity in response to RENCA macrobeads, but might be able to induce p21 through p53-dependent mechanisms.

Our work also investigated the possibility of an association between EGFR expression and RENCA macrobead-mediated MEF2 regulation. We observed that MEF2 activity and MEF2D expression were substantially higher in cells expressing greater levels of functional EGFR (i.e. DU145 and MDA-MB-231 cells) while cell lines with non-functional EGFR or low-levels of receptor displayed reduced ratios of MEF2 activity or MEF2D expression (i.e. DU145/GR and MCF7 cells) (Figure 9 and Figure 10). Although we observed a possible association between EGFR and MEF2, this family of transcription factors serve as endpoints for multiple signaling pathways. For example, MAPK and calcium-dependent signaling have been identified as regulators of MEF2 activity [95], both of which are well known hubs for numerous receptor-mediated signaling pathways. Within the MAPK signaling cascade that includes ERK, p38 kinase and c-Jun N-terminal kinase (JNK), ERK signaling downstream of EGFR activation has been described to play a critical role in the production of MEF2D [329]. In addition, leucine-rich repeat kinase 2 (LRRK2), a kinase enzyme reported to delay EGFR degradation and enhance ERK activation [330] directly regulates MEF2 activity [331]. Additional studies using EGFR knockdown and overexpression constructs in these cell lines as well as analysis of central downstream components will further clarify the role of this receptor in regulating MEF2 behavior in response to RENCA macrobeads.

Lastly, our work identified three specific proteins, RTN4, TSP1 and TIMP2, in conditioned media of mature RENCA macrobeads that contribute to growth regulation of external tumor cells. We show that individual depletion of these proteins from RENCA macrobead conditioned media increases survival of RENCA and DU145 cells (Figures 22-24). We further demonstrate that addition of TIMP2 to naïve cultures can independently decrease cell survival of these same cell lines, while TSP1 only reduced RENCA cell survival. We also demonstrate that RTN4 and TSP1 significantly reduced EGFR activation in RENCA and DU145 cells but not in the DU145/GR cell line (Figures 13-14). In a complementary set of experiments, we show that the addition of RTN4 and TSP1 into naive culture media increases EGFR phosphorylation in the same cell lines. Previous studies have reported the ability of these proteins to restrict the growth of multiple cancers through diverse mechanisms. Regulators of EGFR signaling, like RTN4, TSP1, and TIMP2, can modulate EGFR phosphorylation through physical interactions with the EGFR extracellular domain or through an intracellular event leading to activation or inactivation of the catalytic domain. Prior studies indicate that these proteins regulate EGFR activity through an interaction independent of the ligand binding domain of EGFR [234, 261, 280, 281]. Consistent with these previous studies, we have observed that EGFR blockade using (1) the chimeric anti-EGFR monoclonal antibody, C225, a research grade biosimilar of the drug cetuximab, or (2) the 528 monoclonal antibody, successfully blocked EGF-mediated EGFR phosphorylation but had a negligible effect on RENCA macrobead-mediated EGFR activation (unpublished data). Moreover, the lack of response observed in DU145/GR cells suggests that the intracellular kinase function of EGFR needs to be intact to elicit a response to RENCA macrobead-released RTN4 and TSP1.

Unexpectedly, we noted a substantial reduction in total EGFR levels upon removal of RTN4, TSP1 and TIMP2 from RENCA macrobead conditioned media in RENCA and DU145 cells, suggesting a potential role for these proteins in mediating EGFR stability. Precedence for RTN4-induced stabilization of proteins has been previously established, although studies evaluating EGFR have not been performed. For example, RTN4 promoted clustering and prevented degradation of the ER-localized chaperone, protein disulfide isomerase, in murine spinal motor neurons [332]. In addition, receptors for TSP1 and TIMP2 have been described to regulate EGFR trafficking, protract internalization and reduce EGFR degradation [333, 334] but further studies are necessary to establish whether these proteins working through their cognate receptors regulate EGFR stability in response to RENCA macrobeads.

We also identified a novel role for exogenous RTN4, TSP1 and TIMP2 in modulating MEF2 activity and regulating MEF2 expression. With exception of TSP1 in RENCA cells, depletion of these proteins from RENCA macrobead conditioned media partially diminished MEF2 activity (Figure 16-18). Likewise, addition of proteins to naïve media increased MEF2 activity. We also demonstrated that depletion of RTN4, TSP1 and TIMP2 decreased expression of the MEF2D isoform (Figure 19-21), established to be critical for RENCA macrobead-mediated inhibition. In the same manner, TIMP2 but not RTN4 or TSP1 eluates increased MEF2D expression in RENCA and DU145 cells. Overall, our data underlies an essential role of RTN4, TSP1 and TIMP2 in mediating RENCA macrobead-induced inhibition.

The studies presented in this thesis support a mechanism by which RENCA macrobeads, at least partially, regulate tumor cell growth external to the macrobead. Together, these data demonstrate that cancer cells can respond to external growth control signals and provide a rationale for the hypothesis that in order to better control cancer growth, it may be beneficial to consider tumors as a biological system with dysfunctional, but responsive, growth regulatory mechanisms. As a group of discrete growth-restricted tumor colonies that secrete a large number of tumor-inhibitory signals, RENCA macrobeads can be used as a biological-systems therapeutic to regulate a highly dysregulated cancer system, simultaneously targeting multiple cancer hallmarks to limit the proliferative potential of tumor cells. The RENCA macrobead concept expounds upon principles presented by Prehn [335] whereby the growth of a given tumor may be regulated by biological signals indicating the presence of a tumor mass, even when that mass is not actually present [335-337]. This is based on observations that tumors follow a Gompertzian growth curve that approach an asymptote, similar to normal organs. In other words, growth is represented by an early exponential phase followed by decelerated progression as organ systems enlarge and approach a maximum size whereby some mechanism monitors the ultimate size and precisely regulates its growth along the typical Gompertzian curve toward an asymptotic plateau [89, 90, 338-341]. Individual tumor colonies encapsulated within the agarose matrix of RENCA macrobeads regulate their own growth [1]. That is, tumor colonies reach a maximal size and maintain a constant size through a balance of growth and death processes. Within RENCA macrobeads, the equilibrium maintained by the growth and

death of individual tumor colonies can be viewed as a regulated system, that when applied to freely growing tumor cells, provides a "systems" approach to the treatment of cancers.

Systems biological approaches to regulate cancer growth are increasingly being recognized as critical to address the complexities of cancer. To date, the cancer treatment arsenal has relied on a large array of chemotherapeutics, targeted therapies and immunotherapies; yet, the success of cancer treatments has been limited by inconsistent therapeutic responses, drug resistance, and tumor recurrence, stemming from the astounding heterogeneity in cancers. Recent advances in cancer research, specifically in the field of cancer genomics, has led to the development of a substantial number of novel therapies. Between 2017-2019, the U.S. FDA approved 153 new drugs, of which 46 (30%) were indicated for the treatment of cancers [342-344], illustrating the momentum of these efforts. Despite the initial responsiveness of cancers to a specific treatment, it is evident that most cancers cannot be successfully treated exclusively with single-agent therapies [345, 346]. Based on the potential for additive or synergistic anticancer effects, combination therapies hold tremendous promise for effective clinical outcomes [346] as evidenced by more than 55 new drug combinations approved for joint use by the FDA in the same time frame [347]. The expansive list of cancer driver genes and mutations [348], the multiple hallmarks of cancer described by Hanahan and Weinberg [7, 349], the intricacies of signaling networks [350, 351], and the mutual interactions between cancerous cells and the tumor microenvironment [352] reinforces the requirement to simultaneously target multiple cancer dependencies to achieve growth control. The Halifax project, a recent collaboration of more than 350 researchers globally, similarly supports a "broad-spectrum integrative

design" for cancer therapy that can collectively impact multiple pathways central to the development and progression of cancer [353]. It is our view that RENCA macrobeads, as a complex, non-toxic, biological system, act to provide a multifaceted systems restoration of normal function and interactions. As such, RENCA macrobeads act not as a precision-medicine approach to single targets; but rather, can be considered a biological-systems therapy that reestablishes more normal regulation to a highly dysfunctional and dysregulated cancer system.

With this mindset, it is our contention that the "war on cancer," based on the premise of total eradication of all cancer cells within an individual, may not be the most ideal paradigm for both scientific investigation and clinical care. Between *remission* and *progression*, there is a middle ground where a patient's cancer can be controlled and they can live, even thrive, with the disease. What is now often considered a terminal diagnosis may be able to be managed as a chronic condition. Like cancer, not long ago, a diagnosis of HIV was considered an inevitable death sentence [354, 355]. Yet today, the approximately 1.1 million people living with HIV in the United States [356] are treated with once-daily, combination antiretroviral therapy for the remainder of their lives [357]. These advances in HIV treatment have transformed the life expectancy, quality of life, and health outcomes of newly diagnosed HIV-positive individuals. Indeed, as of 2019, the lifespan of a person living with HIV matched the general population [358-360]. In the same manner, focusing on cancer as a clinically manageable chronic disease offers hope and a new perspective in cancer care, with an emphasis on living with a high quality of life.

Appendix A

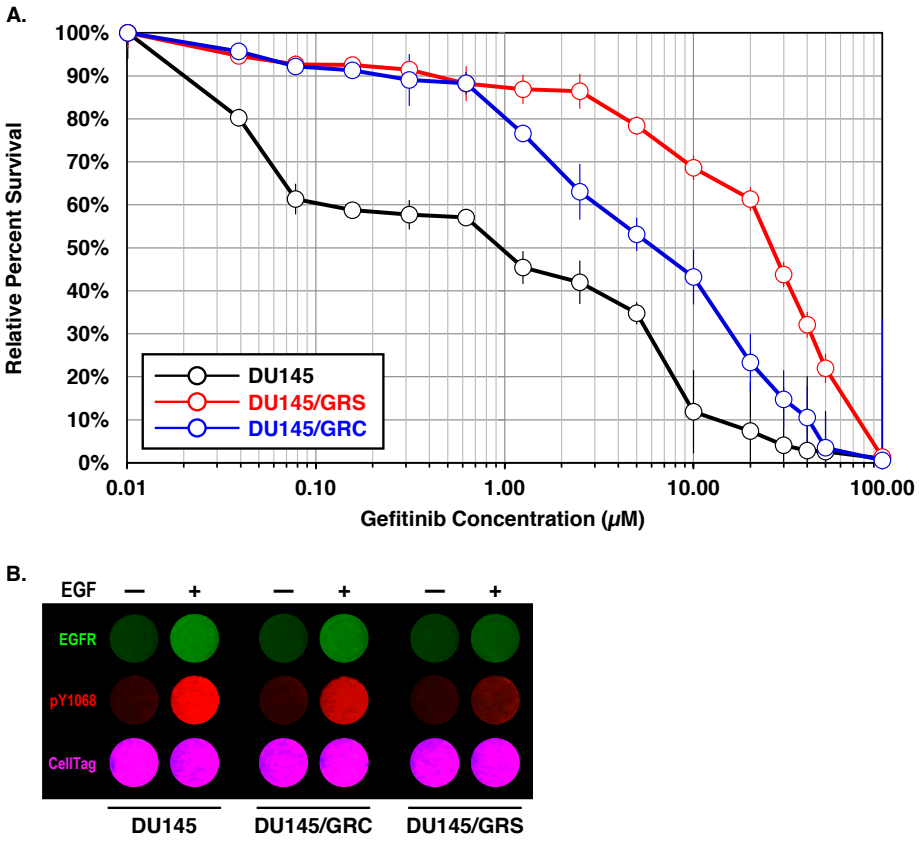

Supplementary Figure 1: Characterization of gefitinib-resistant DU145 cell lines. The DU145/GRS gefitinib-resistant subline was established by culturing parental DU145 cells with incrementally increasing gefitinib concentrations from 1 µM to 3 µM over 6 months. A second gefitinib-resistant subline (DU145/GRC) was generated by continuously culturing parental DU145 cells in high-dose (3 µM) gefitinib. (A) Assessment of resistance to gefitinib in drug-tolerant and resistant populations, and (B) sensitivity to 100 ng/mL EGF in the parental DU145 and drug resistant DU145 sublines.

Supplementary Table 1A: List of mouse primer and probe sequences used for qRT-PCR.

Gene Name	RefSeq No.	Exon Location	Primer	Probe
MEF2a	NM_001033713	5-6	5'-AAGTTCTGAGGTGGCAAGC-3'	5'-/56-FAM/TGCTGAATC/ZEN/TGTCCTCCGAGAGTGG/3IABkFQ/-3'
			5'-CTGATGCTGACGATTACTTTGAG-3'	
MEF2b	NM_001045484	2-3	5'-ATACTGGAAGAGGCGTTGC-3'	5'-/56-FAM/AATGTCGCA/ZEN/GTCACAAAGCACGC/3IABkFQ/-3'
			5'-CTAGACCAAAGGAACAGGCA-3'	
MEF2c	NM_025282	7-9	5'-GTTGCCGTATCCATTCCCT-3'	5'-/56-FAM/AGATCTGAC/ZEN/ATCCGGTGCAGGC/3IABkFQ/-3'
			5'-TGTAACACATAGACCTCCAAGTG-3'	
MEF2d	NM_133665	5-7	5'-TGACATAGCCATTCCCAACG-3'	5'-/56-FAM/CAGGCTCCA/ZEN/TTAGCACTGTTGAGGT/3IABkFQ/-3'
			5'-GCCAGCACTACAGAGAAACAG-3'	
Gapdh	NM_008084	2-3	5'-GTGGAGTCATACTGGAACATGTAG-3'	5'-/56-FAM/TGCAAATGG/ZEN/CAGCCCTGGTG/3IABkFQ/-3'
			5'-AATGGTGAAGGTCGGTGTG-3'	
Tbp	NM_013684	4-5	5'-CCAGAACTGAAAATCAACGCAG-3'	5'-/56-FAM/ACTTGACCT/ZEN/AAAGACCATTGCACTTCGT/3IABkFQ/-3'
			5'-TGTATCTACCGTGAATCTTGGC-3'	

Supplementary Table 1B: List of human primer and probe sequences used for qRT-PCR.

Gene Name	RefSeq No.	Exon Location	Primer	Probe
MEF2A	NM_005587	13-14	5'-GGTTCGGACTTGATGCTGAT-3'	5'-/56-FAM/AACCCTGAG/ZEN/ATAACTGCCCTCCAG/3IABkFQ/-3'
			5'-CACCACCTAGGACAAGCAG-3'	
MEF2B	NM_001145785	1-2	5'-GATGCGGGAGATCTGGATT-3'	5'-/56-FAM/CATCGTCCC/ZEN/AGGCTGAGTGGAAT/3IABkFQ/-3'
			5'-CCCCTGATCTTCGTGCAG-3'	
MEF2C	NM_002397	3-4	5'-TGTTGGTGCTGTTGAAGATGA-3'	5'-/56-FAM/TGCTGTGTG/ZEN/ACTGTGAGATTGCGC/3IABkFQ/-3'
			5'-AGATTACGAGGATTATGGATGAACG-3'	
MEF2D	NM_001271629	11-12	5'-CTGCACTGGTCAACTGGTAA-3'	5'-/56-FAM/CTCCCCTTC/ZEN/TCTTCCATGCCCAC/3IABkFQ/-3'
			5'-CAGTCTACTCATTCGCTCACC-3'	
GAPDH	NM_002046	2-3	5'-TGTAGTTGAGGTCAATGAAGGG-3'	5'-/56-FAM/AAGGTCGGA/ZEN/GTCAACGGATTTGGTC/3IABkFQ/-3'
			5'-ACATCGCTCAGACACCATG-3'	
TBP	NM_003194	5-6	5'-CAAGAACTTAGCTGGAAAACCC-3'	5'-/56-FAM/CACAGGAGC/ZEN/CAAGAGTGAAGAACAGT/3IABkFQ/-3'
			5'-GATAAGAGCCACGAACCAC-3'	

Supplementary Table 1: Primer and probe sequences. List of (A) mouse and (B) human primer and probe sequences used for qRT-PCR.

Appendix B

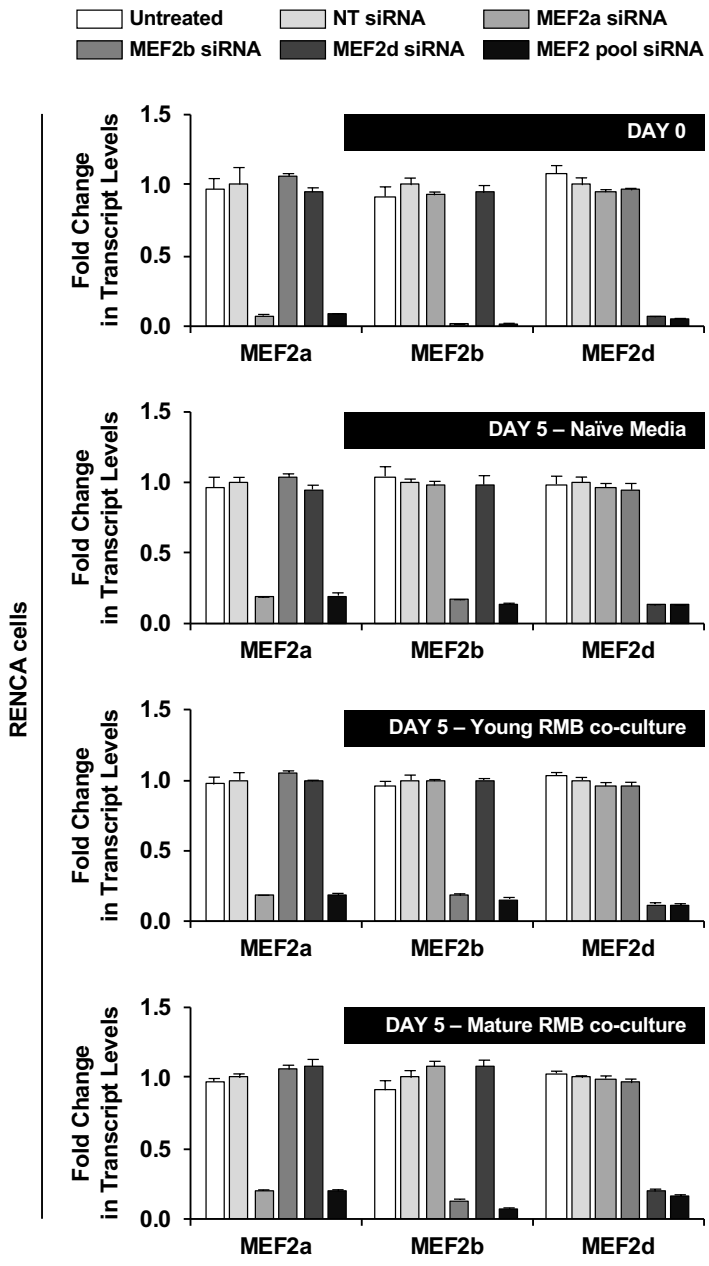

Supplementary Figure 2: MEF2 siRNA induces efficient and isoform-specific in vitro gene silencing. MEF2 isoform transcript levels were analyzed using Taqman based qRT-PCR in RENCA cells transiently transfected with two-rounds of 1 μM non-targeting (NT), isoform-specific, or combined expressed MEF2 isoform (MEF2 pool) siRNA at the beginning (day 0) of the growth inhibition assay and following culture for 5 days in naïve media, or together with young or mature RENCA macrobeads (RMB).

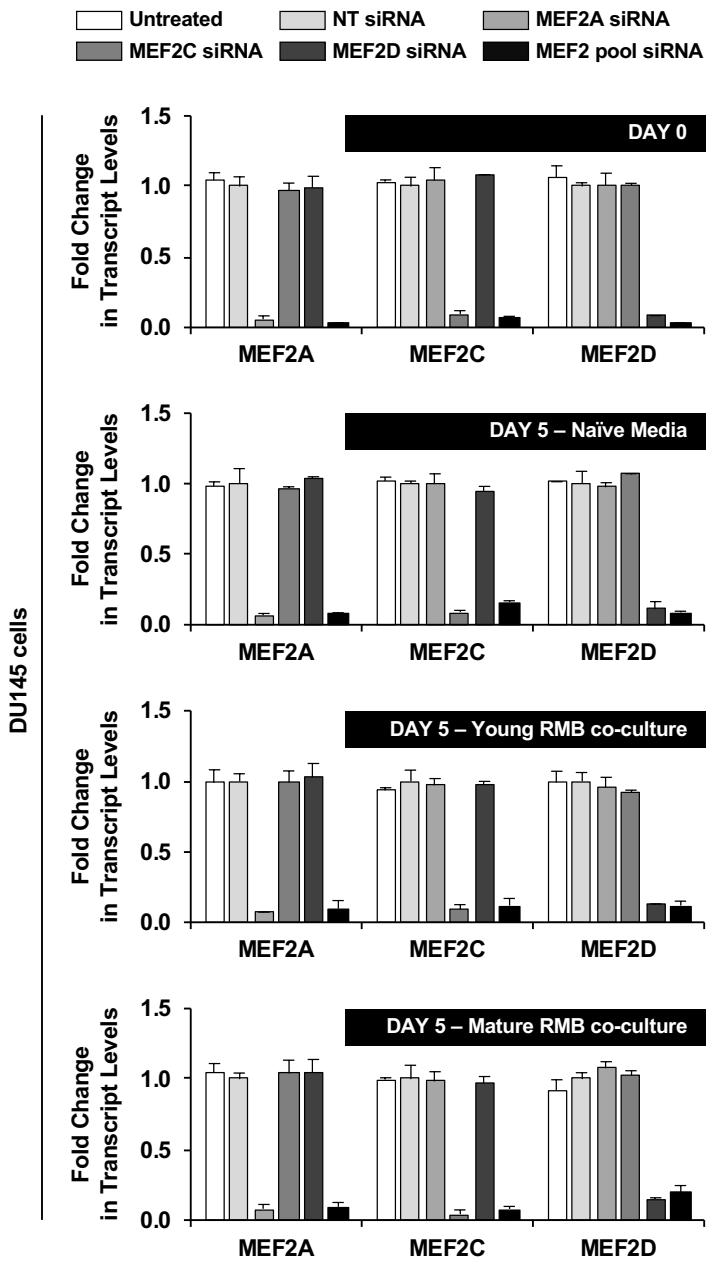

Supplementary Figure 3: MEF2 siRNA induces efficient and isoform-specific in vitro gene silencing. MEF2 isoform transcript levels were analyzed using Taqman based qRT-PCR in DU145 cells transiently transfected with two-rounds of 1 μM non-targeting (NT), isoform-specific, or combined expressed MEF2 isoform (MEF2 pool) siRNA at the beginning (day 0) of the growth inhibition assay and following culture for 5 days in naïve media, or together with young or mature RENCA macrobeads (RMB).

	ELISA	Mock Depleted (ng/mg)	Immunodepleted (ng/mg)	Eluate (ng/mg)
5% NCS	TSP1	10.060 ± 1.801	ND	9.071 ± 1.416
	TIMP2	1.218 ± 0.162	ND	1.102 ± 0.204
	RTN4	0.463 ± 0.077	ND	0.429 ± 0.098
5% FBS	TSP1	11.816 ± 1.765	ND	10.792 ± 1.433
	TIMP2	1.507 ± 0.209	ND	1.465 ± 0.262
	RTN4	0.490 ± 0.093	ND	0.442 ± 0.074

Supplementary Table 2: Protein-specific antibodies effectively deplete RTN4, TSP1 and TIMP2 from mature RENCA macrobead conditioned media. Protein specific anti-IgG antibodies were incubated with RENCA macrobead cultures (5% NCS for use with RENCA cells or 5% FBS for use with DU145 and DU145/GR cells) 24 hours prior to immunodepletion using Protein A magnetic beads. Rb IgG was used as a control (mock depleted). Concentrated media was analyzed by ELISA for RTN4, TSP1 and TIMP2. ND, not detected in tested media. Values represent quantity (ng) of detected protein relative to total protein (mg).

REFERENCES

1. Smith BH, Gazda LS, Conn BL, Jain K, Asina S, Levine DM et al. Three-dimensional culture of mouse renal carcinoma cells in agarose macrobeads selects for a subpopulation of cells with cancer stem cell or cancer progenitor properties. Cancer Res 2011;71(3):716-24.
2. Collaborators GBDCoD. Global, regional, and national age-sex-specific mortality for 282 causes of death in 195 countries and territories, 1980-2017: a systematic analysis for the Global Burden of Disease Study 2017. Lancet 2018;392(10159):1736-88.
3. American Cancer Society. Global Cancer Facts & Figures 4th Edition. Atlanta: American Cancer Society; 2018.
4. Bray F, Ferlay J, Soerjomataram I, Siegel RL, Torre LA, Jemal A. Global cancer statistics 2018: GLOBOCAN estimates of incidence and mortality worldwide for 36 cancers in 185 countries. CA Cancer J Clin 2018;68(6):394-424.
5. Weinberg RA: The biology of cancer; 2014.
6. Vogelstein B, Kinzler KW. The Path to Cancer-Three Strikes and You're Out. N Engl J Med 2015;373(20):1895-8.
7. Hanahan D, Weinberg RA. Hallmarks of cancer: the next generation. Cell 2011;144(5):646-74.
8. Alberts B: Molecular biology of the cell. New York: Garland Science; 2008.
9. Varmus H, Weinberg RA: Genes and the biology of cancer. New York: Scientific American Books; 1996.
10. Marusyk A, Almendro V, Polyak K. Intra-tumour heterogeneity: a looking glass for cancer? Nat Rev Cancer 2012;12(5):323-34.
11. Sonnenschein C, Soto AM. An Integrative Approach Toward Biology, Organisms, and Cancer. Methods Mol Biol 2018;1702:15-26.
12. Soto AM, Sonnenschein C. The tissue organization field theory of cancer: a testable replacement for the somatic mutation theory. Bioessays 2011;33(5):332-40.
13. Bizzarri M, Cucina A, Conti F, D'Anselmi F. Beyond the oncogene paradigm: understanding complexity in cancerogenesis. Acta Biotheor 2008;56(3):173-96.
14. Soto AM, Sonnenschein C. The somatic mutation theory of cancer: growing problems with the paradigm? Bioessays 2004;26(10):1097-107.
15. Idikio HA. Human cancer classification: a systems biology- based model integrating morphology, cancer stem cells, proteomics, and genomics. J Cancer 2011;2:107-15.
16. Gospodarowicz M, Benedet L, Hutter RV, Fleming I, Henson DE, Sobin LH. History and international developments in cancer staging. Cancer Prev Control 1998;2(6):262-8.
17. Brierley J, Gospodarowicz MK, O'Sullivan B, Wittekind C, International Union against C: TNM classification of malignant tumours; 2017.
18. Lu M, Zhan X. The crucial role of multiomic approach in cancer research and clinically relevant outcomes. EPMA J 2018;9(1):77-102.
19. Song Q, Merajver SD, Li JZ. Cancer classification in the genomic era: five contemporary problems. Hum Genomics 2015;9:27.

20. Chan HSL: Understanding cancer therapies. Jackson: University Press of Mississippi; 2007.
21. John C. Reed MD P. Toward a New Era in Cancer Treatment: Message from the New Editor-in-Chief. Mol Cancer Ther 2012;11(8):1621-2.
22. Lin SH, George TJ, Ben-Josef E, Bradley J, Choe KS, Edelman MJ et al. Opportunities and challenges in the era of molecularly targeted agents and radiation therapy. J Natl Cancer Inst 2013;105(10):686-93.
23. Schultz RM. Dawn of a new era in molecular cancer therapeutics. Prog Drug Res 2005;63:1-17.
24. Are C, Berman RS, Wyld L, Cummings C, Lecoq C, Audisio RA. Global curriculum in surgical oncology. Eur J Surg Oncol 2016;42(6):754-66.
25. Zbar AP, Gravitz A, Audisio RA. Principles of surgical oncology in the elderly. Clin Geriatr Med 2012;28(1):51-71.
26. Gunderson LL, Tepper JE. Clinical radiation oncology. 2016.
27. Illidge TM, Hamilton CR. Principles of Clinical Radiation Oncology. 1994:171-201.
28. Jaffray DA, Gospodarowicz MK: Radiation Therapy for Cancer. In: *Cancer: Disease Control Priorities, Third Edition (Volume 3).* edn. Edited by Gelband H, Jha P, Sankaranarayanan R, Horton S. Washington (DC); 2015.
29. Barton MB, Jacob S, Shafiq J, Wong K, Thompson SR, Hanna TP et al. Estimating the demand for radiotherapy from the evidence: a review of changes from 2003 to 2012. Radiother Oncol 2014;112(1):140-4.
30. Baumann M, Krause M, Overgaard J, Debus J, Bentzen SM, Daartz J et al. Radiation oncology in the era of precision medicine. Nat Rev Cancer 2016;16(4):234-49.
31. Domina EA, Philchenkov A, Dubrovska A. Individual Response to Ionizing Radiation and Personalized Radiotherapy. Crit Rev Oncog 2018;23(1-2):69-92.
32. Falzone L, Salomone S, Libra M. Evolution of Cancer Pharmacological Treatments at the Turn of the Third Millennium. Front Pharmacol 2018;9:1300.
33. Ricevuto E, Bruera G, Marchetti P. General principles of chemotherapy. Eur Rev Med Pharmacol Sci 2010;14(4):269-71.
34. Hall AG, Tilby MJ. Mechanisms of action of, and modes of resistance to, alkylating agents used in the treatment of haematological malignancies. Blood Rev 1992;6(3):163-73.
35. Warwick GP. The Mechanism of Action of Alkylating Agents. Cancer Res 1963;23:1315-33.
36. Allegra CJ, Grem JL, Yeh GC, Chabner BA. Antimetabolites. Cancer Chemother Biol Response Modif 1988;10:1-22.
37. Peters GJ. Novel developments in the use of antimetabolites. Nucleosides Nucleotides Nucleic Acids 2014;33(4-6):358-74.
38. Beretta GL, Zunino F. Molecular mechanisms of anthracycline activity. Top Curr Chem 2008;283:1-19.
39. Binaschi M, Bigioni M, Cipollone A, Rossi C, Goso C, Maggi CA et al. Anthracyclines: selected new developments. Curr Med Chem Anticancer Agents 2001;1(2):113-30.

40. Gewirtz DA. A critical evaluation of the mechanisms of action proposed for the antitumor effects of the anthracycline antibiotics adriamycin and daunorubicin. Biochem Pharmacol 1999;57(7):727-41.
41. Moudi M, Go R, Yien CY, Nazre M. Vinca alkaloids. Int J Prev Med 2013;4(11):1231-5.
42. Pienta KJ. Preclinical mechanisms of action of docetaxel and docetaxel combinations in prostate cancer. Semin Oncol 2001;28(4 Suppl 15):3-7.
43. Distelhorst CW. Glucocorticosteroids induce DNA fragmentation in human lymphoid leukemia cells. Blood 1988;72(4):1305-9.
44. Pufall MA. Glucocorticoids and Cancer. Adv Exp Med Biol 2015;872:315-33.
45. Zimmermann S, Dziadziuszko R, Peters S. Indications and limitations of chemotherapy and targeted agents in non-small cell lung cancer brain metastases. Cancer Treat Rev 2014;40(6):716-22.
46. Schirrmacher V. From chemotherapy to biological therapy: A review of novel concepts to reduce the side effects of systemic cancer treatment (Review). Int J Oncol 2019;54(2):407-19.
47. Lheureux S, Denoyelle C, Ohashi PS, De Bono JS, Mottaghy FM. Molecularly targeted therapies in cancer: a guide for the nuclear medicine physician. Eur J Nucl Med Mol Imaging 2017;44(Suppl 1):41-54.
48. Wu HC CD, Huang CT. Targeted Therapy for Cancer. Journal of Cancer Molecules 2006;2(2):57-66.
49. Aragon-Ching JB, Madan RA, Dahut WL. Angiogenesis inhibition in prostate cancer: current uses and future promises. J Oncol 2010;2010:361836.
50. Arora A, Scholar EM. Role of tyrosine kinase inhibitors in cancer therapy. J Pharmacol Exp Ther 2005;315(3):971-9.
51. Surmacz E. Growth factor receptors as therapeutic targets: strategies to inhibit the insulin-like growth factor I receptor. Oncogene 2003;22(42):6589-97.
52. Takeuchi K, Ito F. Receptor tyrosine kinases and targeted cancer therapeutics. Biol Pharm Bull 2011;34(12):1774-80.
53. Schilsky RL, Allen J, Benner J, Sigal E, McClellan M. Commentary: tackling the challenges of developing targeted therapies for cancer. Oncologist 2010;15(5):484-7.
54. de Bono JS, Ashworth A. Translating cancer research into targeted therapeutics. Nature 2010;467(7315):543-9.
55. Groenendijk FH, Bernards R. Drug resistance to targeted therapies: deja vu all over again. Mol Oncol 2014;8(6):1067-83.
56. Sarmento-Ribeiro AB, Scorilas A, Goncalves AC, Efferth T, Trougakos IP. The emergence of drug resistance to targeted cancer therapies: Clinical evidence. Drug Resist Updat 2019;47:100646.
57. Ventola CL. Cancer Immunotherapy, Part 1: Current Strategies and Agents. P T 2017;42(6):375-83.
58. Klener P, Jr., Otahal P, Lateckova L, Klener P. Immunotherapy Approaches in Cancer Treatment. Curr Pharm Biotechnol 2015;16(9):771-81.
59. Inthagard J, Edwards J, Roseweir AK. Immunotherapy: enhancing the efficacy of this promising therapeutic in multiple cancers. Clin Sci (Lond) 2019;133(2):181-93.

60. Remon J, Besse B, Soria JC. Successes and failures: what did we learn from recent first-line treatment immunotherapy trials in non-small cell lung cancer? BMC Med 2017;15(1):55.
61. Fiala O, Sorejs O, Sustr J, Finek J. Side Effects and Efficacy of Immunotherapy. Klin Onkol 2020;33(1):8-10.
62. Hofman P. Is the onset of adverse effects of immunotherapy always bad news for the patients...?-certainly not! Ann Transl Med 2019;7(Suppl 1):S5.
63. Bajwa R, Cheema A, Khan T, Amirpour A, Paul A, Chaughtai S et al. Adverse Effects of Immune Checkpoint Inhibitors (Programmed Death-1 Inhibitors and Cytotoxic T-Lymphocyte-Associated Protein-4 Inhibitors): Results of a Retrospective Study. J Clin Med Res 2019;11(4):225-36.
64. Ventola CL. Cancer Immunotherapy, Part 3: Challenges and Future Trends. P T 2017;42(8):514-21.
65. Bedard PL, Hansen AR, Ratain MJ, Siu LL. Tumour heterogeneity in the clinic. Nature 2013;501(7467):355-64.
66. Ramon YCS, Sese M, Capdevila C, Aasen T, De Mattos-Arruda L, Diaz-Cano SJ et al. Clinical implications of intratumor heterogeneity: challenges and opportunities. J Mol Med (Berl) 2020;98(2):161-77.
67. Stanta G, Bonin S. Overview on Clinical Relevance of Intra-Tumor Heterogeneity. Front Med (Lausanne) 2018;5:85.
68. Gerashchenko TS, Denisov EV, Litviakov NV, Zavyalova MV, Vtorushin SV, Tsyganov MM et al. Intratumor heterogeneity: nature and biological significance. Biochemistry (Mosc) 2013;78(11):1201-15.
69. Rybinski B, Yun K. Addressing intra-tumoral heterogeneity and therapy resistance. Oncotarget 2016;7(44):72322-42.
70. Hiley CT, Swanton C. Spatial and temporal cancer evolution: causes and consequences of tumour diversity. Clin Med (Lond) 2014;14 Suppl 6:s33-7.
71. Swanton C. Cancer evolution: the final frontier of precision medicine? Ann Oncol 2014;25(3):549-51.
72. Gascoigne KE, Taylor SS. Cancer cells display profound intra- and interline variation following prolonged exposure to antimitotic drugs. Cancer Cell 2008;14(2):111-22.
73. Bendall SC, Simonds EF, Qiu P, Amir el AD, Krutzik PO, Finck R et al. Single-cell mass cytometry of differential immune and drug responses across a human hematopoietic continuum. Science 2011;332(6030):687-96.
74. Navin N, Kendall J, Troge J, Andrews P, Rodgers L, McIndoo J et al. Tumour evolution inferred by single-cell sequencing. Nature 2011;472(7341):90-4.
75. Heppner GH, Miller BE. Tumor heterogeneity: biological implications and therapeutic consequences. Cancer Metastasis Rev 1983;2(1):5-23.
76. Dexter DL, Kowalski HM, Blazar BA, Fligiel Z, Vogel R, Heppner GH. Heterogeneity of tumor cells from a single mouse mammary tumor. Cancer Res 1978;38(10):3174-81.
77. Ling S, Hu Z, Yang Z, Yang F, Li Y, Lin P et al. Extremely high genetic diversity in a single tumor points to prevalence of non-Darwinian cell evolution. PNAS 2015;112(47):E6496-505.

78. Vogelstein B, Papadopoulos N, Velculescu VE, Zhou S, Diaz LA, Jr., Kinzler KW. Cancer genome landscapes. Science 2013;339(6127):1546-58.
79. Yin Z, Dong C, Jiang K, Xu Z, Li R, Guo K et al. Heterogeneity of cancer-associated fibroblasts and roles in the progression, prognosis, and therapy of hepatocellular carcinoma. J Hematol Oncol 2019;12(1):101.
80. Giraldo NA, Sanchez-Salas R, Peske JD, Vano Y, Becht E, Petitprez F et al. The clinical role of the TME in solid cancer. Br J Cancer 2019;120(1):45-53.
81. Maeda H, Khatami M. Analyses of repeated failures in cancer therapy for solid tumors: poor tumor-selective drug delivery, low therapeutic efficacy and unsustainable costs. Clin Transl Med 2018;7(1):11.
82. About Chronic Diseases [https://www.cdc.gov/chronicdisease/about/]
83. Nazarian A, Sureshbabu S, Andrada ZP, Thomas J, Arreglado A, Berman N et al. 18F-FDG PET/CT evaluation of tumor response to the implantation of RENCA macrobeads (RMB) in phase I and II clinical trials [INDBB 10091] in advanced, treatment-resistant metastatic colorectal cancer (mCRC). J Clin Oncol 2017;35(15_suppl):e15046-e.
84. Ocean AJ, Parikh T, Berman N, Escalon J, Shah MA, Andrada Z et al. Phase I/II trial of intraperitoneal implantation of agarose-agarose macrobeads (MB) containing mouse renal adenocarcinoma cells (RENCA) in patients (pts) with advanced colorectal cancer (CRC). J Clin Oncol 2013;31(15_suppl):e14517-e.
85. Smith BH, Gazda LS, Conn BL, Jain K, Asina S, Levine DM et al. Hydrophilic agarose macrobead cultures select for outgrowth of carcinoma cell populations that can restrict tumor growth. Cancer Res 2011;71(3):725-35.
86. Smith BH, Gazda LS, Fahey TJ, Nazarian A, Laramore MA, Martis P et al. Clinical laboratory and imaging evidence for effectiveness of agarose-agarose macrobeads containing stem-like cells derived from a mouse renal adenocarcinoma cell population (RMBs) in treatment-resistant, advanced metastatic colorectal cancer: Evaluation of a biological-systems approach to cancer therapy (U.S. FDA IND-BB 10091; NCT 02046174, NCT 01053013). Chin J Cancer Res 2018;30(1):72-83.
87. Smith BH, Parikh T, Andrada ZP, Fahey TJ, Berman N, Wiles M et al. First-in-Human Phase 1 Trial of Agarose Beads Containing Murine RENCA Cells in Advanced Solid Tumors. Cancer Growth Metastasis 2016;9:9-20.
88. Laird AK. Dynamics of Tumor Growth. Br J Cancer 1964;13:490-502.
89. Laird AK. Dynamics of Tumour Growth: Comparison of Growth Rates and Extrapolation of Growth Curve to One Cell. Br J Cancer 1965;19:278-91.
90. Norton L. A Gompertzian model of human breast cancer growth. Cancer Res 1988;48(24 Pt 1):7067-71.
91. Martis PC, Dudley AT, Bemrose MA, Gazda HL, Smith BH, Gazda LS. MEF2 plays a significant role in the tumor inhibitory mechanism of encapsulated RENCA cells via EGF receptor signaling in target tumor cells. BMC Cancer 2018;18(1):1217.
92. Ma Q, Telese F. Genome-wide epigenetic analysis of MEF2A and MEF2C transcription factors in mouse cortical neurons. Commun Integr Biol 2015;8(6):e1087624.
93. Shore P, Sharrocks AD. The MADS-box family of transcription factors. Eur J Biochem 1995;229(1):1-13.

94. Keren A, Tamir Y, Bengal E. The p38 MAPK signaling pathway: a major regulator of skeletal muscle development. Mol Cell Endocrinol 2006;252(1-2):224-30.
95. Potthoff MJ, Olson EN. MEF2: a central regulator of diverse developmental programs. Development 2007;134(23):4131-40.
96. McKinsey TA, Zhang CL, Olson EN. MEF2: a calcium-dependent regulator of cell division, differentiation and death. Trends Biochem Sci 2002;27(1):40-7.
97. Black BL, Olson EN. Transcriptional control of muscle development by myocyte enhancer factor-2 (MEF2) proteins. Annu Rev Cell Dev Biol 1998;14:167-96.
98. Martin JF, Miano JM, Hustad CM, Copeland NG, Jenkins NA, Olson EN. A Mef2 gene that generates a muscle-specific isoform via alternative mRNA splicing. Mol Cell Biol 1994;14(3):1647-56.
99. Wu Y, Dey R, Han A, Jayathilaka N, Philips M, Ye J et al. Structure of the MADS-box/MEF2 domain of MEF2A bound to DNA and its implication for myocardin recruitment. J Mol Biol 2010;397(2):520-33.
100. Coso OA, Montaner S, Fromm C, Lacal JC, Prywes R, Teramoto H et al. Signaling from G protein-coupled receptors to the c-jun promoter involves the MEF2 transcription factor. Evidence for a novel c-jun amino-terminal kinase-independent pathway. J Biol 1997;272(33):20691-7.
101. Clarke N, Arenzana N, Hai T, Minden A, Prywes R. Epidermal growth factor induction of the c-jun promoter by a Rac pathway. Mol Cell Biol 1998;18(2):1065-73.
102. Kato Y, Kravchenko VV, Tapping RI, Han J, Ulevitch RJ, Lee JD. BMK1/ERK5 regulates serum-induced early gene expression through transcription factor MEF2C. The EMBO journal 1997;16(23):7054-66.
103. Kato Y, Tapping RI, Huang S, Watson MH, Ulevitch RJ, Lee JD. Bmk1/Erk5 is required for cell proliferation induced by epidermal growth factor. Nature 1998;395(6703):713-6.
104. Han J, Jiang Y, Li Z, Kravchenko VV, Ulevitch RJ. Activation of the transcription factor MEF2C by the MAP kinase p38 in inflammation. Nature 1997;386(6622):296-9.
105. Andres V, Cervera M, Mahdavi V. Determination of the consensus binding site for MEF2 expressed in muscle and brain reveals tissue-specific sequence constraints. J Biol 1995;270(40):23246-9.
106. Fickett JW. Quantitative discrimination of MEF2 sites. Mol Cell Biol 1996;16(1):437-41.
107. Gossett LA, Kelvin DJ, Sternberg EA, Olson EN. A new myocyte-specific enhancer-binding factor that recognizes a conserved element associated with multiple muscle-specific genes. Mol Cell Biol 1989;9(11):5022-33.
108. Di Giorgio E, Hancock WW, Brancolini C. MEF2 and the tumorigenic process, hic sunt leones. Biochim Biophys Acta Rev Cancer 2018;1870(2):261-73.
109. Taylor MV, Hughes SM. Mef2 and the skeletal muscle differentiation program. Semin Cell Dev Biol 2017;72:33-44.
110. Pon JR, Marra MA. MEF2 transcription factors: developmental regulators and emerging cancer genes. Oncotarget 2016;7(3):2297-312.

111. Pan Y, Yan C, Hu Y, Fan Y, Pan Q, Wan Q et al. Distribution bias analysis of germline and somatic single-nucleotide variations that impact protein functional site and neighboring amino acids. Sci Rep 2017;7:42169.
112. Bai X, Wu L, Liang T, Liu Z, Li J, Li D et al. Overexpression of myocyte enhancer factor 2 and histone hyperacetylation in hepatocellular carcinoma. J Cancer Res Clin Oncol 2008;134(1):83-91.
113. Liu J, Wen D, Fang X, Wang X, Liu T, Zhu J. p38MAPK Signaling Enhances Glycolysis Through the Up-Regulation of the Glucose Transporter GLUT-4 in Gastric Cancer Cells. Cell Physiol Biochem 2015;36(1):155-65.
114. Ma Y, Shi Y, Li W, Sun A, Zang P, Zhang P. Epigallocatechin-3-gallate regulates the expression of Kruppel-like factor 4 through myocyte enhancer factor 2A. Cell Stress Chaperones 2014;19(2):217-26.
115. Wu W, de Folter S, Shen X, Zhang W, Tao S. Vertebrate paralogous MEF2 genes: origin, conservation, and evolution. PloS one 2011;6(3):e17334.
116. Cancer Genome Atlas Research N, Kandoth C, Schultz N, Cherniack AD, Akbani R, Liu Y et al. Integrated genomic characterization of endometrial carcinoma. Nature 2013;497(7447):67-73.
117. Cerami E, Gao J, Dogrusoz U, Gross BE, Sumer SO, Aksoy BA et al. The cBio cancer genomics portal: an open platform for exploring multidimensional cancer genomics data. Cancer Discov 2012;2(5):401-4.
118. Gao J, Aksoy BA, Dogrusoz U, Dresdner G, Gross B, Sumer SO et al. Integrative analysis of complex cancer genomics and clinical profiles using the cBioPortal. Sci Signal 2013;6(269):pl1.
119. Pon JR, Wong J, Saberi S, Alder O, Moksa M, Grace Cheng SW et al. MEF2B mutations in non-Hodgkin lymphoma dysregulate cell migration by decreasing MEF2B target gene activation. Nat Commun 2015;6:7953.
120. Kitano M, Moriyama S, Ando Y, Hikida M, Mori Y, Kurosaki T et al. Bcl6 protein expression shapes pre-germinal center B cell dynamics and follicular helper T cell heterogeneity. Immunity 2011;34(6):961-72.
121. Ryan RJ, Drier Y, Whitton H, Cotton MJ, Kaur J, Issner R et al. Detection of Enhancer-Associated Rearrangements Reveals Mechanisms of Oncogene Dysregulation in B-cell Lymphoma. Cancer Discov 2015;5(10):1058-71.
122. Ying CY, Dominguez-Sola D, Fabi M, Lorenz IC, Hussein S, Bansal M et al. MEF2B mutations lead to deregulated expression of the oncogene BCL6 in diffuse large B cell lymphoma. Nat Immunol 2013;14(10):1084-92.
123. Im JY, Yoon SH, Kim BK, Ban HS, Won KJ, Chung KS et al. DNA damage induced apoptosis suppressor (DDIAS) is upregulated via ERK5/MEF2B signaling and promotes beta-catenin-mediated invasion. Biochim Biophys Acta 2016;1859(11):1449-58.
124. Bea S, Valdes-Mas R, Navarro A, Salaverria I, Martin-Garcia D, Jares P et al. Landscape of somatic mutations and clonal evolution in mantle cell lymphoma. PNAS 2013;110(45):18250-5.
125. Lohr JG, Stojanov P, Lawrence MS, Auclair D, Chapuy B, Sougnez C et al. Discovery and prioritization of somatic mutations in diffuse large B-cell lymphoma (DLBCL) by whole-exome sequencing. PNAS 2012;109(10):3879-84.

126. Morin RD, Mendez-Lago M, Mungall AJ, Goya R, Mungall KL, Corbett RD et al. Frequent mutation of histone-modifying genes in non-Hodgkin lymphoma. Nature 2011;476(7360):298-303.
127. Pasqualucci L, Trifonov V, Fabbri G, Ma J, Rossi D, Chiarenza A et al. Analysis of the coding genome of diffuse large B-cell lymphoma. Nat Genet 2011;43(9):830-7.
128. Homminga I, Pieters R, Langerak AW, de Rooi JJ, Stubbs A, Verstegen M et al. Integrated transcript and genome analyses reveal NKX2-1 and MEF2C as potential oncogenes in T cell acute lymphoblastic leukemia. Cancer Cell 2011;19(4):484-97.
129. Schwieger M, Schuler A, Forster M, Engelmann A, Arnold MA, Delwel R et al. Homing and invasiveness of MLL/ENL leukemic cells is regulated by MEF2C. Blood 2009;114(12):2476-88.
130. Du Y, Spence SE, Jenkins NA, Copeland NG. Cooperating cancer-gene identification through oncogenic-retrovirus-induced insertional mutagenesis. Blood 2005;106(7):2498-505.
131. Krivtsov AV, Twomey D, Feng Z, Stubbs MC, Wang Y, Faber J et al. Transformation from committed progenitor to leukaemia stem cell initiated by MLL-AF9. Nature 2006;442(7104):818-22.
132. Chen G, Han N, Li G, Li X, Li G, Li Z et al. Time course analysis based on gene expression profile and identification of target molecules for colorectal cancer. Cancer Cell Int 2016;16:22.
133. Schuetz CS, Bonin M, Clare SE, Nieselt K, Sotlar K, Walter M et al. Progression-specific genes identified by expression profiling of matched ductal carcinomas in situ and invasive breast tumors, combining laser capture microdissection and oligonucleotide microarray analysis. Cancer Res 2006;66(10):5278-86.
134. Bai XL, Zhang Q, Ye LY, Liang F, Sun X, Chen Y et al. Myocyte enhancer factor 2C regulation of hepatocellular carcinoma via vascular endothelial growth factor and Wnt/beta-catenin signaling. Oncogene 2015;34(31):4089-97.
135. Yu W, Huang C, Wang Q, Huang T, Ding Y, Ma C et al. MEF2 transcription factors promotes EMT and invasiveness of hepatocellular carcinoma through TGF-beta1 autoregulation circuitry. Tumour Biol 2014;35(11):10943-51.
136. Zhang M, Zhu B, Davie J. Alternative splicing of MEF2C pre-mRNA controls its activity in normal myogenesis and promotes tumorigenicity in rhabdomyosarcoma cells. J Biol 2015;290(1):310-24.
137. Prima V, Gore L, Caires A, Boomer T, Yoshinari M, Imaizumi M et al. Cloning and functional characterization of MEF2D/DAZAP1 and DAZAP1/MEF2D fusion proteins created by a variant t(1;19)(q23;p13.3) in acute lymphoblastic leukemia. Leukemia 2005;19(5):806-13.
138. Yuki Y, Imoto I, Imaizumi M, Hibi S, Kaneko Y, Amagasa T et al. Identification of a novel fusion gene in a pre-B acute lymphoblastic leukemia with t(1;19)(q23;p13). Cancer Sci 2004;95(6):503-7.
139. Ma L, Liu J, Liu L, Duan G, Wang Q, Xu Y et al. Overexpression of the transcription factor MEF2D in hepatocellular carcinoma sustains malignant character by suppressing G2-M transition genes. Cancer Res 2014;74(5):1452-62.

140. Zhang R, Zhang Y, Li H. miR-1244/Myocyte Enhancer Factor 2D Regulatory Loop Contributes to the Growth of Lung Carcinoma. DNA Cell Biol 2015;34(11):692-700.
141. Xu K, Zhao YC. MEF2D/Wnt/beta-catenin pathway regulates the proliferation of gastric cancer cells and is regulated by microRNA-19. Tumour Biol 2016;37(7):9059-69.
142. Song Z, Feng C, Lu Y, Gao Y, Lin Y, Dong C. Overexpression and biological function of MEF2D in human pancreatic cancer. Am J Transl Res 2017;9(11):4836-47.
143. Di Giorgio E, Franforte E, Cefalu S, Rossi S, Dei Tos AP, Brenca M et al. The co-existence of transcriptional activator and transcriptional repressor MEF2 complexes influences tumor aggressiveness. PLoS Genet 2017;13(4):e1006752.
144. Clocchiatti A, Di Giorgio E, Viviani G, Streuli C, Sgorbissa A, Picco R et al. The MEF2-HDAC axis controls proliferation of mammary epithelial cells and acini formation in vitro. J Cell Sci 2015;128(21):3961-76.
145. Zhang M, Truscott J, Davie J. Loss of MEF2D expression inhibits differentiation and contributes to oncogenesis in rhabdomyosarcoma cells. Mol Cancer 2013;12(1):150.
146. Tremblay AM, Missiaglia E, Galli GG, Hettmer S, Urcia R, Carrara M et al. The Hippo transducer YAP1 transforms activated satellite cells and is a potent effector of embryonal rhabdomyosarcoma formation. Cancer Cell 2014;26(2):273-87.
147. Badodi S, Baruffaldi F, Ganassi M, Battini R, Molinari S. Phosphorylation-dependent degradation of MEF2C contributes to regulate G2/M transition. Cell Cycle 2015;14(10):1517-28.
148. Di Giorgio E, Gagliostro E, Clocchiatti A, Brancolini C. The control operated by the cell cycle machinery on MEF2 stability contributes to the downregulation of CDKN1A and entry into S phase. Mol Cell Biol 2015;35(9):1633-47.
149. Suzuki E, Guo K, Kolman M, Yu YT, Walsh K. Serum induction of MEF2/RSRF expression in vascular myocytes is mediated at the level of translation. Mol Cell Biol 1995;15(6):3415-23.
150. Wang YN, Yang WC, Li PW, Wang HB, Zhang YY, Zan LS. Myocyte enhancer factor 2A promotes proliferation and its inhibition attenuates myogenic differentiation via myozenin 2 in bovine skeletal muscle myoblast. PloS one 2018;13(4):e0196255.
151. Desjardins CA, Naya FJ. Antagonistic regulation of cell-cycle and differentiation gene programs in neonatal cardiomyocytes by homologous MEF2 transcription factors. J Biol 2017;292(25):10613-29.
152. Estrella NL, Desjardins CA, Nocco SE, Clark AL, Maksimenko Y, Naya FJ. MEF2 transcription factors regulate distinct gene programs in mammalian skeletal muscle differentiation. J Biol 2015;290(2):1256-68.
153. Hu H, Tian M, Ding C, Yu S. The C/EBP Homologous Protein (CHOP) Transcription Factor Functions in Endoplasmic Reticulum Stress-Induced Apoptosis and Microbial Infection. Front Immunol 2018;9:3083.
154. Ullrich A, Coussens L, Hayflick JS, Dull TJ, Gray A, Tam AW et al. Human epidermal growth factor receptor cDNA sequence and aberrant expression of the

amplified gene in A431 epidermoid carcinoma cells. Nature 1984;309(5967):418-25.
155. Downward J, Yarden Y, Mayes E, Scrace G, Totty N, Stockwell P et al. Close similarity of epidermal growth factor receptor and v-erb-B oncogene protein sequences. Nature 1984;307(5951):521-7.
156. Rowinsky EK. The erbB family: targets for therapeutic development against cancer and therapeutic strategies using monoclonal antibodies and tyrosine kinase inhibitors. Annu Rev Med 2004;55:433-57.
157. Salomon DS, Brandt R, Ciardiello F, Normanno N. Epidermal growth factor-related peptides and their receptors in human malignancies. Crit Rev Oncol Hematol 1995;19(3):183-232.
158. Barnes DW. Epidermal growth factor inhibits growth of A431 human epidermoid carcinoma in serum-free cell culture. J Cell Biol 1982;93(1):1-4.
159. Filmus J, Pollak MN, Cailleau R, Buick RN. MDA-468, a human breast cancer cell line with a high number of epidermal growth factor (EGF) receptors, has an amplified EGF receptor gene and is growth inhibited by EGF. Biochem Biophys Res Commun 1985;128(2):898-905.
160. Gill GN, Lazar CS. Increased phosphotyrosine content and inhibition of proliferation in EGF-treated A431 cells. Nature 1981;293(5830):305-7.
161. Imai Y, Leung CK, Friesen HG, Shiu RP. Epidermal growth factor receptors and effect of epidermal growth factor on growth of human breast cancer cells in long-term tissue culture. Cancer Res 1982;42(11):4394-8.
162. Prasad KA, Church JG. EGF-dependent growth inhibition in MDA-468 human breast cancer cells is characterized by late G1 arrest and altered gene expression. Exp Cell Res 1991;195(1):20-6.
163. Schonbrunn A, Krasnoff M, Westendorf JM, Tashjian AH, Jr. Epidermal growth factor and thyrotropin-releasing hormone act similarly on a clonal pituitary cell strain. Modulation of hormone production and inhbition of cell proliferation. J Cell Biol 1980;85(3):786-97.
164. Ali R, Brown W, Purdy SC, Davisson VJ, Wendt MK. Biased signaling downstream of epidermal growth factor receptor regulates proliferative versus apoptotic response to ligand. Cell Death Dis 2018;9(10):976.
165. Armstrong DK, Kaufmann SH, Ottaviano YL, Furuya Y, Buckley JA, Isaacs JT et al. Epidermal growth factor-mediated apoptosis of MDA-MB-468 human breast cancer cells. Cancer Res 1994;54(20):5280-3.
166. Danielsen AJ, Maihle NJ. The EGF/ErbB receptor family and apoptosis. Growth Factors 2002;20(1):1-15.
167. Gulli LF, Palmer KC, Chen YQ, Reddy KB. Epidermal growth factor-induced apoptosis in A431 cells can be reversed by reducing the tyrosine kinase activity. Cell Growth Differ 1996;7(2):173-8.
168. Hognason T, Chatterjee S, Vartanian T, Ratan RR, Ernewein KM, Habib AA. Epidermal growth factor receptor induced apoptosis: potentiation by inhibition of Ras signaling. FEBS Lett 2001;491(1-2):9-15.
169. Kawamoto T, Mendelsohn J, Le A, Sato GH, Lazar CS, Gill GN. Relation of epidermal growth factor receptor concentration to growth of human epidermoid carcinoma A431 cells. J Biol 1984;259(12):7761-6.

170. Kottke TJ, Blajeski AL, Martins LM, Mesner PW, Jr., Davidson NE, Earnshaw WC et al. Comparison of paclitaxel-, 5-fluoro-2'-deoxyuridine-, and epidermal growth factor (EGF)-induced apoptosis. Evidence for EGF-induced anoikis. J Biol 1999;274(22):15927-36.
171. Lehto VP. EGF receptor: which way to go? FEBS Lett 2001;491(1-2):1-3.
172. Ryu JW, Choe SS, Ryu SH, Park EY, Lee BW, Kim TK et al. Paradoxical induction of growth arrest and apoptosis by EGF via the up-regulation of PTEN by activating Redox factor-1/Egr-1 in human lung cancer cells. Oncotarget 2017;8(3):4181-95.
173. Astuti P, Pike T, Widberg C, Payne E, Harding A, Hancock J et al. MAPK pathway activation delays G2/M progression by destabilizing Cdc25B. J Biol 2009;284(49):33781-8.
174. Andersen P, Pedersen MW, Woetmann A, Villingshoj M, Stockhausen MT, Odum N et al. EGFR induces expression of IRF-1 via STAT1 and STAT3 activation leading to growth arrest of human cancer cells. Int J Cancer 2008;122(2):342-9.
175. Chin YE, Kitagawa M, Su WC, You ZH, Iwamoto Y, Fu XY. Cell growth arrest and induction of cyclin-dependent kinase inhibitor p21 WAF1/CIP1 mediated by STAT1. Science 1996;272(5262):719-22.
176. Dangi S, Chen FM, Shapiro P. Activation of extracellular signal-regulated kinase (ERK) in G2 phase delays mitotic entry through p21CIP1. Cell Prolif 2006;39(4):261-79.
177. Chin YE, Kitagawa M, Kuida K, Flavell RA, Fu XY. Activation of the STAT signaling pathway can cause expression of caspase 1 and apoptosis. Mol Cell Biol 1997;17(9):5328-37.
178. Thomas T, Balabhadrapathruni S, Gardner CR, Hong J, Faaland CA, Thomas TJ. Effects of epidermal growth factor on MDA-MB-468 breast cancer cells: alterations in polyamine biosynthesis and the expression of p21/CIP1/WAF1. J Cell Physiol 1999;179(3):257-66.
179. Chen KY, Huang LM, Kung HJ, Ann DK, Shih HM. The role of tyrosine kinase Etk/Bmx in EGF-induced apoptosis of MDA-MB-468 breast cancer cells. Oncogene 2004;23(10):1854-62.
180. Kim HS, Lim JM, Kim JY, Kim Y, Park S, Sohn J. Panaxydol, a component of Panax ginseng, induces apoptosis in cancer cells through EGFR activation and ER stress and inhibits tumor growth in mouse models. Int J Cancer 2016;138(6):1432-41.
181. Wieduwilt MJ, Moasser MM. The epidermal growth factor receptor family: biology driving targeted therapeutics. Cell Mol Life Sci 2008;65(10):1566-84.
182. Lemmon MA, Bu Z, Ladbury JE, Zhou M, Pinchasi D, Lax I et al. Two EGF molecules contribute additively to stabilization of the EGFR dimer. The EMBO journal 1997;16(2):281-94.
183. Schlessinger J. Ligand-induced, receptor-mediated dimerization and activation of EGF receptor. Cell 2002;110(6):669-72.
184. Purba ER, Saita EI, Maruyama IN. Activation of the EGF Receptor by Ligand Binding and Oncogenic Mutations: The "Rotation Model". Cells 2017;6(2).
185. Jorissen RN, Walker F, Pouliot N, Garrett TP, Ward CW, Burgess AW. Epidermal growth factor receptor: mechanisms of activation and signalling. Exp Cell Res 2003;284(1):31-53.

186. Schlessinger J. Cell signaling by receptor tyrosine kinases. Cell 2000;103(2):211-25.
187. Tomas A, Futter CE, Eden ER. EGF receptor trafficking: consequences for signaling and cancer. Trends Cell Biol 2014;24(1):26-34.
188. Goh LK, Sorkin A. Endocytosis of receptor tyrosine kinases. Cold Spring Harb Perspect Biol 2013;5(5):a017459.
189. Haglund K, Dikic I. The role of ubiquitylation in receptor endocytosis and endosomal sorting. J Cell Sci 2012;125(Pt 2):265-75.
190. Roepstorff K, Grandal MV, Henriksen L, Knudsen SL, Lerdrup M, Grovdal L et al. Differential effects of EGFR ligands on endocytic sorting of the receptor. Traffic 2009;10(8):1115-27.
191. Harris RC, Chung E, Coffey RJ. EGF receptor ligands. Exp Cell Res 2003;284(1):2-13.
192. Sabbah DA, Hajjo R, Sweidan K. Review on Epidermal Growth Factor Receptor (EGFR) Structure, Signaling Pathways, Interactions, and Recent Updates of EGFR Inhibitors. Curr Top Med Chem 2020.
193. Wang Z. ErbB Receptors and Cancer. Methods Mol Biol 2017;1652:3-35.
194. Wagner MJ, Stacey MM, Liu BA, Pawson T. Molecular mechanisms of SH2- and PTB-domain-containing proteins in receptor tyrosine kinase signaling. Cold Spring Harb Perspect Biol 2013;5(12):a008987.
195. Oda K, Matsuoka Y, Funahashi A, Kitano H. A comprehensive pathway map of epidermal growth factor receptor signaling. Mol Syst Biol 2005;1:2005 0010.
196. Singh AB, Harris RC. Autocrine, paracrine and juxtacrine signaling by EGFR ligands. Cell Signal 2005;17(10):1183-93.
197. Appella E, Weber IT, Blasi F. Structure and function of epidermal growth factor-like regions in proteins. FEBS Lett 1988;231(1):1-4.
198. Schenk S, Hintermann E, Bilban M, Koshikawa N, Hojilla C, Khokha R et al. Binding to EGF receptor of a laminin-5 EGF-like fragment liberated during MMP-dependent mammary gland involution. J Cell Biol 2003;161(1):197-209.
199. Swindle CS, Tran KT, Johnson TD, Banerjee P, Mayes AM, Griffith L et al. Epidermal growth factor (EGF)-like repeats of human tenascin-C as ligands for EGF receptor. J Cell Biol 2001;154(2):459-68.
200. Luttrell LM, Daaka Y, Lefkowitz RJ. Regulation of tyrosine kinase cascades by G-protein-coupled receptors. Curr Opin Cell Biol 1999;11(2):177-83.
201. Moro L, Venturino M, Bozzo C, Silengo L, Altruda F, Beguinot L et al. Integrins induce activation of EGF receptor: role in MAP kinase induction and adhesion-dependent cell survival. The EMBO journal 1998;17(22):6622-32.
202. Beerli RR, Hynes NE. Epidermal growth factor-related peptides activate distinct subsets of ErbB receptors and differ in their biological activities. J Biol 1996;271(11):6071-6.
203. Yang YS, Strittmatter SM. The reticulons: a family of proteins with diverse functions. Genome Biol 2007;8(12):234.
204. Oertle T, Schwab ME. Nogo and its paRTNers. Trends Cell Biol 2003;13(4):187-94.
205. van de Velde HJ, Roebroek AJ, van Leeuwen FW, Van de Ven WJ. Molecular analysis of expression in rat brain of NSP-A, a novel neuroendocrine-specific

protein of the endoplasmic reticulum. Brain Res Mol Brain Res 1994;23(1-2):81-92.
206. Hu J, Prinz WA, Rapoport TA. Weaving the web of ER tubules. Cell 2011;147(6):1226-31.
207. Park SH, Blackstone C. Further assembly required: construction and dynamics of the endoplasmic reticulum network. EMBO Rep 2010;11(7):515-21.
208. Shibata Y, Hu J, Kozlov MM, Rapoport TA. Mechanisms shaping the membranes of cellular organelles. Annu Rev Cell Dev Biol 2009;25:329-54.
209. Karnezis T, Mandemakers W, McQualter JL, Zheng B, Ho PP, Jordan KA et al. The neurite outgrowth inhibitor Nogo A is involved in autoimmune-mediated demyelination. Nat Neurosci 2004;7(7):736-44.
210. Reindl M, Khantane S, Ehling R, Schanda K, Lutterotti A, Brinkhoff C et al. Serum and cerebrospinal fluid antibodies to Nogo-A in patients with multiple sclerosis and acute neurological disorders. J Neuroimmunol 2003;145(1-2):139-47.
211. Oertle T, van der Haar ME, Bandtlow CE, Robeva A, Burfeind P, Buss A et al. Nogo-A inhibits neurite outgrowth and cell spreading with three discrete regions. J Neurosci 2003;23(13):5393-406.
212. Simonen M, Pedersen V, Weinmann O, Schnell L, Buss A, Ledermann B et al. Systemic deletion of the myelin-associated outgrowth inhibitor Nogo-A improves regenerative and plastic responses after spinal cord injury. Neuron 2003;38(2):201-11.
213. Kim JE, Li S, GrandPre T, Qiu D, Strittmatter SM. Axon regeneration in young adult mice lacking Nogo-A/B. Neuron 2003;38(2):187-99.
214. GrandPre T, Nakamura F, Vartanian T, Strittmatter SM. Identification of the Nogo inhibitor of axon regeneration as a Reticulon protein. Nature 2000;403(6768):439-44.
215. Chen MS, Huber AB, van der Haar ME, Frank M, Schnell L, Spillmann AA et al. Nogo-A is a myelin-associated neurite outgrowth inhibitor and an antigen for monoclonal antibody IN-1. Nature 2000;403(6768):434-9.
216. Prinjha R, Moore SE, Vinson M, Blake S, Morrow R, Christie G et al. Inhibitor of neurite outgrowth in humans. Nature 2000;403(6768):383-4.
217. Cheung HC, Hai T, Zhu W, Baggerly KA, Tsavachidis S, Krahe R et al. Splicing factors PTBP1 and PTBP2 promote proliferation and migration of glioma cell lines. Brain 2009;132(Pt 8):2277-88.
218. Zhao H, Su W, Zhu C, Zeng T, Yang S, Wu W et al. Cell fate regulation by reticulon-4 in human prostate cancers. J Cell Physiol 2019;234(7):10372-85.
219. Fournier AE, GrandPre T, Strittmatter SM. Identification of a receptor mediating Nogo-66 inhibition of axonal regeneration. Nature 2001;409(6818):341-6.
220. McGee AW, Yang Y, Fischer QS, Daw NW, Strittmatter SM. Experience-driven plasticity of visual cortex limited by myelin and Nogo receptor. Science 2005;309(5744):2222-6.
221. Xie F, Zheng B. White matter inhibitors in CNS axon regeneration failure. Exp Neurol 2008;209(2):302-12.
222. Qi B, Qi Y, Liu Q, Qu X. asy andasyip: A new type of apoptosis-inducing gene. Chinese Science Bulletin 2001;46(17):1409-10.

223. Li Q, Qi B, Oka K, Shimakage M, Yoshioka N, Inoue H et al. Link of a new type of apoptosis-inducing gene ASY/Nogo-B to human cancer. Oncogene 2001;20(30):3929-36.
224. Kuang E, Wan Q, Li X, Xu H, Zou T, Qi Y. ER stress triggers apoptosis induced by Nogo-B/ASY overexpression. Exp Cell Res 2006;312(11):1983-8.
225. Teng FY, Tang BL. Nogo/RTN4 isoforms and RTN3 expression protect SH-SY5Y cells against multiple death insults. Mol Cell Biochem 2013;384(1-2):7-19.
226. Tagami S, Eguchi Y, Kinoshita M, Takeda M, Tsujimoto Y. A novel protein, RTN-XS, interacts with both Bcl-XL and Bcl-2 on endoplasmic reticulum and reduces their anti-apoptotic activity. Oncogene 2000;19(50):5736-46.
227. Li M, Liu J, Song J. Nogo goes in the pure water: solution structure of Nogo-60 and design of the structured and buffer-soluble Nogo-54 for enhancing CNS regeneration. Protein Sci 2006;15(8):1835-41.
228. Domeniconi M, Zampieri N, Spencer T, Hilaire M, Mellado W, Chao MV et al. MAG induces regulated intramembrane proteolysis of the p75 neurotrophin receptor to inhibit neurite outgrowth. Neuron 2005;46(6):849-55.
229. Mi S, Miller RH, Lee X, Scott ML, Shulag-Morskaya S, Shao Z et al. LINGO-1 negatively regulates myelination by oligodendrocytes. Nat Neurosci 2005;8(6):745-51.
230. Shao Z, Browning JL, Lee X, Scott ML, Shulga-Morskaya S, Allaire N et al. TAJ/TROY, an orphan TNF receptor family member, binds Nogo-66 receptor 1 and regulates axonal regeneration. Neuron 2005;45(3):353-9.
231. Park JB, Yiu G, Kaneko S, Wang J, Chang J, He XL et al. A TNF receptor family member, TROY, is a coreceptor with Nogo receptor in mediating the inhibitory activity of myelin inhibitors. Neuron 2005;45(3):345-51.
232. Mi S, Lee X, Shao Z, Thill G, Ji B, Relton J et al. LINGO-1 is a component of the Nogo-66 receptor/p75 signaling complex. Nat Neurosci 2004;7(3):221-8.
233. Wang KC, Kim JA, Sivasankaran R, Segal R, He Z. P75 interacts with the Nogo receptor as a co-receptor for Nogo, MAG and OMgp. Nature 2002;420(6911):74-8.
234. Koprivica V, Cho KS, Park JB, Yiu G, Atwal J, Gore B et al. EGFR activation mediates inhibition of axon regeneration by myelin and chondroitin sulfate proteoglycans. Science 2005;310(5745):106-10.
235. Bornstein P. Diversity of function is inherent in matricellular proteins: an appraisal of thrombospondin 1. J Cell Biol 1995;130(3):503-6.
236. Frazier WA. Thrombospondins. Curr Opin Cell Biol 1991;3(5):792-9.
237. PEDIATRIC BONE : biology and diseases. ELSEVIER ACADEMIC Press; 2016.
238. Lamy L, Foussat A, Brown EJ, Bornstein P, Ticchioni M, Bernard A. Interactions between CD47 and thrombospondin reduce inflammation. J Immunol 2007;178(9):5930-9.
239. Liu A, Mosher DF, Murphy-Ullrich JE, Goldblum SE. The counteradhesive proteins, thrombospondin 1 and SPARC/osteonectin, open the tyrosine phosphorylation-responsive paracellular pathway in pulmonary vascular endothelia. Microvasc Res 2009;77(1):13-20.

240. Nor JE, Dipietro L, Murphy-Ullrich JE, Hynes RO, Lawler J, Polverini PJ. Activation of Latent TGF-beta1 by Thrombospondin-1 is a Major Component of Wound Repair. Oral Biosci Med 2005;2(2):153-61.
241. Borsotti P, Ghilardi C, Ostano P, Silini A, Dossi R, Pinessi D et al. Thrombospondin-1 is part of a Slug-independent motility and metastatic program in cutaneous melanoma, in association with VEGFR-1 and FGF-2. Pigment Cell Melanoma Res 2015;28(1):73-81.
242. Jayachandran A, Anaka M, Prithviraj P, Hudson C, McKeown SJ, Lo PH et al. Thrombospondin 1 promotes an aggressive phenotype through epithelial-to-mesenchymal transition in human melanoma. Oncotarget 2014;5(14):5782-97.
243. Roberts DD. Regulation of tumor growth and metastasis by thrombospondin-1. FASEB J 1996;10(10):1183-91.
244. Zubac DP, Bostad L, Kihl B, Seidal T, Wentzel-Larsen T, Haukaas SA. The expression of thrombospondin-1 and p53 in clear cell renal cell carcinoma: its relationship to angiogenesis, cell proliferation and cancer specific survival. J Urol 2009;182(5):2144-9.
245. Hyder SM, Liang Y, Wu J. Estrogen regulation of thrombospondin-1 in human breast cancer cells. Int J Cancer 2009;125(5):1045-53.
246. Gutierrez LS, Suckow M, Lawler J, Ploplis VA, Castellino FJ. Thrombospondin 1--a regulator of adenoma growth and carcinoma progression in the APC(Min/+) mouse model. Carcinogenesis 2003;24(2):199-207.
247. Hsu SC, Volpert OV, Steck PA, Mikkelsen T, Polverini PJ, Rao S et al. Inhibition of angiogenesis in human glioblastomas by chromosome 10 induction of thrombospondin-1. Cancer Res 1996;56(24):5684-91.
248. Sheibani N, Frazier WA. Thrombospondin 1 expression in transformed endothelial cells restores a normal phenotype and suppresses their tumorigenesis. PNAS 1995;92(15):6788-92.
249. Weinstat-Saslow DL, Zabrenetzky VS, VanHoutte K, Frazier WA, Roberts DD, Steeg PS. Transfection of thrombospondin 1 complementary DNA into a human breast carcinoma cell line reduces primary tumor growth, metastatic potential, and angiogenesis. Cancer Res 1994;54(24):6504-11.
250. Iruela-Arispe ML, Dvorak HF. Angiogenesis: a dynamic balance of stimulators and inhibitors. Thromb Haemost 1997;78(1):672-7.
251. Volpert OV, Stellmach V, Bouck N. The modulation of thrombospondin and other naturally occurring inhibitors of angiogenesis during tumor progression. Breast Cancer Res Treat 1995;36(2):119-26.
252. Guo NH, Krutzsch HC, Inman JK, Shannon CS, Roberts DD. Antiproliferative and antitumor activities of D-reverse peptides derived from the second type-1 repeat of thrombospondin-1. J Pept Res 1997;50(3):210-21.
253. Rusnati M, Urbinati C, Bonifacio S, Presta M, Taraboletti G. Thrombospondin-1 as a Paradigm for the Development of Antiangiogenic Agents Endowed with Multiple Mechanisms of Action. Pharmaceuticals (Basel) 2010;3(4):1241-78.
254. Bornstein P. Thrombospondins: structure and regulation of expression. FASEB J 1992;6(14):3290-9.

255. Tan K, Duquette M, Liu JH, Zhang R, Joachimiak A, Wang JH et al. The structures of the thrombospondin-1 N-terminal domain and its complex with a synthetic pentameric heparin. Structure 2006;14(1):33-42.
256. Calzada MJ, Sipes JM, Krutzsch HC, Yurchenco PD, Annis DS, Mosher DF et al. Recognition of the N-terminal modules of thrombospondin-1 and thrombospondin-2 by alpha6beta1 integrin. J Biol 2003;278(42):40679-87.
257. Orr AW, Pedraza CE, Pallero MA, Elzie CA, Goicoechea S, Strickland DK et al. Low density lipoprotein receptor-related protein is a calreticulin coreceptor that signals focal adhesion disassembly. J Cell Biol 2003;161(6):1179-89.
258. Roberts DD, Haverstick DM, Dixit VM, Frazier WA, Santoro SA, Ginsburg V. The platelet glycoprotein thrombospondin binds specifically to sulfated glycolipids. J Biol 1985;260(16):9405-11.
259. Bornstein P. Thrombospondins function as regulators of angiogenesis. J Cell Commun Signal 2009;3(3-4):189-200.
260. Wang XQ, Lindberg FP, Frazier WA. Integrin-associated protein stimulates alpha2beta1-dependent chemotaxis via Gi-mediated inhibition of adenylate cyclase and extracellular-regulated kinases. J Cell Biol 1999;147(2):389-400.
261. Liu A, Garg P, Yang S, Gong P, Pallero MA, Annis DS et al. Epidermal growth factor-like repeats of thrombospondins activate phospholipase Cgamma and increase epithelial cell migration through indirect epidermal growth factor receptor activation. J Biol 2009;284(10):6389-402.
262. Brew K, Nagase H. The tissue inhibitors of metalloproteinases (TIMPs): an ancient family with structural and functional diversity. Biochim Biophys Acta 2010;1803(1):55-71.
263. Stetler-Stevenson WG. The tumor microenvironment: regulation by MMP-independent effects of tissue inhibitor of metalloproteinases-2. Cancer Metastasis Rev 2008;27(1):57-66.
264. Kim HJ, Cho YR, Kim SH, Seo DW. TIMP-2-derived 18-mer peptide inhibits endothelial cell proliferation and migration through cAMP/PKA-dependent mechanism. Cancer letters 2014;343(2):210-6.
265. Seo DW, Li H, Qu CK, Oh J, Kim YS, Diaz T et al. Shp-1 mediates the antiproliferative activity of tissue inhibitor of metalloproteinase-2 in human microvascular endothelial cells. J Biol 2006;281(6):3711-21.
266. Perez-Martinez L, Jaworski DM. Tissue inhibitor of metalloproteinase-2 promotes neuronal differentiation by acting as an anti-mitogenic signal. J Neurosci 2005;25(20):4917-29.
267. Haase G, Pettmann B, Raoul C, Henderson CE. Signaling by death receptors in the nervous system. Curr Opin Neurobiol 2008;18(3):284-91.
268. Lim MS, Guedez L, Stetler-Stevenson WG, Stetler-Stevenson M. Tissue inhibitor of metalloproteinase-2 induces apoptosis in human T lymphocytes. Ann NY Acad Sci 1999;878:522-3.
269. Mitsiades N, Poulaki V, Kotoula V, Leone A, Tsokos M. Fas ligand is present in tumors of the Ewing's sarcoma family and is cleaved into a soluble form by a metalloproteinase. Am J Pathol 1998;153(6):1947-56.
270. Lombard MA, Wallace TL, Kubicek MF, Petzold GL, Mitchell MA, Hendges SK et al. Synthetic matrix metalloproteinase inhibitors and tissue inhibitor of

metalloproteinase (TIMP)-2, but not TIMP-1, inhibit shedding of tumor necrosis factor-alpha receptors in a human colon adenocarcinoma (Colo 205) cell line. Cancer Res 1998;58(17):4001-7.
271. Wang Y, Kong D. LncRNA GAS5 Represses Osteosarcoma Cells Growth and Metastasis via Sponging MiR-203a. Cell Physiol Biochem 2018;45(2):844-55.
272. Tran PL, Vigneron JP, Pericat D, Dubois S, Cazals D, Hervy M et al. Gene therapy for hepatocellular carcinoma using non-viral vectors composed of bis guanidinium-tren-cholesterol and plasmids encoding the tissue inhibitors of metalloproteinases TIMP-2 and TIMP-3. Cancer Gene Ther 2003;10(6):435-44.
273. Brand K, Baker AH, Perez-Canto A, Possling A, Sacharjat M, Geheeb M et al. Treatment of colorectal liver metastases by adenoviral transfer of tissue inhibitor of metalloproteinases-2 into the liver tissue. Cancer Res 2000;60(20):5723-30.
274. Bernardo MM, Fridman R. TIMP-2 (tissue inhibitor of metalloproteinase-2) regulates MMP-2 (matrix metalloproteinase-2) activity in the extracellular environment after pro-MMP-2 activation by MT1 (membrane type 1)-MMP. Biochem J 2003;374(Pt 3):739-45.
275. Zucker S, Drews M, Conner C, Foda HD, DeClerck YA, Langley KE et al. Tissue inhibitor of metalloproteinase-2 (TIMP-2) binds to the catalytic domain of the cell surface receptor, membrane type 1-matrix metalloproteinase 1 (MT1-MMP). J Biol 1998;273(2):1216-22.
276. Strongin AY, Collier I, Bannikov G, Marmer BL, Grant GA, Goldberg GI. Mechanism of cell surface activation of 72-kDa type IV collagenase. Isolation of the activated form of the membrane metalloprotease. J Biol 1995;270(10):5331-8.
277. Deryugina EI, Ratnikov B, Monosov E, Postnova TI, DiScipio R, Smith JW et al. MT1-MMP initiates activation of pro-MMP-2 and integrin alphavbeta3 promotes maturation of MMP-2 in breast carcinoma cells. Exp Cell Res 2001;263(2):209-23.
278. Seo DW, Saxinger WC, Guedez L, Cantelmo AR, Albini A, Stetler-Stevenson WG. An integrin-binding N-terminal peptide region of TIMP-2 retains potent angio-inhibitory and anti-tumorigenic activity in vivo. Peptides 2011;32(9):1840-8.
279. Fernandez CA, Roy R, Lee S, Yang J, Panigrahy D, Van Vliet KJ et al. The anti-angiogenic peptide, loop 6, binds insulin-like growth factor-1 receptor. J Biol 2010;285(53):41886-95.
280. Seo DW, Li H, Guedez L, Wingfield PT, Diaz T, Salloum R et al. TIMP-2 mediated inhibition of angiogenesis: an MMP-independent mechanism. Cell 2003;114(2):171-80.
281. Hoegy SE, Oh HR, Corcoran ML, Stetler-Stevenson WG. Tissue inhibitor of metalloproteinases-2 (TIMP-2) suppresses TKR-growth factor signaling independent of metalloproteinase inhibition. J Biol 2001;276(5):3203-14.
282. Wakeling AE, Guy SP, Woodburn JR, Ashton SE, Curry BJ, Barker AJ et al. ZD1839 (Iressa): an orally active inhibitor of epidermal growth factor signaling with potential for cancer therapy. Cancer Res 2002;62(20):5749-54.
283. Jain K, Yang H, Cai BR, Haque B, Hurvitz AI, Diehl C et al. Retrievable, replaceable, macroencapsulated pancreatic islet xenografts. Long-term engraftment without immunosuppression. Transplantation 1995;59(3):319-24.

284. Livak KJ, Schmittgen TD. Analysis of relative gene expression data using real-time quantitative PCR and the 2(-Delta Delta C(T)) Method. Methods 2001;25(4):402-8.
285. Gazda LS, Martis PC, Laramore MA, Bautista MA, Dudley A, Vinerean HV et al. Treatment of agarose-agarose RENCA macrobeads with docetaxel selects for OCT4(+) cells with tumor-initiating capability. Cancer Biol Ther 2013;14(12):1147-57.
286. Ogryzko VV, Wong P, Howard BH. WAF1 retards S-phase progression primarily by inhibition of cyclin-dependent kinases. Mol Cell Biol 1997;17(8):4877-82.
287. Treda C, Popeda M, Ksiazkiewicz M, Grzela DP, Walczak MP, Banaszczyk M et al. EGFR Activation Leads to Cell Death Independent of PI3K/AKT/mTOR in an AD293 Cell Line. PloS one 2016;11(5):e0155230.
288. Glynne-Jones E, Goddard L, Harper ME. Comparative analysis of mRNA and protein expression for epidermal growth factor receptor and ligands relative to the proliferative index in human prostate tissue. Hum Pathol 1996;27(7):688-94.
289. Pignon JC, Koopmansch B, Nolens G, Delacroix L, Waltregny D, Winkler R. Androgen receptor controls EGFR and ERBB2 gene expression at different levels in prostate cancer cell lines. Cancer Res 2009;69(7):2941-9.
290. Sherwood ER, Van Dongen JL, Wood CG, Liao S, Kozlowski JM, Lee C. Epidermal growth factor receptor activation in androgen-independent but not androgen-stimulated growth of human prostatic carcinoma cells. Br J Cancer 1998;77(6):855-61.
291. Fitzpatrick SL, LaChance MP, Schultz GS. Characterization of epidermal growth factor receptor and action on human breast cancer cells in culture. Cancer Res 1984;44(8):3442-7.
292. El Guerrab A, Bamdad M, Kwiatkowski F, Bignon YJ, Penault-Llorca F, Aubel C. Anti-EGFR monoclonal antibodies and EGFR tyrosine kinase inhibitors as combination therapy for triple-negative breast cancer. Oncotarget 2016;7(45):73618-37.
293. Cuadrado A, Garcia-Fernandez LF, Gonzalez L, Suarez Y, Losada A, Alcaide V et al. Aplidin induces apoptosis in human cancer cells via glutathione depletion and sustained activation of the epidermal growth factor receptor, Src, JNK, and p38 MAPK. J Biol 2003;278(1):241-50.
294. Huang HS, Nagane M, Klingbeil CK, Lin H, Nishikawa R, Ji XD et al. The enhanced tumorigenic activity of a mutant epidermal growth factor receptor common in human cancers is mediated by threshold levels of constitutive tyrosine phosphorylation and unattenuated signaling. J Biol 1997;272(5):2927-35.
295. Chen X, Gao B, Ponnusamy M, Lin Z, Liu J. MEF2 signaling and human diseases. Oncotarget 2017;8(67):112152-65.
296. Madugula K, Mulherkar R, Khan ZK, Chigbu DI, Patel D, Harhaj EW et al. MEF-2 isoforms' (A-D) roles in development and tumorigenesis. Oncotarget 2019;10(28):2755-87.
297. Wee P, Wang Z. Epidermal Growth Factor Receptor Cell Proliferation Signaling Pathways. Cancers (Basel) 2017;9(5).

298. Uhlen M, Fagerberg L, Hallstrom BM, Lindskog C, Oksvold P, Mardinoglu A et al. Proteomics. Tissue-based map of the human proteome. Science 2015;347(6220):1260419.
299. Uhlen M, Bjorling E, Agaton C, Szigyarto CA, Amini B, Andersen E et al. A human protein atlas for normal and cancer tissues based on antibody proteomics. Mol Cell Proteomics 2005;4(12):1920-32.
300. Taylor BS, Schultz N, Hieronymus H, Gopalan A, Xiao Y, Carver BS et al. Integrative genomic profiling of human prostate cancer. Cancer Cell 2010;18(1):11-22.
301. Ciccarelli C, Marampon F, Scoglio A, Mauro A, Giacinti C, De Cesaris P et al. p21WAF1 expression induced by MEK/ERK pathway activation or inhibition correlates with growth arrest, myogenic differentiation and onco-phenotype reversal in rhabdomyosarcoma cells. Mol Cancer 2005;4:41.
302. Raimondi L, Ciarapica R, De Salvo M, Verginelli F, Gueguen M, Martini C et al. Inhibition of Notch3 signalling induces rhabdomyosarcoma cell differentiation promoting p38 phosphorylation and p21(Cip1) expression and hampers tumour cell growth in vitro and in vivo. Cell Death Differ 2012;19(5):871-81.
303. Carlo MI, Khan N, Zehir A, Patil S, Ged Y, Redzematovic A et al. Comprehensive Genomic Analysis of Metastatic Non–Clear-Cell Renal Cell Carcinoma to Identify Therapeutic Targets. JCO Precision Oncology 2019;3.
304. Aude-Garcia C, Collin-Faure V, Bausinger H, Hanau D, Rabilloud T, Lemercier C. Dual roles for MEF2A and MEF2D during human macrophage terminal differentiation and c-Jun expression. Biochem J 2010;430(2):237-44.
305. Blaeser F, Ho N, Prywes R, Chatila TA. Ca(2+)-dependent gene expression mediated by MEF2 transcription factors. J Biol 2000;275(1):197-209.
306. Riquelme C, Barthel KK, Liu X. SUMO-1 modification of MEF2A regulates its transcriptional activity. J Cell Mol Med 2006;10(1):132-44.
307. Li M, Linseman DA, Allen MP, Meintzer MK, Wang X, Laessig T et al. Myocyte enhancer factor 2A and 2D undergo phosphorylation and caspase-mediated degradation during apoptosis of rat cerebellar granule neurons. J Neurosci 2001;21(17):6544-52.
308. Zhang L, Sun Y, Fei M, Tan C, Wu J, Zheng J et al. Disruption of chaperone-mediated autophagy-dependent degradation of MEF2A by oxidative stress-induced lysosome destabilization. Autophagy 2014;10(6):1015-35.
309. Cancer Genome Atlas Research N. The Molecular Taxonomy of Primary Prostate Cancer. Cell 2015;163(4):1011-25.
310. Sebastian S, Settleman J, Reshkin SJ, Azzariti A, Bellizzi A, Paradiso A. The complexity of targeting EGFR signalling in cancer: from expression to turnover. Biochim Biophys Acta 2006;1766(1):120-39.
311. Arteaga CL. Epidermal growth factor receptor dependence in human tumors: more than just expression? Oncologist 2002;7 Suppl 4:31-9.
312. Arteaga CL, Engelman JA. ERBB receptors: from oncogene discovery to basic science to mechanism-based cancer therapeutics. Cancer Cell 2014;25(3):282-303.
313. Yang YP, Ma H, Starchenko A, Huh WJ, Li W, Hickman FE et al. A Chimeric Egfr Protein Reporter Mouse Reveals Egfr Localization and Trafficking In Vivo. Cell Rep 2017;19(6):1257-67.

314. Burke P, Schooler K, Wiley HS. Regulation of epidermal growth factor receptor signaling by endocytosis and intracellular trafficking. Mol Biol Cell 2001;12(6):1897-910.
315. Dong J, Opresko LK, Dempsey PJ, Lauffenburger DA, Coffey RJ, Wiley HS. Metalloprotease-mediated ligand release regulates autocrine signaling through the epidermal growth factor receptor. PNAS 1999;96(11):6235-40.
316. Schoffski P, Guillem V, Garcia M, Rivera F, Tabernero J, Cullell M et al. Phase II randomized study of Plitidepsin (Aplidin), alone or in association with L-carnitine, in patients with unresectable advanced renal cell carcinoma. Mar Drugs 2009;7(1):57-70.
317. Francavilla C, Papetti M, Rigbolt KT, Pedersen AK, Sigurdsson JO, Cazzamali G et al. Multilayered proteomics reveals molecular switches dictating ligand-dependent EGFR trafficking. Nat Struct Mol Biol 2016;23(6):608-18.
318. Sangwan V, Abella J, Lai A, Bertos N, Stuible M, Tremblay ML et al. Protein-tyrosine phosphatase 1B modulates early endosome fusion and trafficking of Met and epidermal growth factor receptors. J Biol 2011;286(52):45000-13.
319. Kholodenko BN, Demin OV, Moehren G, Hoek JB. Quantification of short term signaling by the epidermal growth factor receptor. J Biol 1999;274(42):30169-81.
320. Lemmon MA, Freed DM, Schlessinger J, Kiyatkin A. The Dark Side of Cell Signaling: Positive Roles for Negative Regulators. Cell 2016;164(6):1172-84.
321. Rush JS, Quinalty LM, Engelman L, Sherry DM, Ceresa BP. Endosomal accumulation of the activated epidermal growth factor receptor (EGFR) induces apoptosis. J Biol 2012;287(1):712-22.
322. Sironi JJ, Ouchi T. STAT1-induced apoptosis is mediated by caspases 2, 3, and 7. J Biol 2004;279(6):4066-74.
323. Gartel AL, Tyner AL. The role of the cyclin-dependent kinase inhibitor p21 in apoptosis. Mol Cancer Ther 2002;1(8):639-49.
324. Niculescu AB, 3rd, Chen X, Smeets M, Hengst L, Prives C, Reed SI. Effects of p21(Cip1/Waf1) at both the G1/S and the G2/M cell cycle transitions: pRb is a critical determinant in blocking DNA replication and in preventing endoreduplication. Mol Cell Biol 1998;18(1):629-43.
325. Gartel AL, Tyner AL. Transcriptional regulation of the p21((WAF1/CIP1)) gene. Exp Cell Res 1999;246(2):280-9.
326. Abbas T, Dutta A. p21 in cancer: intricate networks and multiple activities. Nat Rev Cancer 2009;9(6):400-14.
327. Bartek J, Iggo R, Gannon J, Lane DP. Genetic and immunochemical analysis of mutant p53 in human breast cancer cell lines. Oncogene 1990;5(6):893-9.
328. van Bokhoven A, Varella-Garcia M, Korch C, Johannes WU, Smith EE, Miller HL et al. Molecular characterization of human prostate carcinoma cell lines. Prostate 2003;57(3):205-25.
329. Zhu HX, Shi L, Zhang Y, Zhu YC, Bai CX, Wang XD et al. Myocyte enhancer factor 2D provides a cross-talk between chronic inflammation and lung cancer. J Transl Med 2017;15(1):65.
330. Gomez-Suaga P, Rivero-Rios P, Fdez E, Blanca Ramirez M, Ferrer I, Aiastui A et al. LRRK2 delays degradative receptor trafficking by impeding late endosomal budding through decreasing Rab7 activity. Hum Mol Genet 2014;23(25):6779-96.

331. Han KA, Shin WH, Jung S, Seol W, Seo H, Ko C et al. Leucine-rich repeat kinase 2 exacerbates neuronal cytotoxicity through phosphorylation of histone deacetylase 3 and histone deacetylation. Hum Mol Genet 2017;26(1):1-18.
332. Yang YS, Harel NY, Strittmatter SM. Reticulon-4A (Nogo-A) redistributes protein disulfide isomerase to protect mice from SOD1-dependent amyotrophic lateral sclerosis. J Neurosci 2009;29(44):13850-9.
333. Morello V, Cabodi S, Sigismund S, Camacho-Leal MP, Repetto D, Volante M et al. beta1 integrin controls EGFR signaling and tumorigenic properties of lung cancer cells. Oncogene 2011;30(39):4087-96.
334. Caswell PT, Vadrevu S, Norman JC. Integrins: masters and slaves of endocytic transport. Nat Rev Mol Cell Biol 2009;10(12):843-53.
335. Prehn RT. The inhibition of tumor growth by tumor mass. Cancer Res 1991;51(1):2-4.
336. Fisher B, Gunduz N, Coyle J, Rudock C, Saffer E. Presence of a growth-stimulating factor in serum following primary tumor removal in mice. Cancer Res 1989;49(8):1996-2001.
337. DeWys WD. Studies correlating the growth rate of a tumor and its metastases and providing evidence for tumor-related systemic growth-retarding factors. Cancer Res 1972;32(2):374-9.
338. Norton L. Cancer stem cells, self-seeding, and decremented exponential growth: theoretical and clinical implications. Breast Dis 2008;29:27-36.
339. Speer JF, Petrosky VE, Retsky MW, Wardwell RH. A stochastic numerical model of breast cancer growth that simulates clinical data. Cancer Res 1984;44(9):4124-30.
340. Norton L, Simon R, Brereton HD, Bogden AE. Predicting the course of Gompertzian growth. Nature 1976;264(5586):542-5.
341. Laird AK, Tyler SA, Barton AD. Dynamics of normal growth. Growth 1965;29(3):233-48.
342. Administration USFD: 2017 New Drug Therapy Approvals. In: *Advancing Health Through Innovation.* Center for Drug Evaluation and Research; 2018.
343. Administration USFD: 2018 New Drug Therapy Approvals. In: *Advancing Health Through Innovation.* Center for Drug Evaluation and Research; 2019.
344. Administration USFD: 2019 New Drug Therapy Approvals. In: *Advancing Health Through Innovation.* Center for Drug Evaluation and Research; 2020.
345. Vasan N, Baselga J, Hyman DM. A view on drug resistance in cancer. Nature 2019;575(7782):299-309.
346. Bayat Mokhtari R, Homayouni TS, Baluch N, Morgatskaya E, Kumar S, Das B et al. Combination therapy in combating cancer. Oncotarget 2017;8(23):38022-43.
347. Administration USFD: Hematology/Oncology (Cancer) Approvals & Safety Notifications. In: *Development & Approval Process: Drugs.* Approved Drugs; 2020.
348. Bailey MH, Tokheim C, Porta-Pardo E, Sengupta S, Bertrand D, Weerasinghe A et al. Comprehensive Characterization of Cancer Driver Genes and Mutations. Cell 2018;173(2):371-85 e18.
349. Hanahan D, Weinberg RA. The hallmarks of cancer. Cell 2000;100(1):57-70.

350. Azeloglu EU, Iyengar R. Signaling networks: information flow, computation, and decision making. Cold Spring Harb Perspect Biol 2015;7(4):a005934.
351. Ratushny V, Golemis E. Resolving the network of cell signaling pathways using the evolving yeast two-hybrid system. Biotechniques 2008;44(5):655-62.
352. Yuan Y, Jiang YC, Sun CK, Chen QM. Role of the tumor microenvironment in tumor progression and the clinical applications (Review). Oncol Rep 2016;35(5):2499-515.
353. Block KI, Gyllenhaal C, Lowe L, Amedei A, Amin A, Amin A et al. Designing a broad-spectrum integrative approach for cancer prevention and treatment. Semin Cancer Biol 2015;35 Suppl:S276-S304.
354. Selik RM, Chu SY, Buehler JW. HIV infection as leading cause of death among young adults in US cities and states. JAMA 1993;269(23):2991-4.
355. Huber JT. Death and AIDS: a review of the medico-legal literature. Death Stud 1993;17(3):225-32.
356. Estimated HIV incidence and prevalence in the United States, 2010-2016.
357. Kemnic TR, Gulick PG: HIV Antiretroviral Therapy. In: *StatPearls.* edn. Treasure Island (FL); 2020.
358. Samji H, Cescon A, Hogg RS, Modur SP, Althoff KN, Buchacz K et al. Closing the gap: increases in life expectancy among treated HIV-positive individuals in the United States and Canada. PloS one 2013;8(12):e81355.
359. Mascolini M: Increased overall life expectancy but not comorbidity-free years for people with HIV. In: *Conference on Retroviruses and Opportunistic Infections.* Boston, USA; 2020.
360. What is the life expectancy for someone with HIV? [https://www.nhs.uk/common-health-questions/sexual-health/what-is-the-life-expectancy-for-someone-with-hiv/]